ELUCIDATING THE ROLES OF THE CARDIOGENIC FACTORS *TBX20*, *TBX5* AND *HSP27* IN VERTEBRATE HEART DEVELOPMENT

Daniel DeWitt Brown

A dissertation submitted to the faculty of the University of North Carolina at Chapel Hill in partial fulfillment of the requirements for the degree of Doctorate of Philosophy in the Department of Biology.

Chapel Hill
2006

Approved by:

Shawn Ahmed

Victoria Bautch

Frank L. Conlon

Mark Majesky

Larysa Pevny

ABSTRACT

DANIEL BROWN: Elucidating the Roles of the Cardiogenic Factors *Tbx20*, *Tbx5* and *Hsp27* in Vertebrate Heart Development
(Under the direction of Frank Conlon)

The development of a functional multi-chambered contractile heart from a simple patterned tube involves a number of interacting transcriptional networks acting within well-defined temporal and spatial parameters. While many of the regulatory transcription factors have been identified and shown to be required for proper cardiogenesis, much remains to be deciphered regarding how these pathways interact at different times and within different cell populations during cardiogenesis. In addition, very little is currently known as to the specific downstream pathways affected by the various transcriptional regulators known to be involved in cardiac morphogenesis.

In this dissertation, I describe the identification of several novel *Xenopus laevis* (*X. laevis*) genes expressed during heart development, including *T-box 20* (*Tbx20*), *titin novex 3* (*XTn3*), and *heat shock protein 27* (*XHsp27*), thus providing evidence that these genes may be involved in cardiogenesis. By depleting *X. laevis* embryos of TBX20 and the related T-box protein, TBX5, I demonstrate that these proteins are both critical for proper cardiac morphogenesis. In addition, I provide evidence for a physical and functional interaction between TBX20 and TBX5 in cardiogenesis, thus adding one potential point at which multiple pathways may converge during heart development. Results from a microarray-based screen I conducted to identify genes downstream of

Tbx5 function led to the identification of several cell cycle genes putatively misregulated in response to loss of TBX5. This work led directly to a study conducted by Sarah Goetz in which she has demonstrated a requirement for *Tbx5* for proper cell cycle progression, thus further elucidating downstream pathways in heart development. A similar screen I performed to identify genes misregulated in response to loss of *Tbx20* yielded a host of novel cardiac-specific genes, setting up the basis for future studies to come. This microarray experiment further resulted in the identification of *Hsp27*, which I subsequently demonstrated is required for proper fusion of cardiac precursors and for actin cytoskeleton integrity. Thus, this dissertation significantly advances our understanding of cardiogenesis at multiple levels, including the identification of factors involved in cardiogenesis, interactions between these factors, and downstream cellular behaviors affected by these factors.

ACKNOWLEDGEMENTS

The successful completion of any long term scientific endeavor requires patience and determination, but more importantly, it requires a burning passion and excitement for the subject of study. A love of biology was fostered within me in spades thanks to the dedication and talent of several notable mentors in my early training: my high school zoology teacher Bob Ross, my advanced placement biology teacher Ellen Neaville, my molecular biology professor Dr. Kelly Agnew, and my Zoology professor and friend Dr. Matt Moran. For this I will be forever grateful. Of course, everything I have ever accomplished was made possible with the unending love and unquestioning support of my parents, Keith Brown and Pamela Garrison. Furthermore, none of the work reported herein would be possible without the excellent guidance and mentorship of my advisor Dr. Frank Conlon. A certain degree of stress obligatorily comes with the trials and tribulations of learning to be a great scientist, thus a strong support network is as important for graduate school happiness as a heart is for survival. Thus, I would like to thank Dr. Nick Kappas, Jan LaRocque, Emily Fisher, Brian Robertson, Danny Monroe, and Sarah Taylor. But most of all I would like to think the single most important and cherished person in my life: my wife, Leslie Brown. I probably would not have survived a year without her love and support.

TABLE OF CONTENTS

LIST OF TABLES

Chapter IV

Table

LIST OF FIGURES

ABBREVIATIONS

ANF	atrial natriuretic factor
BMP	bone morphogenetic protein
Dkk1	dikkopf 1
FGF	fibroblast growt factor
Fn	fibronectin
HOS	Holt-Oram Syndrome
Hsp27	heat shock protein 27
MHC	myosin heavy chain
ODC	ornithine decarboxylase
sHSP	small heat shock protein
SRF	serum response factor
Tbx1	T-box 1
Tbx3	T-box 3
Tbx5	T-box 5
Tbx20	T-box 20
TEM	Transmission Electron Microscopy
TnIc	Cardiac Troponin I
X. laevis	*Xenopus* laevis
XHsp27	*Xenopus* heat shock protein 27
XTn3	*Xenopus* Titin Novex-3
XTbx5	*Xenopus* T-box 5
XTbx20	*Xenopus* T-box 20

CHAPTER I

GENERAL INTRODUCTION

Of the many known congenital diseases that affect human beings, those affecting development of the heart are among the most severe. A functioning cardiovascular system is integral to nearly every process and system that makes human existence possible. Development of the heart is an incredibly complex process requiring the coordination of many events within well-defined spatial and temporal dimensions (reviewed in Harvey, 2002). The complex nature and multitude of coordinated steps within cardiogenesis make this process inherently sensitive to genetic perturbation. As such, it is not surprising that congenital heart disease is the most common cause of prenatal mortality (Hoffman, 1995a; Hoffman, 1995b; Kochanek et al., 2004), and is estimated to be responsible for 10% to 15% of all maternal mortalities during childbirth (Gei and Hankins, 2001; Klein and Galan, 2004). Furthermore, current data from the Centers for Disease Control estimates that one out of every one hundred and ten babies born in the United States is afflicted with a congenital heart disease (Thom et al., 2006). In addition to the problems associated with congenital heart diseases, a number of adult heart diseases are highly prevalent, including myocardial infarction and hypertrophy. Research has shown that many of these diseases are characterized by a recapitulation of cardiogenic processes and transcriptional programs in the cardiac tissue. For instance, ventricular hypertrophy has been shown to involve upregulation of several of the earliest expressed cardiac transcription factors including *Gata4*, *Nkx2.5*,

Mef2, *eHand* and *dHand* (Bar et al., 2003). Thus, understanding the cellular, molecular, and genetic events involved in the creation of a heart remains one of the biggest and potentially highest impacting challenges facing human health today.

A. Mechanisms of Heart Induction and Development

Cardiac Progenitor Induction

The vertebrate heart is a highly complex muscular pump necessary for the dissemination of nutrition and signaling molecules and for the exchange of gases throughout the body. It also functions to transport wastes away from their tissues of origin to the systems that remove them. In mammals and avians, the heart consists of two separate but fused pumps, each containing one atria and one ventricle, which service the pulmonary and systemic systems of the body, respectively (reviewed in Olson, 2006). In contrast, amphibian and reptile hearts contain two atria and one ventricle all serving as a single pump, although the ventricle is partially divided in reptiles (reviewed in Olson, 2006). In these organisms, blood flows from the heart, through the pulmonary system, and then to the rest of the body (reviewed in Olson, 2006). Further down on the evolutionary ladder, fish hearts consist of one atria and one ventricle and do not have pulmonary circulation (reviewed in Olson, 2006). Despite the differences in chamber number and organization between various vertebrate lineages, early heart development occurs in a nearly identical fashion mechanistically between these organisms (Chen and Fishman, 2000; DeRuiter et al., 1992; Keller, 1976; Lohr and Yost, 2000; Sater and Jacobson, 1989; Stainier et al., 1993).

During gastrulation, when the three germ layers, endoderm, ectoderm and mesoderm, are formed, a bilaterally symmetric pair of cell fields within the mesoderm are specified to

eventually give rise to the heart. However, before this specification can occur, the mesodermal germ layer must first form through an inductive interaction with the endoderm (reviewed in Harland and Gerhart, 1997). Mesoderm induction is followed by a refinement in mesodermal character (e.g. ventral mesoderm versus dorsal mesoderm) via signals emanating from a region in *X. laevis* termed the "Spemann Organizer". The Spemann Organizer, a region of the embryo that shares some similarity to the node in avians and mammals, secretes a host of signaling molecules that function by inhibiting the Wnt and bone morphogenetic protein (BMP) signals emanating from the ventral region of the embryo (Fig. 1.1A). The canonical Wnt pathway involves the binding of Wnt ligands to their Frizzled and LRP family receptors and transduction of signaling to β-catenin, which translocates into the nucleus and forms a complex with TCF transcription factors resulting in activation of Wnt target genes (for a review of the Wnt pathway see Gordon and Nusse, 2006). BMPs are members of the transforming growth factor β (TGFβ) family of proteins and function by binding Type I and Type II receptors, resulting in the binding of receptor SMAD with a co-SMAD and activation of BMP target genes (for a review of the BMP pathway see Nohe et al., 2004). The interplay between Wnt/Bmp signaling from the ventral region of the embryo and Wnt/BMP antagonism by the Spemann organizer results in the formation of ventral mesoderm in regions of high Wnt/Bmp signaling and dorsal mesoderm in regions of low Wnt/Bmp signaling.

Once the dorsal mesoderm is induced, the local environment within the lateral mesoderm becomes permissive for cardiac specification. Studies have shown that at least two independent signaling events must occur for the cardiac progenitors to be specified. First, during gastrulation the dorsal organizer secretes the inhibitors of canonical Wnt signaling,

Dikkopf 1 (*Dkk1*) and *crescent*, and these events are critical for cardiac induction (Marvin et al., 2001; Schneider and Mercola, 2001). Recent work by Foley and Mercola (2005) has demonstrated that canonical Wnt inhibition by *Dkk1* leads to cell-autonomous expression of the homeobox transcription factor *Hex* (Foley and Mercola, 2005). They further show that the repressive activity of *Hex* is required for the production of an unknown signal resulting in cardiac induction, thus demonstrating a non cell-autonomous requirement for *Hex* in cardiogenesis (Foley and Mercola, 2005). Other studies have also implicated Nodal signaling in cardiogenesis and *Hex* regulation, although the specific role of Nodal in heart development is currently unclear (Griffin and Kimelman, 2002; Ladd et al., 1998; Logan and Mohun, 1993; Sugi and Lough, 1994; Yatskievych et al., 1997; Yatskievych et al., 1999). In addition to the requirement for Wnt antagonism from the organizer, it is also well-known that a signal emanating from the endoderm adjacent to the cardiac progenitor region is also necessary for proper cardiac induction (Nascone and Mercola, 1996). This requirement is at least partially due to the secretion of BMPs from the adjacent anterior endoderm. Head mesoderm is induced by the dorsal organizer and requires antagonism of BMP and Wnt signals emanating from the ventral region of the embryo (Niehrs et al., 2001; Perea-Gomez et al., 2001). This is accomplished by the secretion of the Wnt inhibitors *Dkk1* and *crescent*, and the BMP inhibitors *chordin* and *noggin*, among others (Niehrs et al., 2001; Perea-Gomez et al., 2001). In contrast, the cardiac precursors are induced at the lateral edges of the head precursor zone, where Wnt signaling is efficiently inhibited by *Dkk1* and *crescent* but BMP signals are still present (Fig. 1.1A; Marvin et al., 2001; Schneider and Mercola, 2001). Several studies have demonstrated a critical requirement for BMPs in proper cardiac specification (Andree et al., 1998; Ladd et al., 1998; Schlange et al., 2000; Schultheiss et al., 1997; Shi et al., 2000;

Zhang and Bradley, 1996). In addition, several SMAD proteins, which are downstream effectors of BMP signaling, can directly activate *Nkx2.5*, an early cardiac transcription factor (see below; Liberatore et al., 2002; Lien et al., 2002; Schwartz and Olson, 1999; Sparrow et al., 2000). Consistent with the hypothesis that *Dkk1* and Wnt inhibition is required for cardiac induction, the Wnt inhibitors *Dkk1* and members of the Frizzled-like family of proteins are expressed in the anterior endoderm as well as in the aforementioned organizer (Marvin et al., 2001; Schneider and Mercola, 2001). These data combined suggest that interplay between Wnt antagonism and BMP signaling from the organizer and anterior endoderm is partially responsible for cardiac induction. In corroboration of this hypothesis, experiments have shown that non-cardiogenic posterior mesoderm can be induced to form cardiac mesoderm in the presence of both BMP signals and Wnt antagonists (Marvin et al., 2001; Schneider and Mercola, 2001; Tzahor and Lassar, 2001). Furthermore, in *X. laevis* this dual presence can lead to the formation of contractile cardiac tissue lined with an endothelium in the posterior non-cardiogenic mesoderm when induced ectopically (Schneider and Mercola, 2001).

In addition to the requirement for BMP signaling and Wnt antagonism in heart induction, a role for several other signaling pathways has also been implicated. *Fibroblast growth factor 8* (*Fgf8*), which is also expressed in the endoderm, can be induced by BMP signaling and is required for cardiac specification (Alsan and Schultheiss, 2002). Furthermore, mice lacking the Hedgehog receptor *Smoothened* (*Smo*) fail to initiate *Nkx2.5* expression (Zhang et al., 2001). Thus considering that the *Smo* ligand Indian Hedgehog (IHH) is expressed in the endoderm and can induce BMP4 expression, these data suggest that Hedgehog signaling is also an important regulator of cardiogenesis (Zhang et al., 2001). In

summary, many different signaling cascades originating from the surrounding tissues are involved in commitment to the cardiac lineage, including Wnt antagonists, BMPs, FGF8, and Hedgehog signals.

Cardiac Progenitor Migration and Fusion

Once the cardiac precursor fields are specified they undergo two separate migration events as neurulation proceeds (reviewed in Harvey, 2002). The large-scale tissue movements involved in gastrulation and subsequent convergent extension result in the anterior migration of the cardiac progenitors toward more anterior regions (Fig. 1.1B). This process seems to be largely controlled by FGF factors such as FGF8 and FGF4 (Beiman et al., 1996; Ciruna and Rossant, 1999; Gisselbrecht et al., 1996; Sun et al., 1999). The progenitors then migrate ventrally towards the anterior ventral midline (Figs. 1.1C, 1.2; DeHaan, 1963). Expression of fibronectin (Fn) at the junction between the endoderm and mesoderm appears to be required for this migration; mutant mice lacking *Fn* exhibit cardia bifida, which is characterized by unfused cardiac progenitors that independently differentiate into cardiac tissue (George et al., 1997). It has also been well established that the anterior endoderm is required for cardiac progenitor migration. For example, many genes involved in endoderm differentiation and maturation result in cardia bifida when mutated in mice or fish, and it is currently thought that the cardiac defects result from a loss of cardiac migration factors from mature endoderm, such as the aforementioned Fn (Crispino et al., 2001; Kupperman et al., 2000; Reiter et al., 1999; Stainier, 2001).

Linear Heart Tube Formation and Cardiac Looping

Once the presumptive cardiac mesoderm meets at the ventral midline, the two pre-cardiac fields fuse resulting in a single contiguous sheet of mesoderm at the anterior ventral midline (Fig. 1.2; for reviews of this process see Fishman and Chien, 1997; Harvey, 2002) and (Mohun et al., 2003). Dorsal to this mesoderm lays the anterior endoderm, which will eventually form the pharynx, liver, and gut. At this stage, the pre-cardiac mesoderm appears morphologically as a wedge-shaped trough in *X. laevis* (Fig. 1.2) or as a crescent in avians and mammals. Shortly after progenitor fusion at the midline, the lateral edges of the cardiogenic field roll dorsally and medially to form a linear heart tube (Fig. 1.2). The dorsal-most aspect of this tube remains connected to the surrounding lateral mesoderm by way of a thin strip of dorsal mesocardial tissue. As the linear heart tube forms, the surrounding space expands to form the pericardial cavity. While the cardiac field is still in trough form, a layer of endothelial tissue is already evident just dorsal to the layer of myocardial precursors (Fig. 1.2; Stainier et al., 1993). This endothelial tissue is encompassed by the developing heart tube to eventually form the endocardium. Evidence from lineage tracing experiments suggests that the endocardium is also mesodermally-derived; however it is currently unknown whether this mesoderm is the sole ancestor of the endocardium (Fig. 1.2; Raffin et al., 2000).

Once the linear heart tube forms, a further morphogenetic event is necessary to properly position the presumptive atrial and ventricular regions: cardiac looping morphogenesis (Fig. 1.3; for reviews of looping morphogenesis see Fishman and Chien, 1997; Harvey, 2002; Mohun, 2000). The general structure of the heart in all adult vertebrates consists of the atrium (or atria) in the dorsal anterior position and the ventricle (or ventricles)

just ventral and posterior to the atria (Fig. 1.3; DeHaan and Ursprung, 1965). However, in the linear heart tube phase, the relative positions of the future atria and ventricle are precisely opposite of their positions in the adult heart. Initially, the most anterior portion of the heart tube consists of the future ventricle and outflow tract. Conversely the posterior portion consists of the future inflow tract and atria. As development proceeds, the tube undergoes spiral looping whereby the inflow region initially moves leftward, in a process termed "leftward jogging". The future atria then move dorsally and anteriorly, repositioning itself just dorsal and anterior to the future ventricle (Fig. 1.3). At this stage in cardiogenesis, differences in myocardial wall thickness become evident as atrial and ventricular chamber identities develop (Bisaha and Bader, 1991; Christoffels et al., 2000; Edmondson et al., 1994; Mohun, 2000). The primitive heart begins to undergo many processes of chamber formation and remodeling, including septation of the atria, formation of valves and endocardial cushions, and trabeculation of the ventricle (reviewed in Fishman and Chien, 1997). These processes result in the formation of a mature tadpole heart consisting of two small thin-walled atria and a single thick-walled ventricle (Fig. 1.3).

B. Molecular Control of Heart Development

As discussed above, induction of cardiac progenitors requires the interaction of multiple tissues and several signaling pathways, including BMPs, non-canonical Wnts, canonical Wnt inhibitors, and FGFs. These signaling events result in the initiation of many distinct programs of cardiac differentiation leading to many different cardiac cell types reviewed in (Bruneau, 2002; Eisenberg and Markwald, 2004; Fishman and Chien, 1997; Olson, 2006). It is becoming increasingly clear that a complex molecular regulatory network is required in the specification, differentiation, and morphogenesis of a functional heart. The

proteins implicated in controlling these processes include a number of transcription factors from a range of transcription factor families, including the T-box, basic helix-loop-helix homeobox, GATA, zinc finger, and MADS domain families (Cripps and Olson, 2002; Harvey, 2002; Zaffran and Frasch, 2002). Specific transcription factors thus far identified as critical for proper cardiogenesis include *Nkx2.5*, *myocardin*, *Gata4-6*, *SRF*, *Tbx5*, *Tbx20*, and many others. In this introduction I focus on *Nkx2.5, Gata4-6*, *Tbx20*, and *Tbx5*, due to the direct relevance of these factors to the work presented herein.

The homeobox transcription factor *Nkx2.5* is one of the earliest markers of the cardiac precursors. *Nkx2.5*, which was initially identified as critical for *Drosophila* dorsal vessel formation, has been demonstrated to be essential for establishment and maintenance of ventricular gene expression and differentiation (Bodmer, 1993; Bruneau et al., 2000; Lyons, 1995; Tanaka et al., 1999). Furthermore, mice lacking *Nkx2.5* display reduced myocardial growth and a failure of cardiac looping morphogenesis (Lyons, 1995). Expression of *Nkx2.5* has been shown to be largely controlled by the downstream effectors of BMP signaling, SMADs, as well as by GATA factors (Lee et al., 2004; Lien et al., 1999; Schlange et al., 2000; Searcy et al., 1998). Furthermore, dominant-negative experiments in *X. laevis* have suggested that expression of the cardiac transcription factor *myocardin*, which interacts with *serum response factor* (*SRF*) to control transcription, is necessary for high-level *Nkx2.5* expression and cardiac differentiation (Wang et al., 2001).

In addition to the requirement for *Nkx2.5* in cardiac specification and differentiation, three GATA family members have also been demonstrated as critical for cardiogenesis: *gata4*, *gata5*, and *gata6*. As mentioned above, *gata4* and *gata5* are known to be important for proper endoderm maturation and thus important for proper interaction between endoderm

and mesoderm in cardiac formation. However, studies have also demonstrated a role for GATA factors within developing cardiac tissue. Studies in P19 embryonal carcinoma cells have shown that induced cardiac differentiation is arrested when *gata4* or *gata6* is removed by antisense oligonucleotides (Grepin et al., 1995; Narita et al., 1997). Furthermore, a role for GATA factors in cardiogenesis appears to have been conserved throughout evolution, as flies mutant for the *Drosophila* homologue of *gata4*, *pannier*, display defects in cardiac progenitor proliferation (Gajewski et al., 1999).

T-box Genes in Cardiogenesis

In addition to the aforementioned families of cardiogenic transcription factors, members of another class of transcription factors have been shown to be integral regulators of vertebrate cardiogenesis: the T-box proteins. The T-box family of transcription factors is a large family of proteins involved in determining early cell fate decisions, such as those necessary for formation of the basic vertebrate body plan, as well as for controlling differentiation and organogenesis (reviewed in Naiche et al., 2005; Showell et al., 2004). The involvement of T-box genes in these processes is emphasized by the observation that mutation of many T-box members results in dramatic phenotypes in mouse and zebrafish (Beddington et al., 1992; Bruneau et al., 2001; Chapman et al., 1996a; Fujimoto et al., 1991; Garrity et al., 2002; Schier et al., 1997; Schulte-Merker et al., 1994). Furthermore, alterations in T-box gene expression or function have been shown in a number of human congenital malformations and are amplified in a subset of cancers (reviewed in Papaioannou, 2001; Smith, 1999; Wilson and Conlon, 2002). The T-box family has recently been shown to comprise approximately 0.1 % of genomes as diverse as *C. elegans* and human and have

been identified in a wide variety of chordates from ctenophores to humans while being completely absent in genomes from other phyla (*e.g. Arabidopsis thaliana*). For many of these genes clear homologues exist, such as *Brachyury*, which displays a high degree of conservation in sequence, expression pattern, and function between a variety of vertebrates including fish, frog, dog and mouse (Haworth et al., 2001; Herrmann and Lehrach, 1988; Schulte-Merker et al., 1994; Smith et al., 1991). However, other T-box genes appear to be unique to particular species. For instance, *VegT*, a T-box gene thought to be required for endoderm formation in *Xenopus*, has no apparent homologue or orthologue in mouse or human (reviewed in Wilson and Conlon, 2002).

Two sets of clinical studies have provided direct evidence for a role for T-box genes in human heart development and differentiation. Patients with DiGeorge syndrome, a disease characterized by cardiac outflow tract defects as well as defects in other neural-crest-derived structures, are often deleted for the T-box gene *Tbx1* (Baldini, 2004; Chieffo et al., 1997; Jerome and Papaioannou, 2001; Lindsey et al., 2001; Merscher et al., 2001; Yagi et al., 2003). Furthermore, a second congenital heart disease, Holt-Oram Syndrome, has been shown to be associated with mutations in the coding region of another T-box family member, *Tbx5* (Basson et al., 1997; Li et al., 1997). In addition to *Tbx1* and *Tbx5*, recent studies in *Xenopus*, human, mouse, chick and zebrafish have implicated a third member of the T-box gene family, *Tbx20*, in heart development (Brown et al., 2005; Cai et al., 2005; Carson et al., 2000; Griffin et al., 2000; Iio et al., 2001; Kraus et al., 2001; Meins et al., 2000; Stennard et al., 2005; Szeto et al., 2002; Takeuchi et al., 2005).

Tbx20

Tbx20 was initially identified by Meins and colleagues (2000) by searching the human genome for sequences homologous to the *Drosophila* T-box gene *H15* (Meins et al., 2000). This study resulted in the identification of both human and mouse orthologues of *Tbx20*, and demonstrated enrichment of *Tbx20* expression in heart tissues. Shortly thereafter, apparent orthologues of *Tbx20* were identified in chick and zebrafish, and shown to be expressed within the developing heart (Griffin et al., 2000; Iio et al., 2001). In all species examined, *Tbx20* expression begins in the anterior lateral plate mesoderm and gradually becomes restricted to the *Nkx2-5*-expressing cardiac primordia prior to ventral migration and convergence at the midline. This expression continues in the heart throughout the processes of migration, jogging, looping, and cardiac chamber formation. Thus, *Tbx20* is expressed at the same time as and in many regions of the heart that also express the heart markers *Tbx5*, *Nkx2-5*, and *Gata4* (Horb and Thomsen, 1999; Serbedzija et al., 1998; Tonissen et al., 1994). Furthermore, I here report that *Tbx20* expression in the developing heart throughout the entire course of cardiogenesis is conserved in *X. laevis* (see Chapter II; Brown et al., 2003).

Despite our knowledge of the expression pattern of *Tbx20* in several vertebrates, little was known of *Tbx20* function in heart development prior to the experiments reported in this dissertation work. In the zebrafish, it has recently been observed that eliminating endogenous TBX20 (HRT) via morpholinos leads to cardiac defects (Szeto et al., 2002). Specifically, TBX20 knockdown in zebrafish leads to dysmorphic hearts and a loss of blood circulation (Horb and Thomsen, 1999; Szeto et al., 2002). The morphological defects are not apparent until cardiac looping stage, despite high levels of *Tbx20* during the earlier stages of specification and development, suggesting that other T-box genes may act redundantly with

Tbx20 during early heart development. In this dissertation I further demonstrate by TBX20 depletion using antisense morpholinos that TBX20 is critical for proper cardiac growth and morphogenesis in *X. laevis* (see Chapter III; Brown et al., 2003; Brown et al., 2005). In addition, I show that TBX20 can physically and functionally interact with TBX5, and that the neither factor is required for expression of the other. Subsequent to my thesis work, several studies concurrently reported that mutation of *Tbx20* in mice results in cardiac defects (Cai et al., 2005; Stennard et al., 2005; Takeuchi et al., 2005). Findings from these studies corroborate the work reported herein, demonstrating that loss of TBX20 function results in reduced cardiac growth and failure of cardiac looping morphogenesis. Studies from the mouse *Tbx20* mutants further reveal that one role of TBX20 appears to be to repress expression of *Tbx2*, which itself can repress expression of *Nmyc1*, a regulator of cellular proliferation (Cai et al., 2005; Stennard et al., 2005). These results suggest a model in which loss of TBX20 results in overexpression of *Tbx2*, repression of *Nmyc1*, and thus repression of cellular proliferation. Furthermore, a role for *Tbx20* function in cardiogenesis appears to be ancient in evolutionary origin, as recent studies have demonstrated that the *Drosophila* orthologues of *Tbx20*, *H15* and *midline*, are also required for proper development of the dorsal vessel, which is thought to be homologous to the vertebrate heart (Miskolczi-McCallum et al., 2005; Reim et al., 2005).

Tbx5

Along with *Nkx2.5* and *Tbx20*, *Tbx5* is among the first genes expressed in cardiogenic precursor cells (Griffin et al., 2000; Horb and Thomsen, 1999; Tonissen et al., 1994). During vertebrate cardiogenesis, *Tbx5* is expressed throughout the heart in a graded fashion,

excluding the outflow tract. As mentioned above, clinical studies of Holt-Oram Syndrome (HOS) patients have demonstrated a fundamental role for *Tbx5* in heart development. HOS is a highly penetrant autosomal-dominant condition associated with a host of skeletal and cardiac malformations, including defects in upper limb development, atrial and ventricular septal defects, and deficits in cardiac conduction (Newbury-Ecob et al., 1996). Patients with HOS often carry mutations within the coding region of *Tbx5* (Basson et al., 1997; Basson et al., 1999; Benson et al., 1996; Li et al., 1997). Furthermore, *Tbx5* has been shown to be essential for proper heart morphogenesis in several vertebrate species. Studies on mice and zebrafish mutated for *Tbx5*, dominant negative studies in *X. laevis*, and antisense morpholino experiments in zebrafish have demonstrated a requirement for *Tbx5* in proper cardiac looping and morphogenesis (Bruneau et al., 2001; Garrity et al., 2002; Horb and Thomsen, 1999). In mice, despite the early expression of *Tbx5* in the presumptive cardiogenic mesoderm, *Tbx5* appears to be dispensable for cardiac crescent or heart tube formation, but is instead required for growth and differentiation of the left ventricle and atria. *Tbx5* null mice arrest in development at E9.5, and display severely hypoplastic hearts, conduction defects, as well as gross aberrations in cardiac morphology, including an absence of looping. *Tbx5* heterozygous mice display atrial and ventricular septal defects and cardiomegaly, demonstrating that precise *Tbx5* dosage is important for proper heart development (Bruneau et al., 2001). Coincident with these morphological defects, *atrial natriuretic factor* (*ANF*) and *connexin 40* (*cx40*) expression is diminished or absent (Bruneau et al., 2001). Studies in *X. laevis* have shown that when *Tbx5* function is inhibited by dominant-negative hormone-inducible TBX5, the heart is grossly abnormal and reduced in size or absent (Horb and Thomsen, 1999). Furthermore, *myosin light chain 2* (*MLC2*), *Nkx2-5*, and endogenous *Tbx5* levels are reduced

in embryos injected with the dominant negative *Tbx5* (Horb and Thomsen, 1999). These studies demonstrate that mice heterozygous for mutations in *Tbx5* display many of the phenotypic abnormalities of HOS patients, and show that TBX5 is required for growth and differentiation of the left ventricle and atria as well as for proper development of the cardiac conduction system. Expression of *Tbx5* has also been shown to increase differentiation of P19C16 cells, further suggesting a role for *Tbx5* in cardiac differentiation. Similar results are seen in the zebrafish *Tbx5* mutation, *heartstrings*, characterized by a lack of cardiac looping and subsequent degeneration of both the atrium and ventricle, suggesting that the expression and function of TBX5 is conserved throughout vertebrate evolution (Garrity et al., 2002).

Potential Interactions Between *Tbx5* and *Tbx20*

Tbx20 expression is observed in a graded pattern with the highest levels being expressed caudally (Carson et al., 2000; Stennard et al., 2003). This is very similar to the pattern of *Tbx5* expression, which also lies in a caudal-high gradient along the long axis of the heart (Bruneau et al., 1999). Furthermore, the temporal onset of *Tbx5* expression occurs near the same time as that of *Tbx20* (2 hours earlier in zebrafish; (Griffin et al., 2000). Thus, both *Tbx5* and *Tbx20* are expressed throughout cardiogenesis in overlapping domains. However, while *Tbx20* and *Tbx5* share overlapping domains of expression within the developing heart, there are some differences in their expression. Of note is the fact that the outflow tract is a site of major *Tbx20* expression, in contrast to *Tbx5*, which is not significantly expressed in the outflow tract, while *Tbx5* and not *Tbx20* is expressed in the common cardinal and hepatic veins. Nonetheless, the similarity in expression domains and

homology within the DNA-binding domain of *Tbx20* and *Tbx5* suggest that perhaps the two genes cooperate to regulate cardiogenesis.

In addition to expression evidence suggesting the possibility of an interaction occurring between *Tbx20* and *Tbx*5, data on the physical interactions of TBX20 and TBX5 also indicate such a possibility. For instance, both TBX20 and TBX5 have been shown to physically interact with NKX2-5 and GATA4 to synergistically activate transcription of target genes (Bruneau et al., 2001; Garg et al., 2003; Stennard et al., 2003). Furthermore, the mesodermal T-box gene *brachyury* has been shown to bind DNA as a homodimers (Muller and Herrmann, 1997). Recent studies have also reported homodimerization of another T-domain protein, TBX1, which is associated with the congenital heart disease DiGeorge Syndrome (Sinha et al., 2000). Thus, considering that both TBX5 and TBX20 share interacting partners and are both present in overlapping domains, combined with evidence that T-box proteins can at least homodimerize, it seems highly possible that TBX20 and TBX5 may physically interact with one another to heterodimerize or exist within the same complex to control cardiogenesis.

Titin Novex-3

As described above, formation of a functioning heart requires the activity of many transcription factors that act by regulating target gene expression. The end goal of this complex regulatory network is the formation of contractile muscle tissue. Muscles are composed of myofibers, which are in turn made of bundles of smaller myofibrils. Thus, differentiation of cardiomyocytes results in the production of various structural proteins that can assemble to form individual myofibrils. Contractile myofibrils consist of an organized

structure of thin actin-based filaments and thick myosin-based filaments held in place by filaments composed of another structural protein termed "Titin". The giant muscle protein titin is the largest known protein in the biological world and the single human titin gene contains 363 exons with a coding potential of 38,138 amino acids. Many splice-variants of titin have been described and full-length isoforms have been shown to span half the sarcomere length from the Z-line to the M-line, serving to link the two regions and stabilize sarcomere length by acting as a molecular spring (reviewed in Granzier et al., 2002). To date, the cloning or expression of *Xenopus* titin orthologues has not been reported. Recently a novel human titin exon, termed novex-3, was identified within the human titin locus and shown to encode an alternative C-terminal exon resulting in a truncated titin isoform that is too short to reach the A-band (Bang et al., 2001). This isoform was shown to be expressed in human skeletal and cardiac muscle (Bang et al., 2001). In this dissertation, I report the identification of a *X. laevis* orthologue of *titin novex 3* (*XTn3*) and demonstrate that *XTn3* expression is developmentally regulated during cardiac and skeletal myogenesis. These data suggest a potential role for *XTn3* in muscle differentiation.

Hsp27

As described above, ventral migration and fusion of the cardiac fields require the coordination of many processes, including proper cardiomyocyte differentiation (Reiter et al., 1999; Yelon et al., 2000), signaling from the endoderm (Alexander et al., 1999; Kikuchi et al., 2000; Reiter et al., 1999; Schier et al., 1997), epithelial organization of the cardiac fields, and migration cues from the midline (Trinh and Stainier, 2004). Studies have implicated many molecules as being required for proper cardiac fusion, such as the extracellular matrix

protein *fibronectin* (*Fn*), which has been demonstrated to be necessary for proper epithelial integrity and migration of the cardiac progenitors (Trinh and Stainier, 2004). It has also been established that the anterior endoderm is required for cardiac progenitor migration (reviewed in (Lough and Sugi, 2000). For example, mutation of many genes involved in endoderm differentiation and maturation, including *Gata4*, *Gata5*, *one-eyed pinhead* (*oep*), *casanova*, and *miles apart* result in cardia bifida (Kuo et al., 1997; Kupperman et al., 2000; Reiter et al., 1999; Stainier, 2001). Furthermore, studies have shown that proper myocardial differentiation is integral to the cardiac fusion process (Reiter et al., 1999; Yelon et al., 2000). In this dissertation I report an additional requirement for proper cardiac fusion: expression and function of the small heat shock protein, *Hsp27*.

Hsp27 is one of the most widely distributed and most studied of the small heat shock proteins (reviewed in Ferns et al., 2006). The small heat shock proteins (sHSP) are a ubiquitous family of molecular chaperones, consisting of ten members in humans (Kappe et al., 2003). Proteins in the sHSP family have molecular weights ranging from 16 to 25 kDa and generally consist of a conserved carboxy-terminal α-crystallin domain, a variable amino terminus and a short variable carboxy tail. Functionally, sHSPs have been demonstrated to be cytoprotective in response to cellular stress, and have been implicated in many cellular processes, including cytoskeletal dynamics and apoptosis. Furthermore, sHSP function has been implicated in a variety of human disease states, such as cataract, cancer, ischemic injury, myopathy, and neuropathy (reviewed in (Sun and MacRae, 2005). Changes in *Hsp27* expression have been observed in cells and tissues exposed to many stress conditions, including oxidative damage (Arrigo, 2001; Baek et al., 2000; Dalle-Donne et al., 2001; Escobedo et al., 2004; Huot et al., 1996; Komatsuda et al., 1999; Mehlen et al., 1995), metal

toxicity (Bonham et al., 2003; Leal et al., 2002; Somji et al., 1999), and ischemia (Hollander et al., 2004; Reynolds and Allen, 2003; Shelden et al., 2002; Vander Heide, 2002), as well as in disease states such as cardiac hypertrophy (Knowlton et al., 1998; Scheler et al., 1999), and muscle myopathies (Benndorf and Welsh, 2004). In addition, a role for HSP27 function has been implicated in many cellular processes, including protein chaperone activity (Jakob et al., 1993), regulation of cellular glutathione levels (Arrigo, 2001; Baek et al., 2000), apoptotic signaling (Bruey et al., 2000; Paul et al., 2002), inhibition of actin polymerization (Benndorf et al., 1994; Miron et al., 1991; Rahman et al., 1995), and stabilization of actin filament arrays (Huot et al., 1996; Lavoie et al., 1993a; Lavoie et al., 1993b; Lavoie et al., 1995). *Hsp27* has been shown to be expressed during both skeletal and cardiac muscle development in several organisms, including human (Shama et al., 1999), mouse (Gernold et al., 1993), pig (David et al., 2000) and zebrafish (Mao et al., 2005; Mao and Shelden, 2006). However, the biological significance of this developmentally regulated expression has not been analyzed in developing embryos. Furthermore, previous attempts to identify *Xenopus laevis* (*X. laevis*) orthologues of the *Hsp27* family have reportedly failed (Norris et al., 1997). In the present studies I report the sequence and expression of the *X. laevis* orthologue of *heat shock protein 27* (*XHsp27*). I demonstrate using anti-sense morpholinos that XHSP27 is required for proper fusion of cardiac precursors and for actin organization in developing cardiac and skeletal muscle. I further demonstrate that cardiac specification and differentiation appear unaltered as assayed by several markers of cardiac precursor and differentiated cardiomyocyte populations.

Figure 1.1. Diagram Depicting Cardiac Precursor Induction and Migration

(A) Blastula stage 10 embryo shown in cross section. Image on the left shows orientation and tissue domains of image on the right. Wnt and BMP inhibitors from Spemann organizer antagonize Wnt and BMP signals from ventral region. Cardiac precursors are specified in regions of Wnt signal inhibition and BMP signaling. (B) Neurulation stage 14 embryo shown laterally. Heart field precursors migrate anteriorly during this stage. (C) Early tailbud stage 26. Heart precursors migrate ventrally to fuse at the ventral midline.

Figure 1.1. Diagram Depicting Cardiac Precursor Induction and Migration

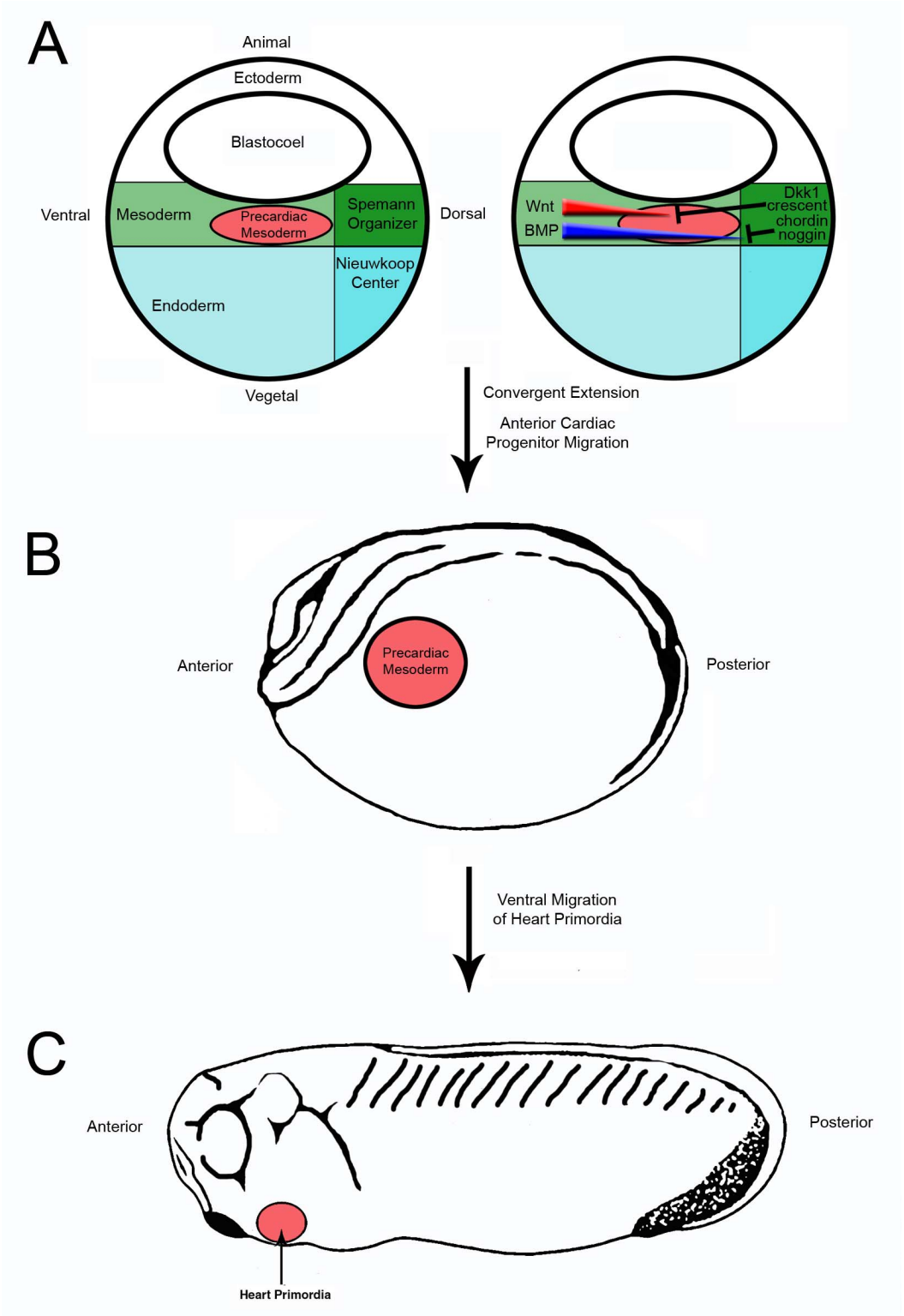

Figure 1.2. Diagram Depicting Cardiac Precursor Fusion

Diagram of transversely cross sectioned embryos at indicated stages. Heart precursors fuse at the midline, endocardium migrates dorsally and medially, and the endocardium is enveloped by differentiating myocardium.

Figure 1.2. Diagram Depicting Cardiac Precursor Fusion

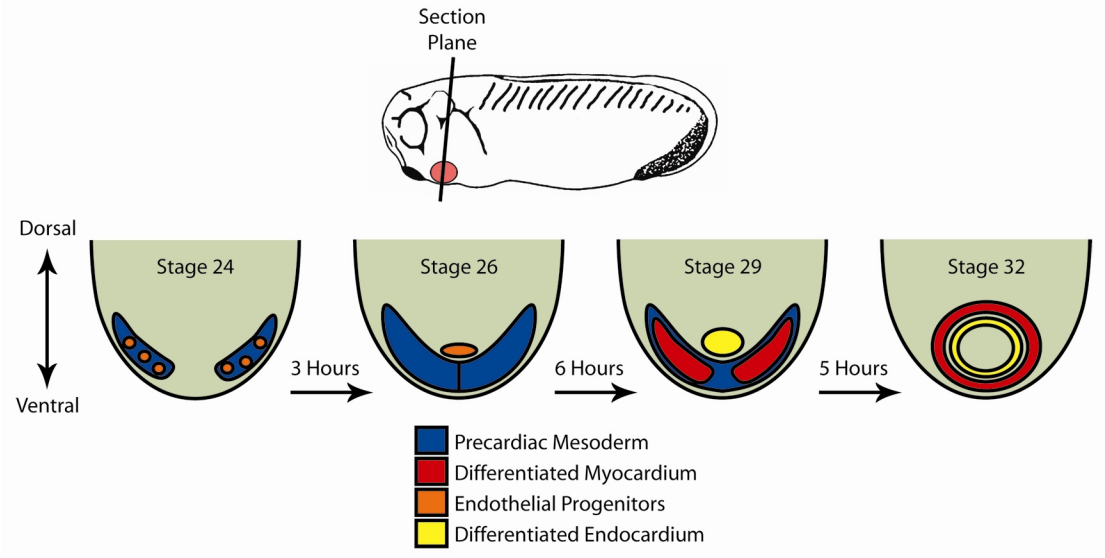

Figure 1.3. Diagram Depicting Cardiac Looping Morphogenesis

Lateral views of heart tubes from stage 29 through stage 38 embryos depicting rearrangement of the chamber regions in the developing heart. Blue arrows indicate inflow and red arrows indicate outflow.

Figure 1.3. Diagram Depicting Cardiac Looping Morphogenesis

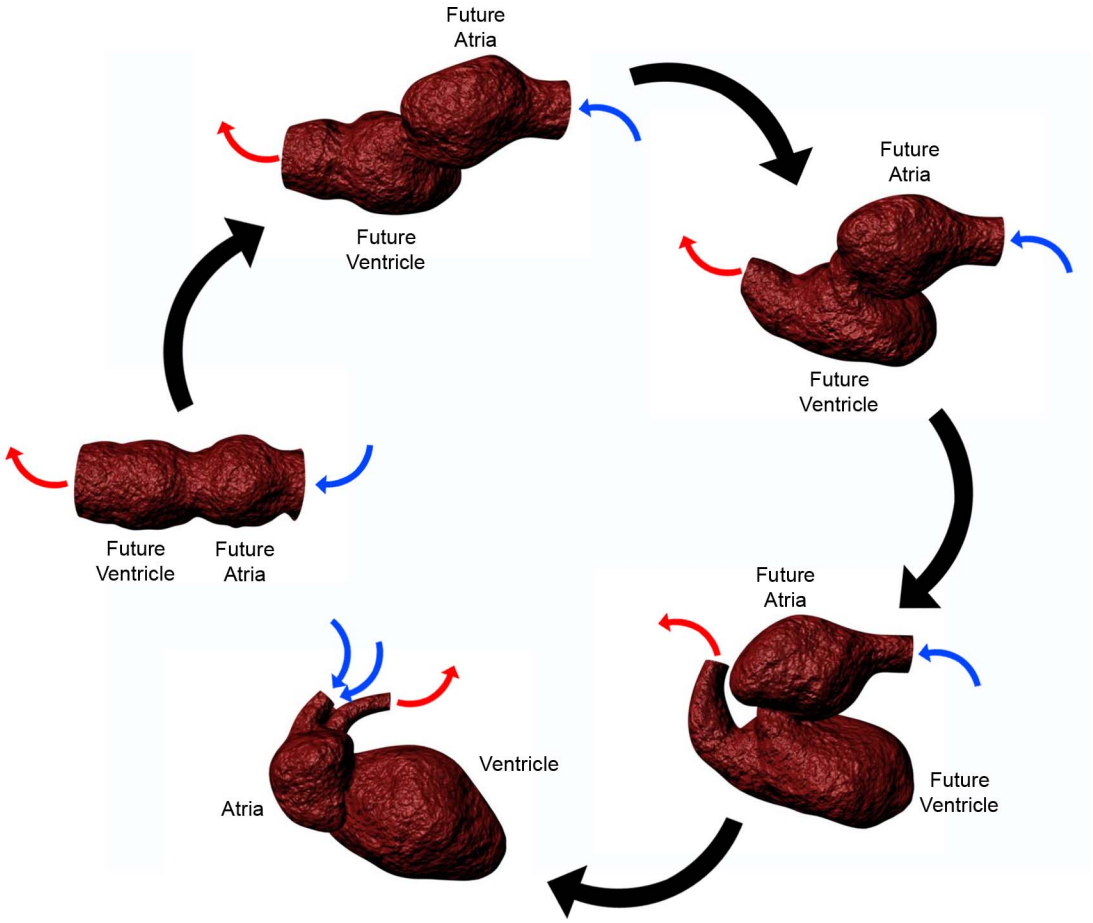

CHAPTER II

DEVELOPMENTAL EXPRESSION OF THE *XENOPUS LAEVIS TBX20* ORTHOLOGUE[1]

A. Introduction

The T-box family of transcription factors is a large family of proteins required for both early cell fate decisions, such as those necessary for formation of the basic vertebrate body plan, as well as for differentiation and organogenesis. The role of the T-box genes in these processes is emphasized by the observation that T-box genes when mutated give dramatic phenotypes in mouse and zebrafish. Furthermore, T-box genes are implicated in a number of human congenital malformations and are amplified in a subset of cancers (reviewed in Papaioannou, 2001; Smith, 1999; Wilson and Conlon, 2002). The T-box family has recently been shown to comprise approximately 0.1 % of genomes as diverse as *C. elegans* and human and have been identified in a wide variety of chordates from ctenophore to human while being completely absent in genomes from other phyla (*e.g. Arabidopsis thaliana*). For many of these genes clear homologues exist such as *Brachyury*, which displays a high degree of sequence similarity, expression pattern, and function between a variety of vertebrates including fish, frog, dog and mouse. However, other T-box genes appear to be unique to a particular species. For instance, *VegT*, a T-box gene thought to be

[1] This work was originally published in Brown, D. D., Binder, O., Pagratis, M., Parr, B. A. and Conlon, F. L. (2003). Developmental expression of the Xenopus laevis Tbx20 orthologue. *Dev Genes Evol* 212, 604-7..

required for endoderm formation in *Xenopus*, has no apparent homologue or orthologue in mouse or human (reviewed in Wilson and Conlon, 2002).

Two sets of clinical studies have provided direct evidence for a role for T-box genes in heart development and differentiation with *Tbx1* deleted in patients with the DiGeorge syndrome (Jerome and Papaioannou, 2001; Lindsey et al., 2001; Merscher et al., 2001), and *Tbx5* often mutated in patients with the congenital heart disease, Holt-Oram Syndrome (Basson et al., 1999; Li et al., 1997). In addition to *Tbx1* and *Tbx5*, recent studies in human, mouse, chick and zebrafish have implicated a third member of the T-box gene family, *Tbx12/20*, in heart development (Ahn et al., 2000; Carson et al., 2000; Griffin et al., 2000; Iio et al., 2001; Kraus et al., 2001; Meins et al., 2000). To further address the role of *Tbx20* in early heart development, I have identified and analyzed the expression of a *Tbx20* orthologue in *Xenopus laevis* (*X. laevis*).

B. Materials and Methods

Isolation of *Tbx20* cDNA

Degenerate primers were designed based on *Drosophila* H15 and *C. elegans* Tbx12 sequences (Agulnik et al., 1997; Brook and Cohen, 1996a). RT-PCR was performed using these primers on stage 36 *X. laevis* RNA. Additional *X. laevis* sequence was obtained by a second round of amplification using primers derived from mouse, human, and zebrafish *Tbx20* sequences (Ahn et al., 2000; Carson et al., 2000; Griffin et al., 2000; Meins et al., 2000). This 928bp clone was used to screen a cDNA mixed stage (19-26) *X. laevis* cDNA library (generous gift of Aaron Zorn) by PCR. Partial sequencing and restriction mapping

were used to construct a full-length copy of the gene by cloning overlapping fragments into pBluescript II KS (Stratagene).

Ribonuclease Protection Assay

To make the RNase probe, the 3-prime end of *Tbx20* was subcloned into pGEM-4Z (Promega). This probe does not contain sequences within the putative T-box domain and is assumed to be *Tbx20*-specific. *Ornithine decarboxylase* (*ODC)* was used as an internal loading control and tRNA was used as a negative control (Isaacs et al., 1992). Briefly, the constructs were linearized and probe was synthesized using ^{32}P-UTP (PerkinElmer). Total RNA was isolated from staged embryos from early gastrula (stage 10) to early tadpole (stage 36) using TRIZOL reagent according to manufacturer (Invitrogen). Probe was hybridized to labeled RNA in 1X PIPES Buffer (Sigma) and 50% formamide (Sigma). Unprotected probe was degraded for 30 minutes at 37°C using 200 U RNase T1 (Ambion) in 0.1M Tris, pH 7.4 (Sigma), 0.05M EDTA (Sigma) and 0.3M NaCl (Sigma). Phenol/chloroform extracted probe was then run on 6% polyacrylamide gel and the dried gel was exposed to X-OMAT-AR film (Kodak).

Reverse Transcription Polymerase Chain Reaction

RNA was isolated from ten embryos per stage per condition using the RNeasy kit (Qiagen) according to the manufacturer's instructions. The resulting RNA was quantified using a UV spectrophotometer (Shimadzu UV-1601), and 100 ng of RNA for each reaction was used to synthesize cDNA with Superscript II reverse transcriptase (Invitrogen). Total

reaction volume for cDNA synthesis was 20 μl. Resulting cDNA (2 μl) was then used as template in PCR reactions with Taq polymerase.

Whole-mount RNA *in situ* hybridization

Whole-mount *in situ* hybridizations were performed as previously described (Harland 1991). *XTbx20* digoxigenin-labeled probes were synthesized using T7 RNA polymerase from pXTbx20Δ5'3' (the initially identified partial *Tbx20* cDNA clone) linearized with XhoI. Embryos were cleared using 2:1 benzyl benzoate/benzyl alcohol.

C. Results

XTbx20 Shares High Sequence Homology to *Tbx20* Orthologues

To isolate *X. laevis Tbx20*, we designed a set of degenerate primers based on the published *Drosophila* H15 and *C. elegans* Tbx12 sequences (Agulnik et al., 1997; Brook and Cohen, 1996a). These primers were used to isolate a clone from Stage 36 *X. laevis* RNA. Additional *X. laevis* sequence was obtained by a second round of amplification using primers derived from mouse, human, and zebrafish *Tbx20* sequences (Ahn et al., 2000; Carson et al., 2000; Griffin et al., 2000; Meins et al., 2000). This 928bp clone was in turn used to screen a cDNA mixed stage (19-26) *X. laevis* cDNA library (generous gift of Aaron Zorn) by PCR. Partial sequencing and restriction mapping were used to construct a full-length copy of the gene by cloning overlapping fragments into pBluescript II KS (Stratagene). The clone was sequenced from both ends with a minimum of 4-fold coverage and shown to contain a 1741bp insert with an open reading frame of 441 amino acids (GenBank Accession number: AY154394; Fig. 2.1A). Sequence analysis revealed the clone to have 84% identity with

human *Tbx20* (Meins et al., 2000), 90% with mouse *Tbx12/20* (Carson et al., 2000; Kraus et al., 2001), and 91% to chicken *Tbx20* (Fig. 2.1B; Iio et al., 2001; Showell et al., 2004). Based on sequence (Fig. 2.1), expression analysis (Fig 2.2, 2.3), and current T-box nomenclature, we refer to this gene as the *X. laevis* orthologue of *Tbx20*.

XTbx20 Expression is Developmentally Regulated in Heart, Brain, Eye, and Cement Gland

I determined the onset and relative levels of *Tbx20* during *X. laevis* development by RNase protection analysis using a probe derived from the 3-prime end of *Tbx20* on staged embryos from early gastrula (stage 10) to early tadpole (stage 36; Fig. 2.2). This probe does not contain sequences within the putative T-box domain and therefore is assumed to be *Tbx20* specific. *Ornithine decarboxylase* (*ODC)* was used as an internal loading control and tRNA was used as a negative control. *Tbx20* transcripts are first detected at low but consistent levels by early neural stage (stage 16) with expression then increasing by stage 19 and remaining relatively constant until a sharp drop off at later neurula stages (stages 23 to 28). However, there is a sharp increase in expression between early (stage 30) and mid-tadpole stages (stage 36; Fig. 2.2). RT-PCR analysis shows no maternal expression as judged in unfertilized eggs and early gastrula embryos (stage 10).

To determine the spatial pattern of expression I performed whole mount *in situ* hybridizations on staged *X. laevis* from early gastrula (stage 10) to mid-tadpole (stage 40). Consistent with RNase protection and RT-PCR analysis, we first detect *Tbx20* expression by *in situ* hybridization at late gastrula stages in the region of the most anterior developing cement gland (stage 13; Fig. 2.3A) and at slightly later stages, in the heart field (stage 16;

Fig. 2.3B). *Tbx20* is expressed in the heart field before fusion of the primordium along the ventral midline. Thus, together with *Tbx5* (Horb and Thomsen, 1999) and the *Nkx* paralogues (Newman, 1998), *Tbx20* is one of the earliest markers of *X. laevis* cardiac tissue. Expression of *Tbx20* in the heart gradually increases during development (compare Fig. 2.3B with Fig. 3D) and by mid-tadpole (stage 35), expression is found throughout the cardiac region (Fig. 2.3E, F, I, K) including the atrial and ventricular tissue, the inflow and outflow tract, and the septum transversum (Fig. 2.3F), while being completely absent from more posterior tissues such as the liver (Fig. 2.3C-E, I). In addition, *Tbx20* is expressed in both tissue layers of the heart, with relatively high levels in the myocardial layer and lower levels in the endocardial layer (Fig. 2.3K). Therefore, *Tbx20* is expressed at the same time and in many regions of the heart that also express the heart markers *Tbx5* and *Nkx2.5* (Horb and Thomsen, 1999; Tonissen et al., 1994).

In the cement gland, the most anterior neural ectodermal tissue, *Tbx20* is gradually restricted to the ventral half of the gland by stage 27 (Fig. 2.3C), and expression decreases during neurula and early tadpole stages (Fig. 2.3E, I) such that by stage 40, *Tbx20* can no longer be detected in the tissue. In addition to the cement gland and heart, high levels of *Tbx20* expression are found in the external jugular vein, the lung bud (Fig. 2.3F), and the cloacal aperture (Fig. 2.3H) and very low levels in the retina and transient low levels in the notochord (Fig. 2.3E). Similar to reports in mouse, chick, and zebrafish (Ahn et al., 2000; Carson et al., 2000; Iio et al., 2001; Kraus et al., 2001), we also observe expression in rhombomeres 2, 4, 6, and 8 (Fig. 2.3E-G, I), and as shown by transverse and parasagittal sections through stage 35 embryos, in a subset of motor neurons emerging from these rhombomeres (Fig. 2.3I, J, L). However, in contrast to the mouse, we never detect *Tbx20*

expression in the liver (Fig. 2.3C-E, I; (Kraus et al., 2001). Therefore, although *Tbx20* displays a very high degree of sequence conservation across species, only a subset of tissues, such as the rhombomeres, show a conservation of expression, while other sites of expression appear to be unique to *X. laevis*, such as the lung bud and jugular vein.

D. Discussion

In this study I have successfully isolated the *X. laevis* orthologue of *Tbx20.* Protein sequence analysis reveals that *XTbx20* shares high homologies with other known orthologues of *Tbx20*, ranging from 84% to 91% identity . Furthermore, I have demonstrated that expression of *XTbx20* during embryogenesis appears to be highly conserved between *X. laevis* and other vertebrates. Expression analysis reveals that *XTbx20* is expressed throughout the developing heart and throughout the entire course of cardiogenesis. In addition *XTbx20* mRNA can be detected in domains within specific rhombomeres in the hindbrain, in the eye, in the cement gland, and in the peri-anal region. Considering the very high sequence homology as well as conservation in expression between *XTbx20* and its homologues, these data suggest that the function of *XTbx20* is likely conserved as well. Furthermore, the high degree of conservation suggests that whatever roles *XTbx20* plays in embryogenesis are possibly integral to proper morphogenesis. *XTbx20* expression within cardiac precursors begins during early stages of precursor migration, prior to fusion at the midline. These data suggest that *XTbx20* may be involved in specification or differentiation of these precursors. These observations further implicate *Tbx20* as a potential candidate in leading to human congenital disorders when mutated.

Figure 2.1. *X. laevis Tbx20* is highly homologous to other *Tbx20* family members

(A, B) Comparative sequence analysis of *Tbx20*. Analysis was performed with the GeneDoc program. (A) Alignment of vertebrate *Tbx20* proteins. Fully conserved amino acids including those containing conservative substitutions are shaded in dark gray. Lighter shading represents lower conservation. The conserved T-box domain is underlined in black. (B) Vertebrate *Tbx20* amino acid conservation. The percentage of identical amino acid residues (identity) and the percentage of conservative substitutions and identical residues (similarity) are given for comparison between *Tbx20* proteins.

Figure 2.1. *X. laevis Tbx20* is highly homologous to other *Tbx20* family members

A.

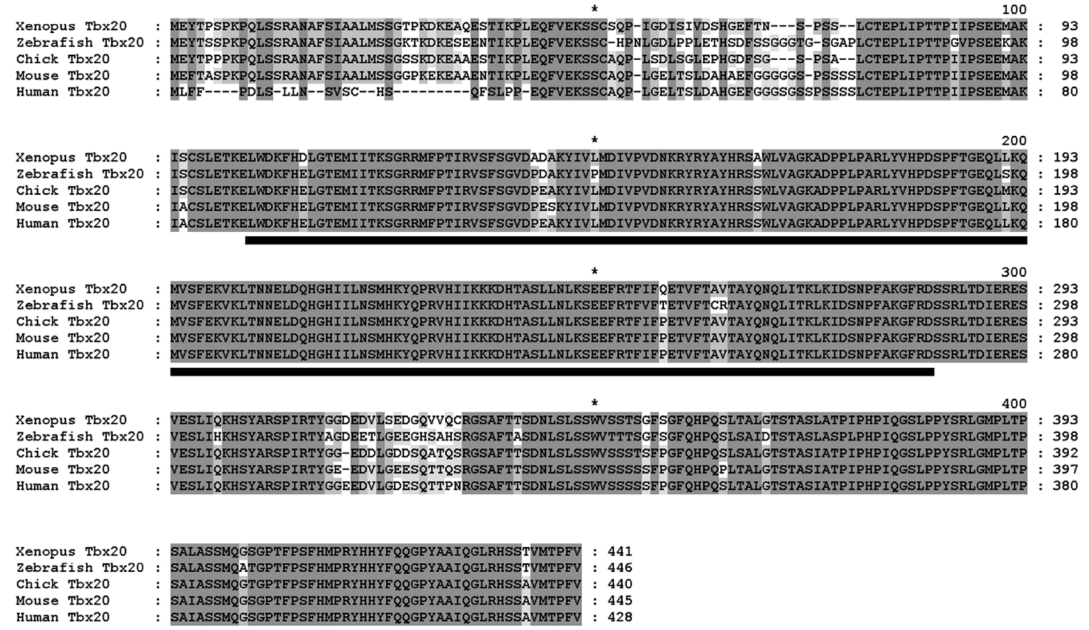

B.

		hTbx20	mTbx20	cTbx20	zTbx20
% Identity	**xTbx20**	84	90	91	85
% Similarity		89	94	95	92
% Identity	**zTbx20**	79	85	85	
% Similarity		86	92	91	
% Identity	**cTbx20**	86	92		
% Similarity		90	95		
% Identity	**mTbx20**	90			
% Similarity		92			

Figure 2.2. Expression of *Tbx20* is temporally regulated during embryogenesis.

Temporal expression of *X. laevis Tbx20* as detected by RNase Protection Assay. *ODC* is included in the lower panel as an internal loading control.

Figure 2.2. Expression of *Tbx20* is temporally regulated during embryogenesis.

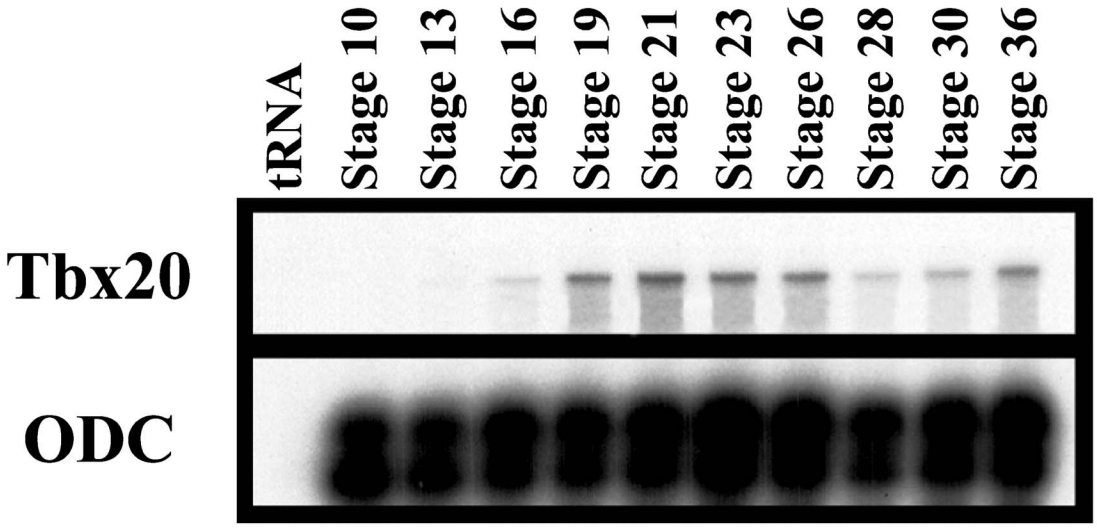

Figure 2.3. *Tbx20* is expressed in the developing heart, eye, cement gland, and hindbrain

(A-L) Expression of *Tbx20* during *Xenopus laevis* development as detected by whole mount *in situ* hybridization. (A) Anterior view of a stage 13 embryo. Dorsal side is facing up. (B) Anterior view of a stage 16 embryo. Dorsal side is facing up. (C) Ventral view of the anterior portion of a stage 27 embryo. (D) Ventral view of the anterior portion of a stage 32 embryo. (E) Lateral view of the anterior portion of a stage 35 embryo. (F) Higher magnification of (E). (G) Dorsolateral view of a stage 35 embryo. (H) Ventral view of the posterior portion of a stage 27 embryo. (I-L) Sections of stage 35 embryos. (I) Anterior view of a parasagittal section. (J) Transverse section through the anterior region. (K, L) Higher magnifications of (J). *ca* cloacal aperture, *cg* cement gland, *e* endocardium, *ey* eye, *h* heart, *hb* hindbrain, *hp* heart primordium, *it* inflow tract, *jv* jugular vein, *l* liver, *lb* lung bud, *m* myocardium, *mn* motor neuron, *nch* notochord, *ot* outflow tract, *st* septum transversum, *R2-R8* rhombomeres 2, 4, 6, and 8.

Figure 2.3. *Tbx20* is expressed in the developing heart, eye, cement gland, and hindbrain

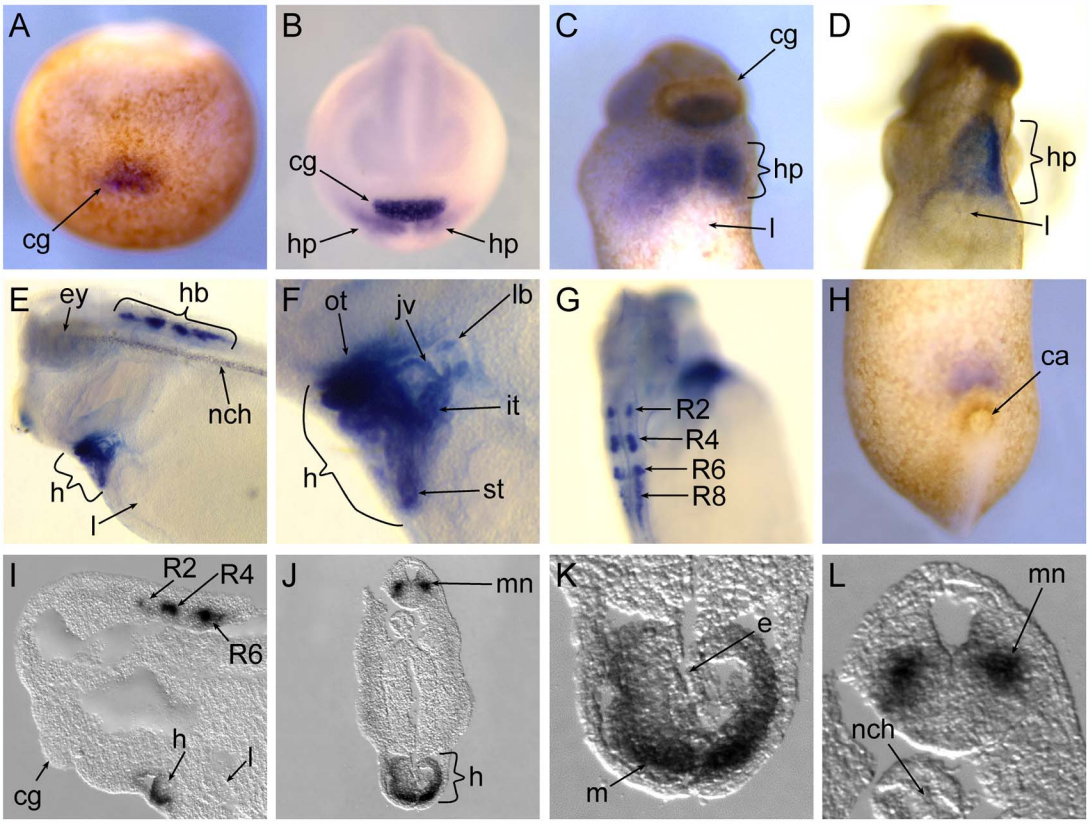

CHAPTER III

TBX5 AND *TBX20* ACT SYNERGISTICALLY TO CONTROL VERTEBRATE HEART MORPHOGENESIS[2]

A. Introduction

The vertebrate heart constitutes the earliest functional organ in the developing embryo and about 1% of all live births exhibit congenital heart disease (Hoffman, 1995a; Hoffman, 1995b; Payne et al., 1995). It is becoming increasingly clear that a complex molecular regulatory network is required to initiate and complete the formation of a functional heart. The proteins implicated in this process include a number of transcription factors from a range of transcription factor families, including the T-box, basic helix-loop-helix homeodomain, zinc finger, and MADS domain families (Cripps and Olson, 2002; Harvey, 2002; Zaffran and Frasch, 2002).

The T-box family of transcription factors is a large family of proteins involved in determining early cell fate decisions and controlling differentiation and organogenesis. Two sets of clinical data have provided direct evidence for the involvement of T-box genes in human heart development (Packham and Brook, 2003; Ryan and Chin, 2003). Deletions of *Tbx1* have been found in patients with DiGeorge syndrome (Baldini, 2004; Chieffo et al., 1997; Jerome and Papaioannou, 2001; Lindsey et al., 2001; Merscher et al., 2001; Yagi et al.,

[2] This work was originally published in Brown, D. D., Martz, S. N., Binder, O., Goetz, S. C., Price, B. M. J., Smith, J. C. and Conlon, F. L. (2005). Tbx5 and Tbx20 act synergistically to control vertebrate heart morphogenesis. *Development* 132, 553-563.

2003), and mutations in *Tbx5* are associated with Holt-Oram Syndrome (HOS), a congenital heart disease characterized by defects in heart formation and upper limb development (Basson et al., 1997; Li et al., 1997). Clinical studies of HOS patients have demonstrated a fundamental role for *Tbx5* in heart development. HOS is a highly penetrant autosomal dominant condition associated with skeletal and cardiac malformations (Newbury-Ecob et al., 1996). Patients with HOS often carry mutations within the coding region of the T-box transcription factor *Tbx5* (Basson et al., 1997; Basson et al., 1999; Benson et al., 1996; Li et al., 1997). The role of *Tbx5* in heart development, and in the HOS disease state, is further supported by recent gene-targeting experiments in mouse. These studies demonstrate that mice heterozygous for mutations in *Tbx5* display many of the phenotypic abnormalities of HOS patients (Bruneau et al., 2001) and show that TBX5 is required for growth and differentiation of the left ventricle and atria as well as for proper development of the cardiac conduction system (Moskowitz et al., 2004). Similar defects are seen in the zebrafish *Tbx5* mutant *heartstrings*, suggesting that the expression and function of TBX5 is conserved throughout vertebrate evolution (Garrity et al., 2002).

Previously, I described the cloning and expression of the *Xenopus laevis* (*X. laevis*) *Tbx20* orthologue, *Tbx20* (Chapter II; Brown et al., 2003). Studies of *Tbx20* have demonstrated that along with *Tbx5*, *Tbx20* is one of the first genes expressed in the vertebrate cardiac lineage. Moreover, *Tbx20* is expressed at the same time and in many of the same regions of the heart that also express the heart markers *Tbx5*, *Nkx2-5*, and *Gata4* (Horb and Thomsen, 1999; Laverriere et al., 1994; Serbedzija et al., 1998; Tonissen et al., 1994).

Despite our knowledge of the expression pattern of *Tbx20*, little is known of *Tbx20* function in heart development. In the zebrafish, it has recently been observed that eliminating

endogenous TBX20 (HrT) via morpholinos leads to cardiac defects (Szeto et al., 2002). Specifically, TBX20 knockdown in zebrafish leads to dysmorphic hearts and a loss of blood circulation. The morphological defects are not apparent until the cardiac looping stage, despite high levels of *Tbx20* during the earlier stages of specification and development suggesting that other T-box genes may act redundantly with *Tbx20* during early heart development.

In this study I investigate the cellular and molecular relationship between *Tbx5* and *Tbx20* in *X. laevis*. I show that the phenotypes of knocking down TBX5 and TBX20 are highly similar, with embryos derived from either *Tbx5* or *Tbx20* morpholino injections displaying profound morphological defects including pericardial edema, reduced cardiac mass, and loss of circulation. In addition, I show that the morphological phenotype is not a reflection of alterations in the specification, commitment, or differentiation of cardiac tissue. Thus, in addition to sharing a number of molecular properties, I show that *Tbx5* and *Tbx20* function in a non-redundant fashion and are essential for cardiac morphogenesis. However, despite the similarities in phenotype and shared molecular properties, *Tbx5* and *Tbx20* also have independent roles in heart development.

Given the similarity in TBX5 and TBX20 morphant phenotypes, I investigated the pathways by which *Tbx5* and *Tbx20* function. I show that TBX5 and TBX20 do not function in a linear pathway (i.e. *Tbx20* does not act downstream of *Tbx5*, and vice versa), but rather imply a synergistic role for these two proteins during early heart development. Consistent with this proposal, I show that TBX5 and TBX20 can physically interact, map the interaction domains, and show an interaction for the two proteins in cardiac development, therefore providing the first evidence for interaction between members of the T-box gene family.

B. Materials and Methods

DNA Constructs

To construct pXTbx20-V5-His the coding region of *XTbx20* minus the stop site was PCR-amplified from pXTbx20-Full-length using sequence-specific primers (XTbx20-Forward - 5' CCCAAGCTTGGGATGGAATACACTCCTTCT 3', XTbx20-reverse - 5' CCGCTCGAGCGGTACAAATGGTGTCATCAC 3'). The forward primer contained a flanking HindIII site and the reverse primer contained a flanking XhoI site for other cloning purposes. The resulting PCR product was then TA-cloned into pcDNA3.1/V5-His TOPO TA (Invitrogen) in-frame with the V5 epitope. pXTbx20Δ5'3' is the original partial XTbx20 clone containing a 928 bp *XTbx20* fragment (nt 627-1554 of full-length cDNA) encompassing most of the T-Box and the 3' end and lacking most of the 5' and part of the 3' end (Brown et al., 2003). The pXTbx20-Full-length construct is our original full length *XTbx20* cDNA construct (Brown et al., 2003). *XANF* was generously provided by Paul Krieg (Small and Krieg, 2000). The *cardiac troponin I* pXTnIc plasmid was generously provided by Tim Mohun (Logan and Mohun, 1993). pXTbx5 contains the full-length coding region of *XTbx5* cloned into pBLUESCRIPT II KS+ with HindIII and NotI (Frank Conlon). Sequence analysis revealed that the clone shows extensive homology to a partial sequence of the second *X. laevis* allele of *Nkx2-5* (accession AF283102). The clone is predicted to be full-length and *in vitro* translation of the protein gave a band of the correct size. The clone is referred to as pCRNkx-2.5B (accession number AY644403). To construct the pBS-*Nkx2-5* hybridization probe, *Nkx2-5* was subcloned into pBLUESCRIPT II KS+.

Transient Transfections

293T cells were plated at 1 X 10^6 cells/well in six-well tissue culture plates 24 hours prior to transfection. Plasmids used in transients are: the *Nppa* promoter-luciferase reporter (Bruneau et al., 2001), p*Tbx5*-V5, p*Tbx20*-V5, pCMV-*LacZ*; pBS/KS. The amount of luciferase reporter plasmid DNA was kept constant at 100 ng for *Tbx5*, while titering in *Tbx20* (25 ng-100 ng). Expression vector plasmid DNA was kept constant at 100 ng total and 50 ng of *LacZ* reporter plasmid was used. Total amount of DNA was kept constant at 2 µg and transfected using Lipofectamine 2000 (Invitrogen). Plasmid DNA was diluted in OPTI-MEM (GibcoBRL) and complexes were allowed to form for 25 minutes at RT and added to each well. 48 hours post-transfection, cells were harvested using M-PER (Pierce) with gentle shaking. Luciferase activity was normalized to ß-galactosidase activity. All assays were done three independent times in triplicate. Results were graphed using normalized Relative Luciferase Units (RLUs).

Nuclear Localization

NIH/3T3 cells were seeded in chamber slides at 6 x 10^3 cells/chamber 24 hours prior to transfection. Cells were transfected with 187.5 ng p*Tbx20*-V5 or p*Tbx5*-V5 per chamber using 1.25 µl Polyfect (QIAgen) transfection reagent according to manufacturer's protocol. At 48 hours, cells were washed twice with PBS and fixed in MEMFA for 1 hour (2 ml 10X MEM, 2 ml Formaldehyde, 16 ml H_2O) at 4°C. Cells were washed twice with PBST (PBS + 0.1% Triton), blocked in PBST + 10% Fetal Bovine Serum for 1 hour at 4°C, incubated at 4°C overnight with anti-V5 (Invitrogen) diluted 1:1000 in PBST+Serum. Cells were washed three times, blocked for 1 hour, then incubated for 1 hour at RT with goat anti-mouse Cy2

(Jackson ImmunoResearch) diluted 1:200 in PBST+Serum. This process was repeated using anti-phosphotyrosine (Upstate Biotechnology) as 1° antibody to visualize the cytoplasmic compartment and goat anti-mouse Cy3 (Jackson ImmunoResearch) 2° antibody. Cells were washed three times, cover-slipped and analyzed by confocal microscopy on a Zeiss LSM 410.

Embryo Injections

Preparation and injection of *X. laevis* embryos was carried out as previously described (Wilson and Hemmati-Brivanlou, 1995). Embryos were staged according to Nieuwkoop and Faber (Nieuwkoop and Faber, 1967). Two antisense morpholino oligonucleotides each were designed against the *Tbx5* and *Tbx20* 5' UTRs and start sites. Morpholinos were obtained from Gene Tools, LLC. with the following sequences: *Tbx20*-MO1, 5' AAT CCA CTT CCA AGG GCA GTT GCT T 3'; *Tbx20*-MO2, 5' GTT TGG GAG AAG GAG TGT ATT CCA T 3'; *Tbx5*-MO1, 5' TTA GGA AAG TGT CTC TGG TGT TGC C 3'; *Tbx5*-MO2, 5' CAT AAG CCT CCT CTG TGT CCG CCA T 3'; Control MO, 5' CCT CTT ACC TCA GTT ACA ATT TAT A 3'. The human ß-globin splice-mutant standard control morpholino from Gene Tools was used as control. Equal amounts of both *Tbx5* morpholinos were used in all injections. This combination is referred to in the text and figures as "TBX5MO". *Tbx20* morpholinos were also injected in combination, and referred to as "TBX20MO". TBX5MO was injected at the optimal (40 ng) or suboptimal (20 ng) doses, and TBX20MO was injected at the optimal (80 ng) or suboptimal (40 ng) doses. "Optimal dose" is defined as the dose empirically found to be efficient at blocking protein translation both *in vitro* and *in vivo*, and inducing a cardiac phenotype in nearly 100% of

injected embryos, while "suboptimal dose" refers to the dose empirically found to be below the threshold of the full cardiac phenotype-inducing dose.

Whole-mount RNA *in situ* hybridization

Whole-mount *in situ* hybridizations were performed as previously described (Harland 1991). *XANF* digoxigenin-labeled probes were synthesized using T7 RNA polymerase from pXANF linearized with BamHI (Small and Krieg, 2000). *XTbx5* digoxigenin-labeled probes were synthesized using T7 RNA polymerase from pXTbx5 linearized with HindIII. *XNkx2.5* digoxigenin-labeled probes were synthesized using T7 RNA polymerase from pXNkx2.5 linearized with XhoI (Tonissen et al., 1994). *XTbx20* digoxigenin-labeled probes were synthesized using T7 RNA polymerase from pXTbx20Δ5'3' linearized with XhoI. To make the *cardiac troponin I* probe pXTnIc was cut with Not1 and anti-sense digoxigenin-labeled probe was synthesized using T7 RNA polymerase. Embryos were cleared using 2:1 benzyl benzoate/benzyl alcohol.

Immunohistochemistry

Embryos were collected and fixed for 2 hours at 4 ºC in 4% paraformaldehyde and rinsed in PBS, incubated overnight in 30% sucrose in PBS at 4 ºC, mounted in OCT cryosectioning medium (Tissue Tek) and snap frozen. Cryostat sections (14 μm) sections were rinsed with wash buffer (PBS, 1% Triton, 1% serum), incubated at 4°C overnight with anti-tropomyosin (1:50; Developmental Studies Hybridoma Bank) (Kolker et al., 2000), and phalloidin conjugated to Alexa 488 flourophore (Molecular Probes). Sections were then rinsed with wash buffer and incubated with anti-mouse Cy3-conjugated secondary antibody

(1:200), (Sigma). Sections were rinsed and incubated for 20 minutes at RT with DAPI, cover slipped and visualized on a Zeiss LSM410 confocal microscope.

Translation Inhibition by Morpholinos

In vitro translations were performed using TNT® Coupled Reticulocyte Lysate System (Promega) following the manufacturer's protocol. We have recently demonstrated that *X. laevis* SHP-2 is uniformly expressed throughout early development (Y. Langdon and FLC, unpublished data) and anti-PTP1D/SHP2 1° antibody was used at 1:2500 (Transduction Laboratories) as a loading control with peroxidase-conjugated AffiniPure donkey anti-mouse (H+L) 2° antibody (1:10,000). V5-tagged proteins were probed with anti-V5 1° antibody (Invitrogen) at 1:5000 dilution, and peroxidase-conjugated AffiniPure Donkey anti-mouse (H+L) 2° antibody (Jackson ImmunoResearch Laboratories) at 1:10,000 dilution. For *in vivo* translation analyses, embryos were injected with MOs and mRNA at the one-cell stage and animal caps cut at stage 8. At sibling stage 10, and 10 animal caps per treatment were collected and lysed in 100 µl of lysis buffer: 200 mM NaCl, 20 mM NaF, 50 mM Tris pH 7.5, 5 mM EDTA, 1% IGEPAL, 1% Triton X-100 (Sigma), Complete EDTA-free Protease Inhibitor (Roche). Lysates were resolved on 12% SDS-PAGE gels, and visualization was carried out using Western Lightning Chemiluminescence Reagent Plus (PerkinElmer Life Sciences, Inc.).

Benzidine Staining

Erythrocytes were detected using a modified version of the benzidine histochemical staining method (Hemmati Brivanlou and Thomsen, 1995; Orkin et al., 1975). Briefly,

embryos were fixed at stage 43 in 12% glacial acetic acid and 4% benzidine (Sigma) for 5 minutes and stained with the addition of 0.3% hydrogen peroxide. The staining reaction was allowed to proceed for 10 minutes at RT. The embryos were washed with 12% glacial acetic acid three times, fixed for 1.5 hours in MEMFA, and cleared using 2:1 benzyl benzoate/benzyl alcohol.

Glutathione-S-Transferase Pulldown Assays

GST pulldown assays were performed using the MicroSpin GST Purification Module (Amersham Biosciences) according to the manufacturer's protocol. GST constructs were transformed into BL21-Gold (DE3) cells (Stratagene) for protein induction. Transformed cells were grown at 37°C to $O.D._{A600}$=0.8 and GST proteins were induced for 1.5 hours at 20-27°C with 1mM IPTG (Amersham Biosciences). Hemagglutinin (HA)-tagged putative interacting proteins were produced in 293T cells. Lysates were sonicated 3 times for 10 seconds prior to centrifugation at 12,000 rpm at 4°C for 10 minutes, and the supernatant was collected. GST-fusion protein lysates and putative interacting protein lysates were loaded on GST columns, incubated for 1.5 hours at 25°C, eluted, electrophoresed on a 12% SDS-PAGE gel, and transferred to PolyScreen PVDF Transfer Membranes. HA-tagged proteins were detected with mouse HA.11 primary antibody (1:1,000, Covance Research Products) and with peroxidase-conjugated AffiniPure donkey anti-mouse (H+L) secondary antibody (1:10,000). GST-fusion proteins were detected with rabbit anti-GST primary antibody (1:25,000, Sigma-Aldrich) and with Peroxidase-conjugated AffiniPure donkey anti-rabbit (H+L) secondary antibody (1:10,000, Jackson ImmunoResearch Laboratories).

C. Results

TBX5 and TBX20 are Required for Heart Morphogenesis

To analyze the requirement for *Tbx5* and *Tbx20* in cardiogenesis, antisense morpholinos were designed against the 5' UTRs and translational start sites of the respective cDNAs (Fig. 3.1A; Heasman et al., 2000). Due to the lack of antibodies against endogenous TBX5 or TBX20, I tested the efficiency and specificity of morpholino translation inhibition using V5 epitope-tagged versions of TBX5 and TBX20 both *in vitro* and *in vivo*. To this end, transcription/translation reactions were incubated with each cDNA construct alone and together with increasing concentrations of morpholinos (Fig. 3.1B, C). TBX20MO was included as control for TBX5MO and vice versa, and a ControlMO used for both. Results from these assays show that TBX5MO blocks translation of TBX5-V5 while TBX20MO and ControlMO do not. Similarly, TBX20MO blocks translation of TBX20-V5 *in vitro* (Fig. 3.1B, C).

To determine if TBX5MO and TBX20MO block translation *in vivo*, I injected *Tbx5-V5* or *Tbx20-V5* mRNA alone or in the presence of morpholinos into one-cell stage embryos. Animal caps were cut at stage 8 and allowed to develop to stage 10, at which point Western blot analyses were performed. Results from these studies demonstrate that in animal caps, TBX5MO blocks TBX5-V5 translation, while TBX20MO blocks TBX20-V5 translation (Fig. 3.1D, E). I have further shown via sequence alignments that *Tbx5* does not contain binding sites for the *Tbx20* morpholinos and vice versa (Fig. 3.2). I did note that the introduction of TBX20MO results in a slight decrease in TBX5 *in vivo*, and vice versa (see Discussion).

To address the question of whether *Tbx20* morpholinos can theoretically bind the *Tbx5* transcript or whether *Tbx5* MOs can bind the *Tbx20* transcript, I performed sequence alignments using the GeneDoc program. I could find no significant homology between either *Tbx5* MO and the *Tbx20* transcript or *Tbx20* MOs on the *Tbx5* transcript (Fig. 3.2). The alignments shown represent the best matches identified by the GeneDoc software, yet even these matches have a high degree of mismatch as well as gaps. Studies have shown that introducing as few as four mismatches into a morpholino can result in complete abrogation of the morpholino effects (Araki and Brand, 2001). Thus, the *in vitro* translation results, sequence alignments, and published data on morpholino efficacy suggest that our morpholinos do not cross react.

To determine the requirement of TBX5 and TBX20 in heart development, I injected TBX5MO, TBX20MO, or ControlMO into one-cell stage embryos. No significant differences are seen between TBX5 morphants, TBX20 morphants, control morphants, or uninjected siblings throughout gastrulation and neurulation stages. However, a slight delay in developmental stage is evident in TBX5 and TBX20 morphants relative to control morphants and uninjected embryos by neurulation stage, (~st. 16). By cardiac looping stages, (~st. 38) (Kolker et al., 2000; Mohun and Leong, 1999; Mohun, 2000; Newman and Krieg, 1999) a reduction in cardiac mass is evident in the morphants, and by stage 38 both morphants display grossly abnormal heart morphology (Fig. 3.3A- F). At this stage, 82% of TBX5 morphants and 100% of TBX20 morphants display prominent cardiac defects, as scored by the presence of an unlooped heart tube, a reduction in cardiac mass and the presence of a pericardial edema (Fig. 3.3G). After terminal cardiomyocyte differentiation has begun (~st. 45; Kolker et al., 2000; Mohun and Leong, 1999; Mohun, 2000; Newman and Krieg, 1999)

TBX5 and TBX20 morphants display dramatically smaller hearts and in many embryos cardiac tissue is barely detectable (Fig. 3.3E, F). However, the remaining cardiac tissue still retains some degree of contractility, but confined to a small patch of contractile tissue in the dorsal-most aspect of the cardiac cavity. Both TBX5 and TBX20 morphants also display abnormal eyes, which is consistent with studies showing the involvement of both genes in eye development (Carson et al., 2004; Koshiba-Takeuchi et al., 2000; Leconte et al., 2004). In addition, TBX20 morphants appear to be defective in motor function, as 100% of Tbx20 morpholino-injected embryos fail to exhibit swim reflexes in response to touch (data not shown). Embryos derived from injection of *Tbx20* morpholinos directed against the antisense transcript, *Tbx5* morpholinos containing mismatches, MOs directed against zebrafish *Tbx5* and Gene Tools, LLC's MO control, gave no observable phenotype at any concentration (data not shown). These observations, and the findings that the TBX5 and TBX20 protein levels can be reduced or eliminated both *in vitro* and *in vivo*, suggest that the phenotypes we observe are specific for knocking down TBX5 and TBX20.

Tbx20 is expressed in the developing outflow tract and dorsal aorta progenitors (Brown et al., 2003; Szeto et al., 2002). Furthermore, *Tbx5* is expressed in the developing common cardinal and hepatic veins (Fig. 3.4). Based on the expression of both genes in specific regions of the vasculature, I tested whether a loss of either protein results in loss of blood flow. Both TBX5 and TBX20 morphants display a lack of blood circulation at optimal morpholino doses (Fig. 3.5B, C), despite the retention of contractility in the cardiac tissue (data not shown). To examine blood flow in the double morphants I visualized the presence of blood using benzidine to detect hemoglobin. Similar to individual optimal injections, embryos coinjected with suboptimal doses of TBX5MO and TBX20MO exhibit a lack of

blood circulation despite the heart retaining contractility (Fig. 3.5D; data not shown). It should be noted that the heart defects become apparent well before the onset of circulation. Blood is still detected in these embryos, albeit at lower levels. Control embryos display prominent blood staining throughout the heart and vasculature, in contrast to TBX5, TBX20, and double morphants that do not show any blood staining in the heart. Furthermore, blood is seen to pool in the peri-anal region and gut region. The above results suggest that, in addition to the requirement for TBX5 and TBX20 individually in proper cardiogenesis and heart function, the combined activity of the two is also required for cardiac development, function, and blood circulation.

To further define the requirements for *Tbx5* and *Tbx20* during cardiogenesis, we carried out a detailed analysis of TBX5MO and TBX20MO derived hearts relative to those from ControlMO injections. For these analyses, staged-matched TBX5MO, TBX20MO, and ControlMO embryos were collected at stage 37, serial sectioned and stained for the terminal differentiation markers *tropomyosin* and *cardiac actin*, and counterstained with DAPI (Fig. 3.6). Results from this analysis clearly demonstrate that TBX5MO and TBX20MO derived hearts fail to undergo cardiac looping and chamber formation. In addition, quantification of total cardiac cell number by serial sectioning shows that both TBX5MO and TBX20MO hearts have a significant reduction in cell number compared to controls, and TBX20MO-derived hearts have a significantly fewer cardiomyocytes than those from TBX5MO (Fig. 3.6M).

In addition to these defects we note some unique features to both the TBX5MO and TBX20MO derived hearts, most notably TBX5MO hearts remain as an open cardiac trough (Mohun et al., 2000) throughout development and fail to form a cardiac tube (Fig. 3.6E-H).

In contrast, TBX20MO derived embryos form a cardiac tube; however, the lumen often collapses and the hearts concomitantly show a dramatic decrease in the presence of cardiac actin (Fig. 3.6I-L). We also note a decrease in *cardiac actin* in TBX20MO-derived hearts (Fig. 3.6L) compared to TBX5MO or control hearts (Fig. 3.6D, H). Together this data demonstrates a requirement for both *Tbx5* and *Tbx20* in normal heart morphogenesis, and implies that TBX5 cannot compensate for the loss of TBX20, nor can TBX20 compensate for the loss of TBX5 and suggests that *Tbx5* and *Tbx20* play non-redundant roles during normal heart development.

Analysis of hearts derived from TBX5MO and TBX20MO embryos shows a significant decrease in cardiac cell number. To determine if this is due to alterations in cardiac cell commitment, I performed whole-mount *in situ* hybridization with the early heart marker, *Nkx2.5* (Fig. 3.7). This analysis was carried out on staged matched embryos derived from TBX5MO, TBX20MO and ControlMO embryos over the period of cardiac cell commitment and migration and differentiation (stages 16-36). I could detect no obvious difference in the number or spatial distribution of *Nkx2.5*-expressing cells prior to stage 24 (Fig. 3.7). Consistent with initial analysis, after stage 24 the hearts from TBX5MO and TBX20MO embryos are morphologically abnormal and smaller in size, and therefore show a reduced domain of *Nkx2.5* expression.

The above results demonstrate that *Tbx5* and *Tbx20* are required for normal heart morphogenesis, but not for specification and migration of the cardiac precursors. To extend these findings, whole-mount *in situ* hybridizations were performed on stage 36 morphants and controls using the late heart markers *atrial natriuretic factor* (*XANF*; Small and Krieg, 2000) and *cardiac troponin I* (*XTnIc*; Drysdale et al., 1994). As shown in Fig. 3.8, the

terminally differentiated cardiomyocyte marker *XTnIc* displays properly localized expression in the cardiac tissue of morphant embryos and appears to be expressed to the same degree, although due to the reduced cardiac mass it is expressed in fewer cells (Fig. 3.8D-F). *XANF* is a putative target of *Tbx5*, and its expression is reduced in the absence of *Tbx5* in mice (Bruneau et al., 2001). In agreement with these findings, I show that *Xenopus* TBX5 activates transcription of a rat *Nppa/ANF* reporter plasmid (Fig. 3.10) and consistent with TBX5MO blocking TBX5, *XANF* expression is either greatly reduced or absent in TBX5 morphants, however, *XANF* is still detected in TBX20 morphants (Fig. 3.8A-C). These results indicate that terminal differentiation still occurs in both TBX5 and TBX20 morphant embryos and implies that *XANF* is an evolutionarily conserved target of TBX5.

Tbx5 and *Tbx20* are Not Dependent on Each Other's Expression

Since *Tbx5* and *Tbx20* are co-expressed within the heart and have similar requirements in heart development, I next asked whether *Tbx5* and *Tbx20* function linearly within the same molecular pathway. To address this question, I analyzed the expression of *Tbx20* in TBX5MO-injected embryos and *Tbx5* expression in TBX20MO-injected embryos. I could detect no differences in the expression of either gene in morpholino-injected embryos (Fig. 3.9); both genes remain expressed in the forming heart tissue, despite the reduction of cardiac tissue mass in morpholino-injected embryos. Based on these results we conclude TBX5 is not essential for *Tbx20* expression, nor is *Tbx20* dependent on TBX5.

TBX5 affects TBX20 transcriptional activity

My results strongly suggest that *Tbx5* and *Tbx20* do not function linearly within the same pathway yet have a similar requirement in heart development. We therefore carried out a series of experiments to test if TBX5 and TBX20 have either competing or complimentary functions at the molecular level. We first tested the cellular localization of TBX5 and TBX20. For these studies V5 epitope-tagged versions of the full-length cDNAs were transfected into NIH/3T3 cells. Immunohistochemistry on the transfected cells show that similar to TBX5 (Collavoli et al., 2003; Fan et al., 2003; Zaragoza et al., 2004), TBX20 is localized exclusively to the nucleus. (Fig. 3.10C-H)

We next tested if TBX5 and TBX20 can function to regulate the levels of transcription of the TBX5 target gene *Nppa/ANF*. To test for DNA specific binding and transcriptional activities, we transfected in full-length versions of *Tbx5* and *Tbx20*, either alone or in combination, with the putative *Tbx5* target *Nppa/ANF* reporter construct into 293T cells. Consistent with studies using the mouse *Tbx5* orthologue (Bruneau et al., 2001; Hiroi et al., 2001), TBX5 can weakly activate the rat *Nppa/ANF* reporter. In contrast, *Tbx20* alone can activate the *Nppa/ANF* in a dose dependent fashion. However, in the presence of TBX5, TBX20 can have the converse effect on the *Nppa/ANF* reporter. In the presence of TBX5, at high and low doses of TBX20 there is increased activation of the reporter construct, while at moderate doses there is a repressive effect (Fig. 3.10I). Thus, the presence of TBX5 appears to alter TBX20 transcriptional activity.

TBX5 and TBX20 physically interact with one another

Given the similarity in phenotypes of TBX5 and TBX20 morphant embryos, and the observation that *Tbx5* and *Tbx20* are not dependent on one another's expression, I next assessed whether TBX5 and TBX20 can physically interact. TBX5 fused to Glutathione-S-Transferase (GST) was incubated with HA-tagged TBX20 or NKX2-5. Pulldown experiments were then performed to assess whether TBX20 can bind to TBX5. NKX2-5 has been shown to interact with TBX5 and thus serves as a positive control (Bruneau et al., 2001; Hiroi et al., 2001). As shown in Fig. 3.11A, bacterially translated GST-TBX5 is able to bind HA-TBX20 and HA-NKX2-5 produced from 293T cells, in contrast to GST alone, which does not bind either protein. These results reveal that TBX5 and TBX20 can interact *in vitro*. This is the first report of physical interaction between T-box proteins.

Having demonstrated that TBX5 and TBX20 interact, I next mapped the interaction domains of TBX5 and TBX20. To this end, I constructed a deletion series of both GST-tagged TBX5 and HA-tagged TBX20. As shown in Fig. 3.11B, GST-TBX5 proteins lacking the C-terminus still bind HA-TBX20, however when the small N-terminus and T-box domain are removed from GST-TBX5, HA-TBX20 fails to bind. Thus, the domain responsible for TBX20 binding lies within the N-terminus and T-domain of TBX5. Similarly, a C-terminal deletion of HA-TBX20 still binds to GST-TBX5, in contrast to deletions of the HA-TBX20 N-terminus and T-domain (Fig. 3.11C). As seen in the ΔN/C lane in Fig. 3.11E, the HA-TBX20 deletion containing only the T-box domain did not bind GST-TBX5. However, we were unable to obtain comparable amounts of the HA-T20-ΔN/C protein, as seen in the input lane. This could be due to mRNA or protein instability. In an attempt to circumvent this problem, the amount of HA-T20-ΔN/C protein incubated with GST-TBX5 was increased 2-

fold as compared to the rest of the experiments. These results indicate that the N-terminus and possibly the T-domain of TBX20 are required for its interaction with TBX5, although we cannot rule out the possibility that the amount of HA-T20-ΔN/C protein was insufficient to identify a requirement for the T-domain. In summary, my results reveal that the domains responsible for the interaction between TBX20 and TBX5 map to within the N-terminal and T-box domains in both proteins.

Tbx5 and *Tbx20* cooperate to regulate heart morphogenesis

Given that TBX5 and TBX20 physically interact with one another, I hypothesized that *Tbx5* and *Tbx20* may function cooperatively to control cardiogenesis. To test this hypothesis, I coinjected concentrations of TBX5MO and TBX20MO below the threshold at which cardiac phenotypes are efficiently induced when injected individually. At a concentration of 40 ng per embryo for *Tbx5* morpholinos and 80 ng per embryo for *Tbx20* morpholinos, injections yield consistent heart phenotypes in 82% of TBX5MO-injected embryos and in 100% of TBX20MO-injected embryos (Fig. 3.3). I refer to this dose as the "optimal" dose, because it is the dose hat efficiently blocks translation of TBX5 and TBX20 *in vivo* (Fig. 3.1 D, E) and the dose that gives efficient and penetrant cardiac phenotypes. At half doses, 20 ng per embryo for TBX5MO and 40 ng per embryo for TBX20MO, each morpholino yields significantly fewer and weaker heart phenotypes compared to the full dose (Fig. 3.12M, data not shown). I refer to this concentration as the "suboptimal" dose for inducing cardiac defects. The terms "optimal" and "suboptimal" are only used to refer to the concentrations that yield fully penetrant or partially penetrant cardiac phenotypes, respectively.

To address the question of whether *Tbx5* and *Tbx20* cooperate in cardiogenesis, I injected TBX5MO and TBX20MO individually at suboptimal doses in combination with ControlMO to keep total morpholino concentrations equal in all injections. TBX5MO was then coinjected with TBX20MO, each at the suboptimal dose. ControlMO injected at 80ng/embryo served as control. As shown in Figure 3.12, only 4% of embryos injected with suboptimal TBX5MO/ControlMO displayed pericardial edema, unlooped heart tubes, and reduction in cardiac mass. Suboptimal TBX20MO/ControlMO yields only 13% cardiac defects. In suboptimal injections, the majority of embryos appeared normal, while the few cardiac phenotypes produced were much less severe than at optimal doses (e.g. barely detectable reduction in cardiac mass, slight perturbation of looping and little or no pericardial edema). When coinjected at suboptimal doses, 74% of TBX5MO/TBX20MO coinjected embryos display dramatic cardiac defects compared to 0% of ControlMO-injected embryos (Fig. 3.12D, H, L). The observation that the percentage of heart defects in double morphants is more than additive suggests that *Tbx5* and *Tbx20* synergistically act to control heart morphogenesis.

If *Tbx5* and *Tbx20* cooperate to regulate cardiogenesis, one might expect a more severe alteration in cardiac morphology and marker expression when the levels of both proteins are reduced. To address this question I performed *in situ* hybridizations on stage 36 embryos from the above double injection experiment using *Nkx2-5*, *XANF*, and *XTnIc* probes. As shown in Figure 3.12, all three markers are expressed normally in embryos injected with suboptimal doses of TBX5MO and TBX20MO as compared to ControlMO. However, heart marker expression in the double morphant embryos is markedly reduced, particularly *XANF*. Both *Nkx2-5* and *XTnIc* are still detectable in the heart region, albeit in

fewer cells. Thus, the synergistic cooperation of TBX5 and TBX20 are required for proper heart development.

D. Discussion

Members of the T-box family of proteins play a fundamental role in patterning the developing vertebrate heart, however, the precise cellular requirements for any one family member remains largely unknown. In this study, I demonstrate that TBX5 and TBX20 are both required for early cardiac morphogenesis. Moreover, I show that TBX5 and TBX20 function in the same pathway implying a synergistic role for these two proteins during early heart development. Consistent with this proposal, I show that TBX5 and TBX20 can physically and functionally interact, therefore providing the first evidence for direct interaction between members of the T-box gene family.

Functions of *Tbx5* and *Tbx20* in Cardiac Morphogenesis

Our studies show that *Tbx5* and *Tbx20* are required for similar cellular processes in the developing heart. This data demonstrates a non-redundant function for TBX5 and TBX20 during cardiac morphogenesis; neither protein can compensate for the other in heart morphogenesis. The lack of redundancy at the molecular level is corroborated by the observation that the putative TBX5 target gene *XANF* either is not expressed or is expressed very weakly in TBX5 morphant embryos, while being expressed at the proper time, place and levels in TBX20 morphant embryos. Together this data suggests that TBX5 and TBX20 act in a non-redundant fashion to control morphogenetic movements of early heart tissue.

The cardiac defects in response to a reduction of either TBX5 or TBX20 appear to represent a block in an early morphological step in heart formation. Since the spatial distribution of *Nkx2.5* is unaltered throughout early development in TBX5MO, TBX20MO and ControlMO injected embryos, and since *Nkx2.5*, *Tbx5*, and *Tbx20* continue to be expressed until the later stages of heart development, and TBX5 and TBX20 morphants express markers of terminal muscle differentiation, neither *Tbx5* nor *Tbx20* appear to be required for commitment, migration or terminal differentiation of cardiac tissue. Thus, both *Tbx5* and *Tbx20* appear to be required to direct the coordinated events that occur during the early steps of heart morphogenesis.

Consistent with this hypothesis, both TBX5 and TBX20 morphant hearts are greatly extended along the anterior-posterior axis, and the heart tube fails to correctly loop and undergo chamber formation. As a result, embryos display pericardial edemas, have impaired blood flow (Fig. 3.5), an irregular heartbeat (data not shown) and ultimately die. Thus, the alteration in heart morphology appears to be the primary outcome of perturbing TBX5 or TBX20 function.

Past attempts to interfere with *Tbx5* function in *X. laevis* were carried out by the misexpression of a putative interfering form of *Tbx5* that leads to either the absence or severe malformations of the heart (Horb and Thomsen, 1999). In instances in which the heart does form, there is a reduction or block in myocardial tissue formation and a failure of the heart to undergo looping. My results with *Tbx5*-specific morpholinos show a less severe heart phenotype than those reported with the dominant interfering *Tbx5* but bear a close resemblance to those reported for the zebrafish *Tbx5* mutant, *heartstrings* (Garrity et al., 2002). This may be due to the dominant-interfering form of *Tbx5* used in the *X. laevis* studies

interfering with the function of both *Tbx5* and *Tbx20* or possibly other T-box family members expressed in the developing heart, e.g. *Tbx1* and *Tbx2* (Chapman et al., 1996b), as has been shown for other *Engrailed* fusions (Horb and Thomsen, 1997). However, in the absence of a TBX5 specific antibody, we cannot formally rule out the possibility that some residual TBX5 protein is present in morphant embryos leading to a less severe phenotype in our studies.

Tbx5 and *Tbx20* are Not Dependent on One Another's Function

The phenotypes of TBX5 and TBX20 morphant embryos do not appear to act in a linear pathway since the spatial and temporal expression of *Tbx5* appears unaltered in TBX20 morphants, and vice versa. These findings are in agreement with studies showing normal expression of *Tbx20* in *Tbx5* mutant mice (Stennard et al., 2003) but in apparent conflict with a second study reporting the downregulation of *Tbx5* in zebrafish embryos injected with a *Tbx20* morpholino (Szeto et al., 2002). Although the zebrafish and *X. laevis* orthologues of *Tbx20* share a very high degree of identity at the protein level (86%), the differences between the two orthologues may reflect a species difference as, for example, has been reported for the endodermal-inducing activities of the T-box-containing gene *Brachyury* (Marcellini et al., 2003). Although no alterations in *Tbx5* or *Tbx20* RNA levels were observed in morphant embryos, I did observe a downregulation of TBX5 protein in response to *Tbx20* morpholinos *in vivo*, and vice versa, but not *in vitro* (Fig. 3.1), raising the interesting possibility that cross-regulation may be occurring between TBX5 and TBX20 at the level of translation. Since similar studies have not been conducted in zebrafish, it is not possible at this time to know

the mechanisms of cross-regulation or if this is a conserved response to interfering with TBX5 or TBX20.

TBX5 and TBX20 Heterodimerization

Although *Tbx5* and *Tbx20* are coexpressed and both function in early heart development, the genes appear to be regulated through separate pathways. For example, *Tbx20* but not *Tbx5* can be induced in response to *BMP2* signaling (Plageman and Yutzey, 2004). Taken together with my results demonstrating a physical interaction between TBX5 and TBX20, these data would suggest that TBX5 and TBX20 function in parallel pathways that converge upon TBX5:TBX20 heterodimerization. This model is also supported by my results showing a functional interaction between TBX5 and TBX20; embryos derived from injections of suboptimal doses of *Tbx5* and *Tbx20* morpholinos have only minor effects on heart development in a small proportion of the embryos. However, when injected in combination 74% of all embryos examined displayed grossly abnormal heart formation.

What are the possible cellular functions of TBX5 and TBX20 in heart development? Past studies on T-box genes have shown a direct link between members of the T-box gene family and cell adhesion. For example, embryos homozygous for mutations in *Brachyury*, the founding member of the T-box gene family, show an inability of the mesoderm to properly migrate along the extracellular matrix leading to an inability of the mesodermal germ layer to complete the morphogenetic movements normally associated with gastrulation (Showell et al., 2004). An analogous model for TBX5 and TBX20 function may include regulation of cell polarity or adhesion events associated with heart morphogenesis. It is possible that TBX5 and TBX20 function to control polarity or adhesive properties of cardiac tissue once the two

heart fields merge along the anterior midline, and that target specificity is regulated through TBX5 and TBX20 protein-protein interactions. It is also possible that TBX5 and TBX20 may work in concert to regulate cell division and proliferation. In agreement with this proposal, we have recently shown that alterations in cardiac cell numbers, survival and proliferation in TBX5MO-derived embryos are a consequence of disrupting TBX5 function (Goetz et al., 2006).

It is worth noting that neither TBX5 nor TBX20 have strong transcriptional activation or repression activity by themselves (Fig. 3.10; Bruneau et al., 2001; Hiroi et al., 2001; Plageman and Yutzey, 2004; Stennard et al., 2003). Thus, transcriptional activity appears to be governed by protein-protein interactions. Past studies have identified several other interacting partners for both TBX5 and TBX20. For example, both TBX5 and TBX20 have been shown to interact with the homeobox-containing transcription factor NKX2-5 (Bruneau et al., 2001; Hiroi et al., 2001; Stennard et al., 2003), consistent with clinical studies showing that HOS patients and humans heterozygous for NKX2-5 display many of the same cardiac defects (Elliott et al., 2003; Goldmuntz et al., 2001; Prall et al., 2002).

How might TBX5:TBX20 heterodimerization affect target choice? It may be that the role of TBX5:TBX20 dimerization is to sequester TBX5 and thereby block its interaction with other proteins such as NKX2.5 thereby indirectly inhibiting the induction of cardiac specific genes such as *XANF*. However, several lines of evidence argue against such a proposal. For example, at low and high concentrations TBX20 can increase transcription of the *Nppa/ANF* reporter in the presence of TBX5, while showing a repressive activity at intermediate concentrations, suggesting that in certain contexts TBX20 can cooperate with TBX5 to activate transcription, while antagonizing TBX5 activity in others. An alternative

possibility is that TBX20 target choice and ability to function as a transcriptional activator or repressor is governed by its choice of interacting partners. Consistent with this hypothesis, Stennard et al (2003) have shown that NKX2.5, GATA4, and GATA5 interact with TBX20, and the interactions occur through the same domain of TBX20 that we have shown interacts with TBX5, at least in the cases of NKX2.5 and GATA4 (Stennard et al., 2003). Furthermore, the authors demonstrated that TBX20 can repress synergistic activation of a *connexin 40* reporter by NKX2.5 and GATA4, while synergistically activating the same reporter with NKX2.5 and GATA5. Thus, TBX20 may be able to function both as a transcriptional activator or repressor, and this decision is based on its choice of protein partners. In addition, TBX5 and TBX20 have been shown to display different binding affinities for different T-box binding sites (Stennard et al., 2003). For example, TBX20 unlike TBX5 can bind to the *Brachyury* target site while TBX5 has a higher affinity than TBX20 for the T-box binding site in the *Nppa*/*ANF* promoter. Thus, downstream target selection may be dictated by homodimerization verses heterodimerization. This is supported by the recent findings that several genes involved in heart development are found to contain multiple T-box binding sites (R. Schwartz personnel communication, FLC unpublished findings). Our model would suggest that TBX5 and TBX20 target selection and transcriptional activity is based on partner choice in a specific tissue at a specific time. However, it still remains to be established which protein interactions take place in the developing heart and in turn, what governs the choice of partners for TBX5 or TBX20.

Figure 3.1. *Tbx5* and *Tbx20* morpholinos block translation of their respective target proteins.

(A) TBX5MO and TBX20MO positions relative to *Tbx5* and *Tbx20* cDNA. (B) Inhibition of TBX5-V5 translation *in vitro* by TBX5MO. TBX20MO and ControlMO serve as controls. Each reaction contains 1 μg of *Tbx5*-V5 circular plasmid along with the indicated amounts of MO. (C) Inhibition of TBX20-V5 translation in vitro by TBX20MO. TBX5MO and ControlMO serve as controls. Each reaction contains 1 μg of *Tbx20*-V5 circular plasmid along with the indicated amounts of MO. (D) Inhibition of TBX5-V5 translation by TBX5MO in animal caps. TBX20MO and ControlMO serve as controls. Probed with anti-V5 and re-probed with anti-PTP1D/SHP2 as a loading control. Embryos injected with 2 ng mRNA and the indicated amounts of MO. (E) Inhibition of TBX20-V5 translation by TBX20MO in animal caps. TBX20MO and ControlMO serve as controls. Probed with anti-V5 and re-probed with anti-PTP1D/SHP2 as a loading control. Embryos injected with 2 ng mRNA and the indicated amounts of MO.

Figure 3.1. *Tbx5* and *Tbx20* morpholinos block translation of their respective target proteins.

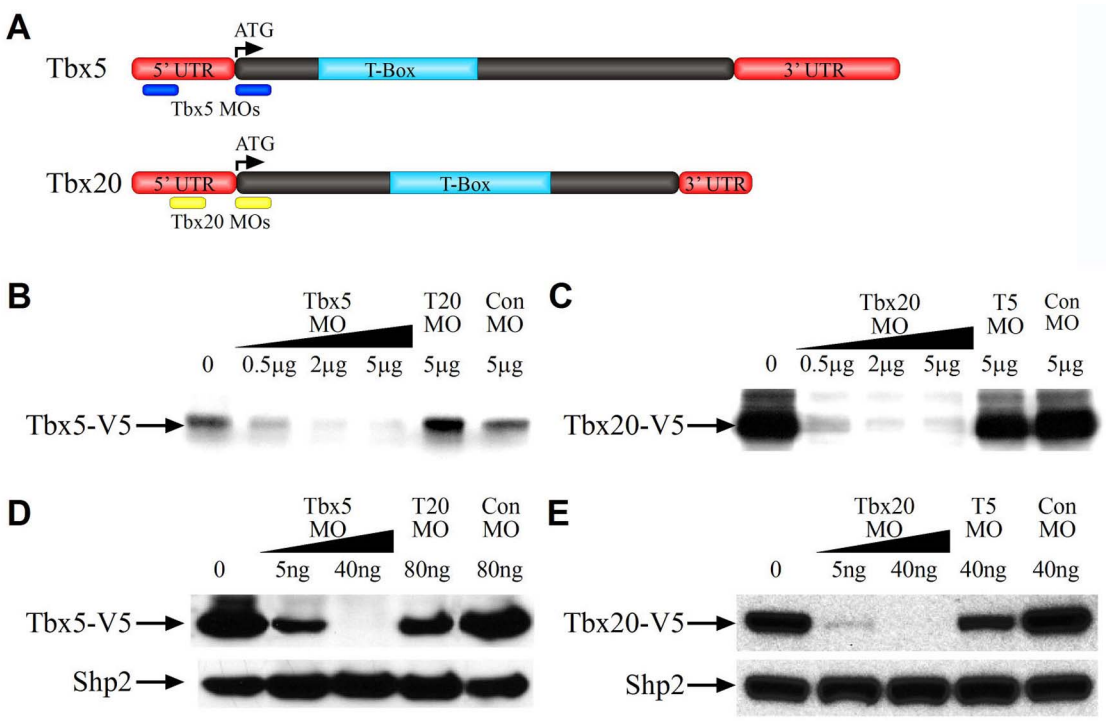

Figure 3.2. Sequence alignments suggest that *Tbx5* and *Tbx20* morpholinos cannot cross react.

(A) Alignments of *Tbx5* morpholinos (complementary sequence) with *Tbx5* and *Tbx20* mRNA sequence. (B) Alignments of *Tbx20* morpholinos (complementary sequence) with *Tbx5* and *Tbx20* mRNA sequence.

Figure 3.2. Sequence alignments suggest that *Tbx5* and *Tbx20* morpholinos cannot cross react.

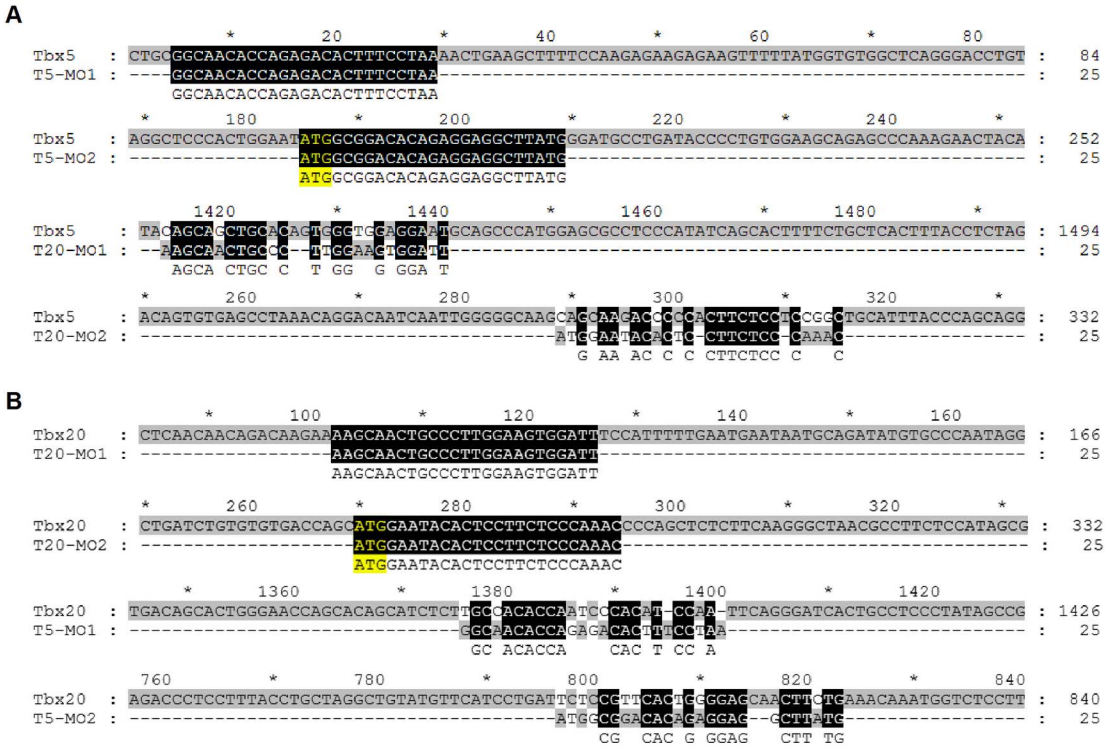

Figure 3.3. *Tbx5* and *Tbx20* are required for proper cardiogenesis.

(A-F) Morpholino-injected tadpoles at the indicated stages. Control morphant embryos (A, D), TBX5 morphant embryos (B, E), TBX20 morphant embryos (C, F). Arrows indicate the heart region, arrowheads indicate the eye. (G) Chart displaying the percentage of morphants surviving and displaying cardiac abnormalities as scored by the presence of an unlooped heart tube, a reduction in cardiac mass and the presence of a pericardial edema.

Figure 3.3. *Tbx5* and *Tbx20* are required for proper cardiogenesis.

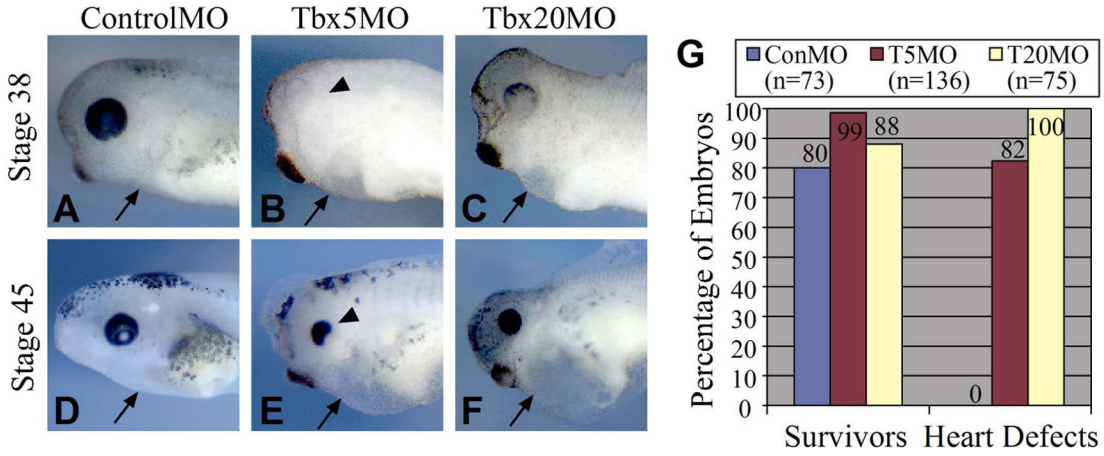

Figure 3.4. *Tbx5* is expressed in the common cardinal and anterior hepatic veins.

(A, B) Whole mount *in situ* hybridization of *Xenopus* embryos at stage 36 (A) and 42 (B). Parasaggital section show expression in the myocardium (m), endocardium (e), and pericardium (p). (C, D) Oblique sections through a stage 36 embryo showing expression in the common cardinal (cc) and anterior hepatic veins (h).

Figure 3.4. *Tbx5* is expressed in the common cardinal and anterior hepatic veins.

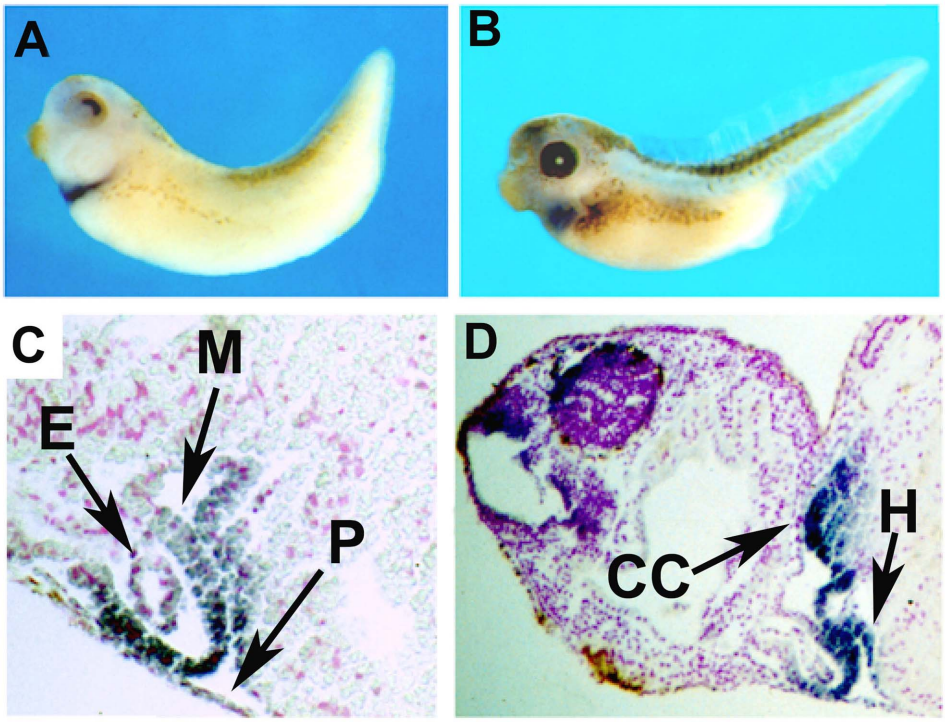

Figure 3.5. *Tbx5* and *Tbx20* morpholinos block the formation of a functional heart as assayed by benzidine staining of erythrocytes in stage 42 tadpoles.

(A) Uninjected control, (B) TBX5MO injected at optimal dose, (C) TBX20MO injected at optimal dose, (D) TBX5MO and TBX20MO injected together at suboptimal doses. Note: Blood staining in the heart region (h) of control embryos but not morphant embryos.

Figure 3.5. *Tbx5* and *Tbx20* morpholinos block the formation of a functional heart as assayed by benzidine staining of erythrocytes in stage 42 tadpoles.

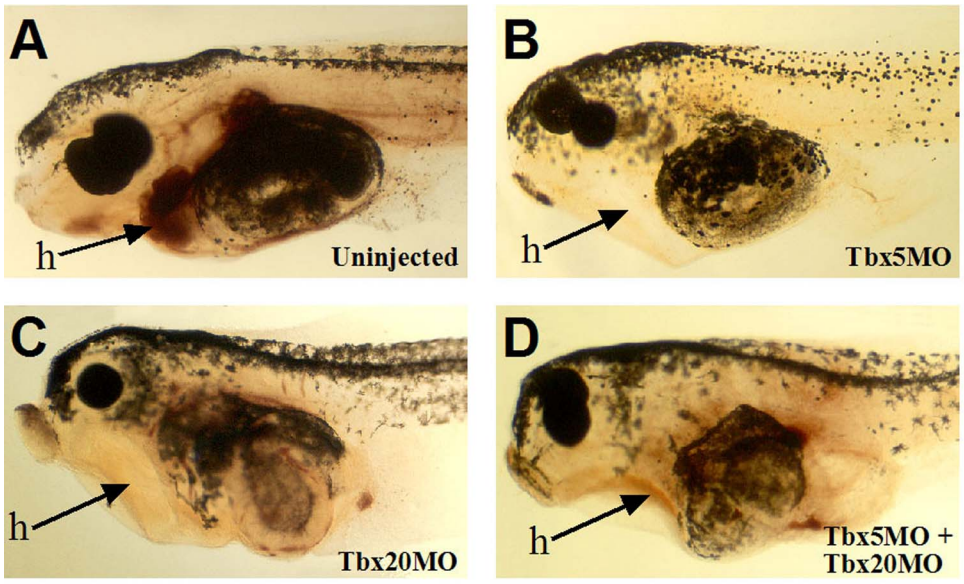

Figure 3.6. TBX5 and TBX20 morphants fail to undergo looping and chamber formation and display reduced cardiac cell numbers.

Cryosections of TBX5 and TBX20 morphant hearts taken at the anterior (outflow), middle (ventricular), and posterior (atrial) regions. (A-D) ControlMO, (E-H) TBX5MO, and (I-L) TBX20MO. Sections stained for *tropomyosin* (red), DAPI (blue), and *cardiac actin* (green). (D, H, L) Same sections as B, F, and J stained with *cardiac actin*. Note that in the looped control heart, the middle ventricular section also contains the atrium. (M) Mean number of cells per hearts obtained by cell counts of heart tissue in serial sections of derived from a minimum of three embryos.

Figure 3.6. TBX5 and TBX20 morphants fail to undergo looping and chamber formation and display reduced cardiac cell numbers.

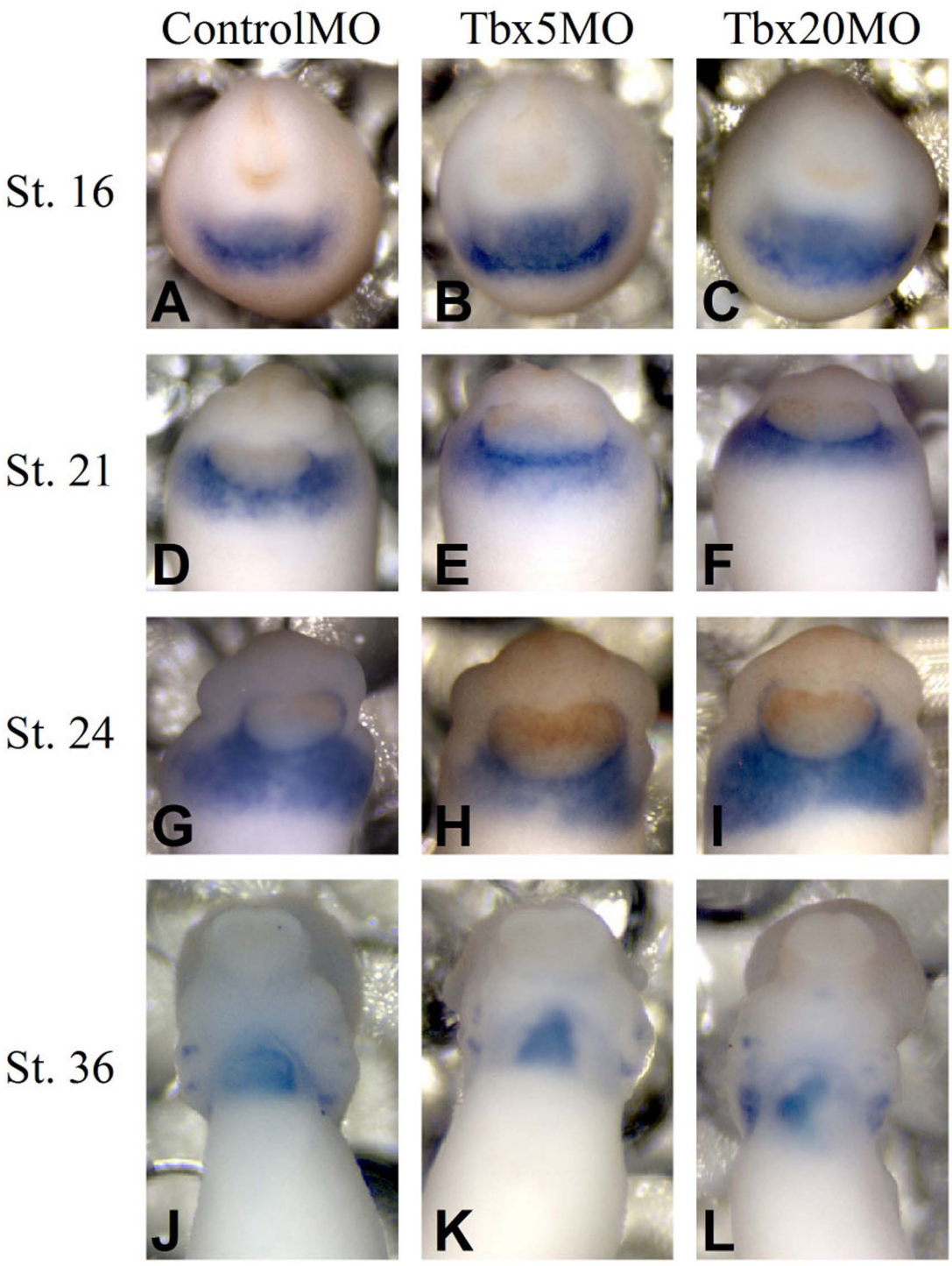

Figure 3.7. Cardiac specification is unaltered in TBX5 and TBX20 morphants.

Whole-mount *in situ* hybridization with *Nkx2.5* on stage matched (A, D, G, J) ControlMO-, (B, E, H, K) TBX5MO-, or (C, F, I, L) TBX20MO-derived embryos.

Figure 3.7. Cardiac specification is unaltered in TBX5 and TBX20 morphants.

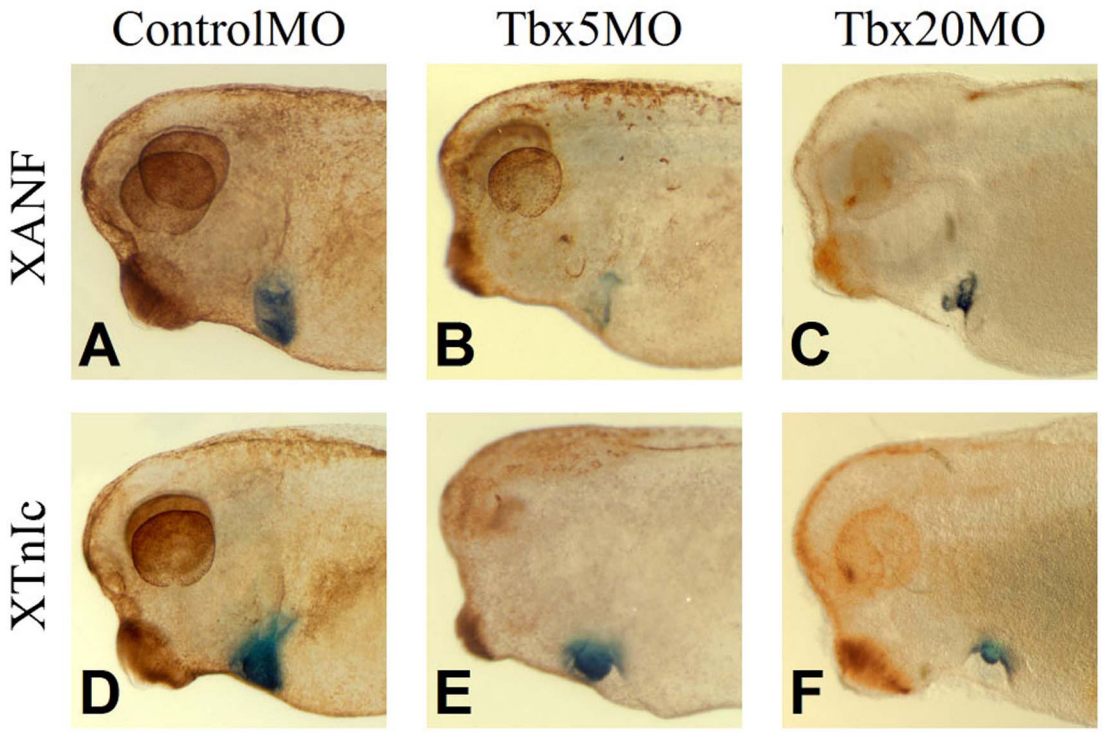

Figure 3.8. TBX5 and TBX20 morphants display dramatic morphological defects.

Whole-mount *in situ* hybridizations of cleared stage 36 embryos. (A-C) *ANF* whole mount *in situ* hybridization. (D-F) *XTnIc* whole mount *in situ* hybridization. (A, D) ControlMO. (B, E), TBX5MO, (C, F) TBX20MO.

Figure 3.8. TBX5 and TBX20 morphants display dramatic morphological defects.

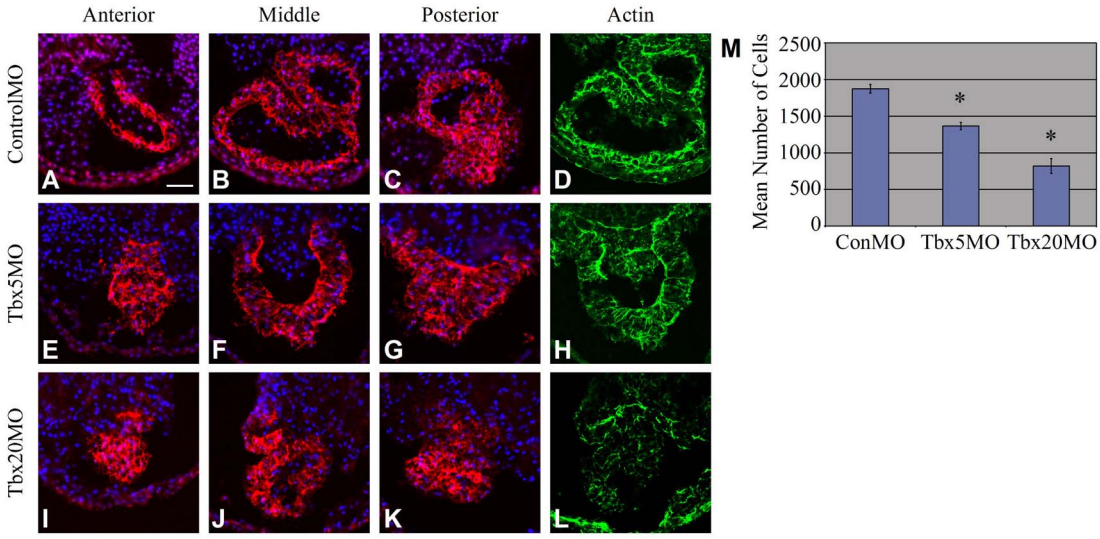

Figure 3.9. *Tbx5* and *Tbx20* are localized to the nucleus and can activate transcription on the *Nppa*/*ANF* promoter.

(A) Schematic depicting the amino acid positions of the T-box domains of *Tbx5* and *Tbx20*. (B) Schematic of Rat *Nppa*/*ANF*-*luciferase* reporter construct showing T-box binding site consensus sequences and their relative position within the promoter relative to translation start site. (C, F) Transfected cells were stained with anti-V5 (Cy2, green) for TBX5-V5 and TBX20-V5 and (D, G) anti-phosphotyrosine (Cy3, red) to visualize cytoplasmic compartment. (E, H) Overlay image of Cy2 and Cy3 staining. (I) Rat *ANF*-*luciferase* co-transfected with a constant amount of *Tbx5* (100 ng) and increasing amounts of *Tbx20* (25, 50, 100 and 500 ng) in 293T cells and level of transcriptional activation expressed as Relative Luciferase Units based on average of three independent experiments performed in triplicate.

Figure 3.9. *Tbx5* and *Tbx20* are localized to the nucleus and can activate transcription on the *Nppa/ANF* promoter.

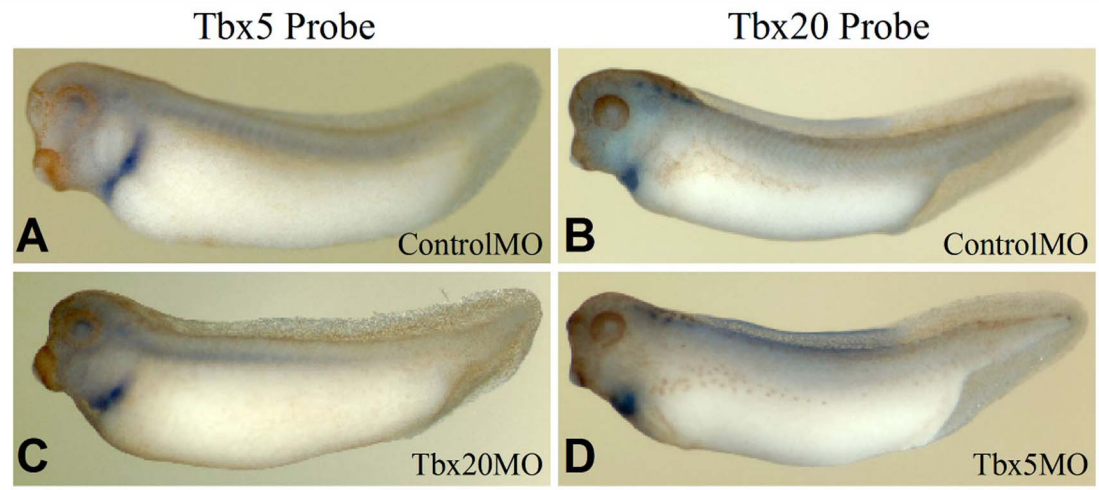

Figure 3.10. *Tbx5* and *Tbx20* are not required for each other's expression.

Embryos injected at the one-cell stage with ControlMO, TBX5MO, or TBX20MO. (A, C) Whole-mount *in situ* hybridization showing *Tbx5* expression. (B, D) Whole-mount *in situ* hybridization showing *Tbx20* expression.

Figure 3.10. *Tbx5* and *Tbx20* are not required for each other's expression.

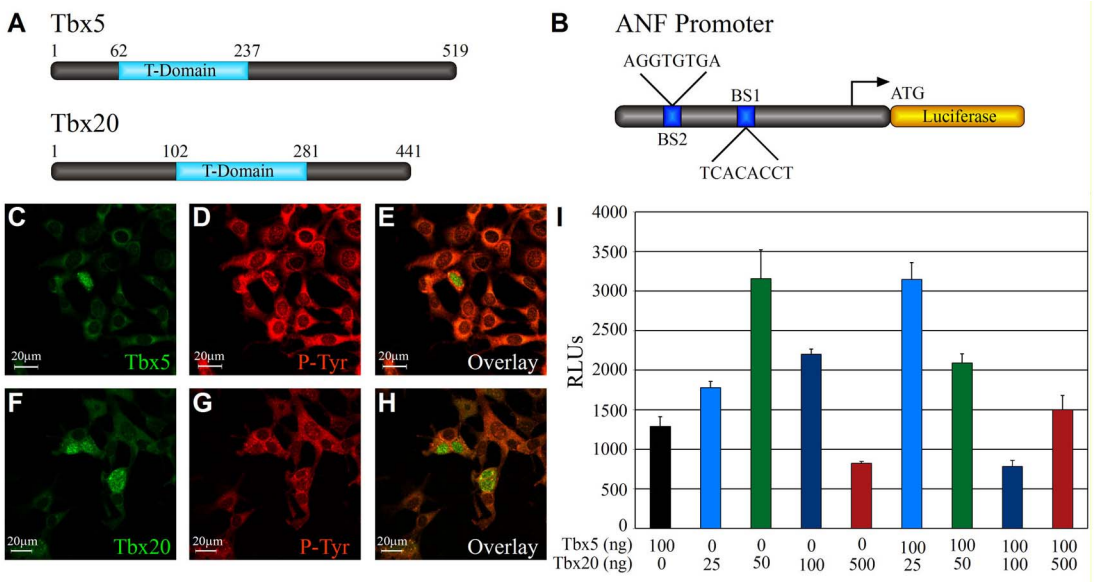

Figure 3.11. TBX5 and TBX20 can physically interact.

Cell lysates containing GST- and/or HA-tagged proteins were incubated on GST and eluted, and separated by SDS-PAGE. GST proteins were detected using anti-GST antibodies and HA-tagged proteins were detected with anti-HA antibodies. (A) Association of TBX5 with TBX20 is shown by pulldown of HA-TBX20 with GST-TBX5. HA-NKX2-5 serves as positive control. 15% of output and 7.5% of input was probed. (B, C) Pulldown of full-length HA-TBX20 with a GST-tagged TBX5 deletion series reveals an interaction domain in the N-terminus and T-box region of TBX5. Each reaction was probed with anti-HA antibodies. 7.5% of input and 15% of output was probed. (D, E) Pulldown of HA-TBX20 deletion series with full-length GST-TBX5 reveals an interaction domain within the N-terminus and T-box of TBX20. Each reaction was probed with anti-HA antibodies. 7.5% of input and 15% of output was probed, except in the case of ΔN/C in which the amount of protein probed was only 4% due to the increase in total amount of ΔN/C protein used in pulldown (see text).

Figure 3.11. TBX5 and TBX20 can physically interact.

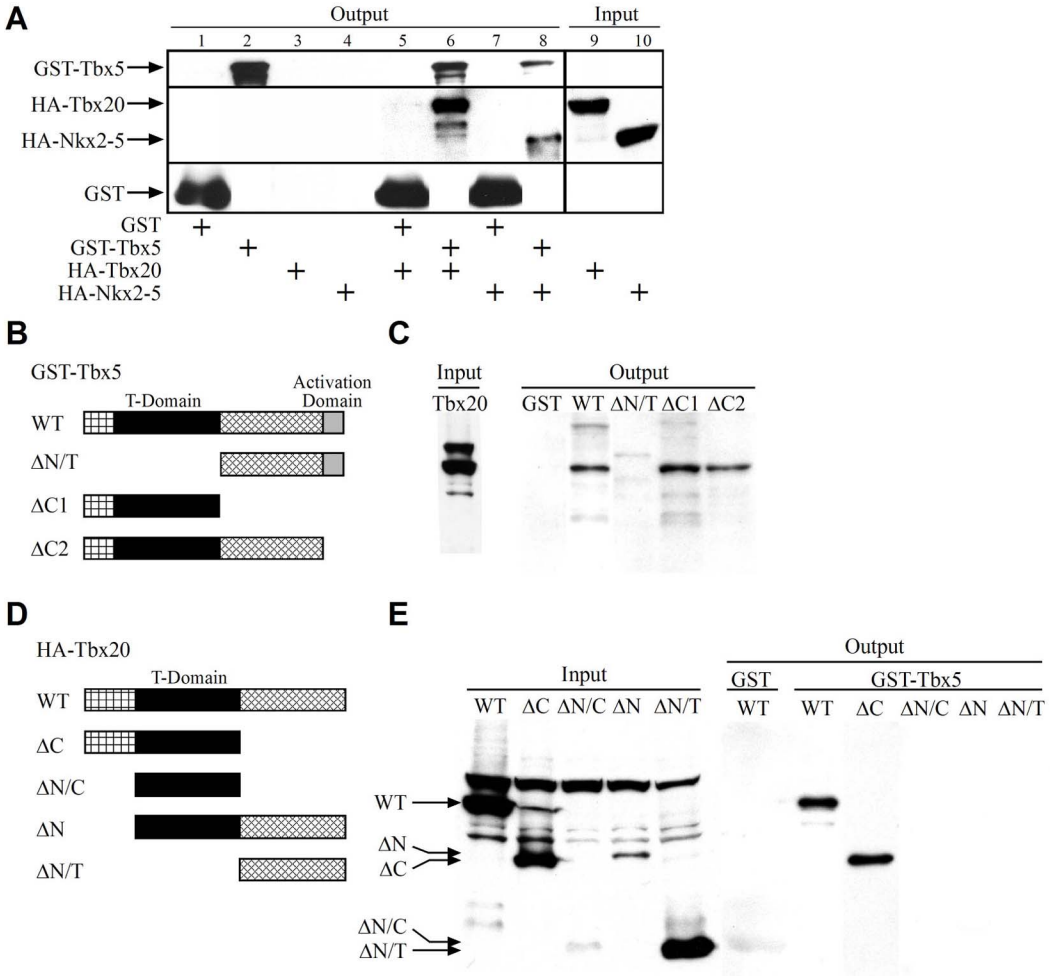

Figure 3.12. *Tbx5* and *Tbx20* synergistically act to regulate cardiac gene expression. (A-L) Embryos injected with the indicated morpholinos at the one-cell stage. (A-D) *Nkx2-5* whole mount *in situ* hybridization. (E-H) *XANF* whole mount *in situ* hybridization. (I-L) *XTnIc* whole mount *in situ* hybridization. (A, E, I) ControlMO, (B, F, J) TBX5MO injected at suboptimal dose, (C, G, K) TBX20MO injected at suboptimal dose, (D, H, L) TBX5MO and TBX20MO injected in combination at suboptimal doses. All embryos were cleared to reveal heart expression. (M) Statistics for embryos injected with suboptimal doses of TBX5MO and TBX20MO in combination with each other or with ControlMO. Hearts were judged as having defects if they displayed a pericardial edema, an unlooped heart tube, or reduction in cardiac mass.

Figure 3.12. *Tbx5* and *Tbx20* synergistically act to regulate cardiac gene expression.

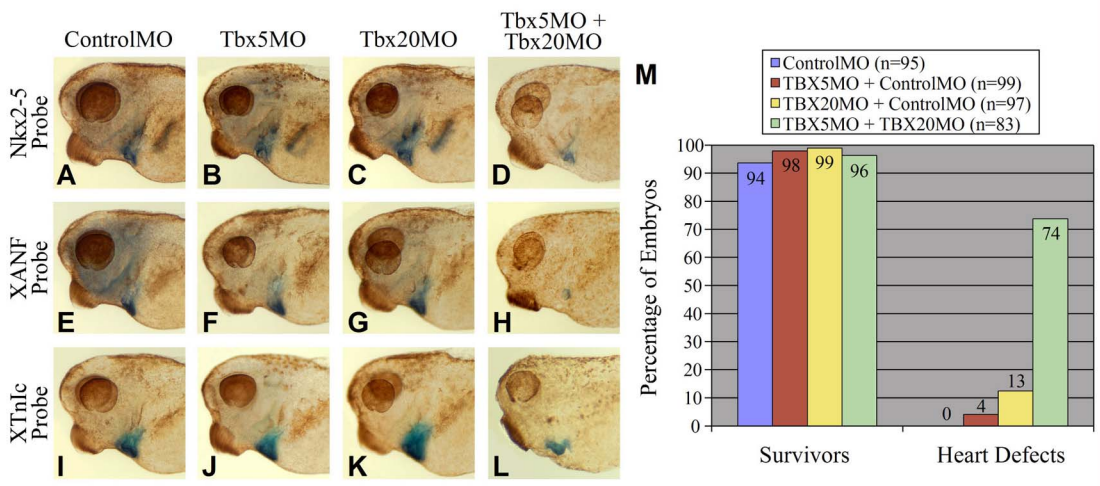

CHAPTER IV

A MICROARRAY-BASED SCREEN FOR TARGETS OF TBX20 AND TBX5 FUNCTION

A. Introduction

Work from our lab and others has demonstrated that both *Tbx5* and *Tbx20* function are required for proper cardiac morphogenesis (Chapter III; Brown et al., 2005; Bruneau et al., 2001; Cai et al., 2005; Garrity et al., 2002; Horb and Thomsen, 1999; Stennard et al., 2005; Takeuchi et al., 2005). Despite the known requirements for these transcription factors in heart development, very few direct targets of their transcriptional activity have been identified. *Tbx5* has been shown to directly bind to elements within the promoters of *connexin40* (*cx40*) and atrial natriuretic factor (ANF; Bruneau et al., 2001; Ghosh et al., 2001). Furthermore, TBX5 has been shown to bind the consensus *Brachyury* (*T*) T-box binding element (TBE) *in vitro* (Ghosh et al., 2001). However, it is unknown whether other targets exist for TBX5 function or whether these targets contain consensus TBEs or different binding elements. Recently, TBX20 was shown to bind to the promotor of *Tbx2*, resulting in repression of *Tbx2* expression (Cai et al., 2005). In addition, TBX2 was itself shown to bind to the promoter of *Nmyc1*, a regulator of cell proliferation (Cai et al., 2005). Binding of TBX2 to the *Nmyc1* promoter was further shown to inhibit *Nmyc1* expression, resulting in a reduction of cardiomyocyte proliferation (Cai et al., 2005). These results suggest a possible explanation for the cardiac defects apparent in embryos depleted for TBX20; loss of TBX20

results in a de-repression of *Tbx2*, in turn leading to repression of cell proliferation by TBX2 activity on *Nmyc1*. Thus, studies have resulted in the identification of only two direct targets of TBX5 activity and one target of TBX20 activity.

Since the putative targets of TBX20 and TBX5 are reported to act during chamber formation, and thus, at later stages of heart development than the stages at which we have reported TBX20 and TBX5 to function in morphogenesis, we sought to identify early targets of these transcription factors (Chapter III; Brown et al., 2005; Bruneau et al., 2001; Cai et al., 2005; Ghosh et al., 2001). To this end we here report a microarray-based screen for genes misregulated in response to loss of TBX20 or TBX5. These results have yielded two sets of genes misregulates in TBX20 and TBX5 morphant embryos, providing the basis for future studies. We demonstrate that a subset of cell cycle regulators are misregulated in *Tbx5* morphant embryos. In addition, we report the identification of several novel cardiac-specific genes, including the *Xenopus* orthologues of *titin novex-3* (*Xtn3*) and *heat shock protein 27* (*XHsp27*).

B. Materials and Methods

Microarray Assay

7 μg of total RNA was used to synthesize cDNA. A custom cDNA kit from Life Technologies was used with a T7-$(dT)_{24}$ primer for this reaction. Biotinylated cRNA was then generated from the cDNA reaction using the BioArray High Yield RNA Transcript Kit. The cRNA was then fragmented in fragmentation buffer (5X fragmentation buffer: 200mM Tris-acetate, pH8.1, 500mM KOAc, 150mM MgOAc) at 94^{o}C for 35 minutes before the chip hybridization. 15 μg of fragmented cRNA was then added to a hybridization cocktail (0.05

μg/μl fragmented cRNA, 50 pM control oligonucleotide B2, *BioB*, *BioC*, *BioD*, and *cre* hybridization controls, 0.1 mg/ml herring sperm DNA, 0.5 mg/ml acetylated BSA, 100mM MES, 1M Na^+, 20mM EDTA, 0.01% Tween 20). 10 μg of cRNA was used for hybridization. Arrays were hybridized for 16 hours at 45°C in the GeneChip Hybridization Oven 640. The arrays were washed and stained with R-phycoerythrin streptavidin in the GeneChip Fluidics Station 400. After this, the arrays were scanned with the Hewlett Packard GeneArray Scanner. Affymetrix GeneChip Microarray Suite 5.0 software was used for washing, scanning, and basic analysis. Sample quality was assessed by examination of 3' to 5' intensity ratios of certain genes.

Whole-mount RNA *in situ* Hybridization

Briefly, each EST clone was obtained from either OpenBiosystems for I.M.A.G.E. clones or from the National Institute for Basic Biology (Japan) for all others. Known genes were obtained as follows. *Ath5a* (generous gift from M Vetter; Kanekar et al., 1997), *Mmp9* (kind gift from J. Henry; Carinato et al., 2000)), *tropomyosin beta 44* (*Tmb44*; generous git of P.Thiebaud; Hardy and Thiebaud, 1992), and *Vent2* (generous gift from J. Gurdon; Ladher et al., 1996). Whole-mount *in situ* hybridizations were performed as previously described (Harland, 1991).

C. Results

In order to identify genes downstream of TBX20 and TBX5 function, we initiated a microarray-based screen for genes misregulated in TBX20- and TBX5-depleted embryos. We used the Affymetrix *Xenopus* GeneChip, which consists of ~14,400 transcripts and

15,503 features. Approximately 3500 known genes, constituting all named *X. laevis* transcripts at manufacturing time are included on the microarray. Each probe on the chip is 25 nucleotides in length and each feature consists of 16 random probes. Furthermore, control features containing mismatch reference probes for each probe set are inluded on the microarray. Sequences on the array were selected from the several public data sources, including GenBank (release 135.0, April 2003), dbEST (June 2003), and UniGene (build 36, June 2003). Briefly, embryos were injected at the one-cell stage with either 60ng TBX20MO, 40ng TBX5MO, or 60ng ControlMO, and allowed to develop to stage 26, prior to observable cardiac defects in morphant embryos (Chapter III; Brown et al., 2005)). The anterior 1/3 of each embryo was then dissected to enrich for cardiac-specific genes and collected for total RNA isolation. For each treatment, 40 embryos were pooled for RNA isolation and this was performed in triplicate, resulting in three RNA samples for each treatment. Furthermore, the entire experimental procedure was performed twice for the *Tbx20* morphant microarray, totalling six samples for each treatment.

Statistical analysis of the microarray data was performed using GeneChip Microarray Suite 5.0 (Affymetrix) and GeneSpring microarray analysis software (Agilent Technologies). Hybridization of total RNA to the microarrays and initial processing of raw data was performed by the UNC Functional Genomics Core Facility (see materials and methods). The intensity reading for each feature was normalized to the mismatch reference feature for each probe set. In order to narrow down the putative list of misregulated targets, a minimum of 2-fold change in expression was used as a selection criterion. The list of genes misregulated at least 2-fold was further culled by analysis of variance (ANOVA) tests to identify genes that were significantly misregulated at least 2-fold at a significance value of $p \leq 0.05$.

Depletion of TBX20 resulted in the identification of 45 transcripts significantly misregulated at least 2-fold (Table 4.1). The vast majority of these transcripts were found to be uncharacterized ESTs, with only 4 transcripts, *atonal homologue 5a* (*Ath5a*), *matrix metalloprotease 9* (*Mmp9*), *tropomyosin beta 44* (*Tmb44*), and *Vent2*, having been previously cloned and annotated (Carinato et al., 2000; Hardy and Thiebaud, 1992; Kanekar et al., 1997; Ladher et al., 1996). In order to corroborate the misregulation of these transcripts, a secondary screen by whole-mount *in situ* hybridization was performed. Briefly, Tbx20MO or ControlMO were injected at the one-cell stage and embryos were collected at neurula stage (stage 19), early tailbud stage (stage 26), or late tailbud stage (stage 36). Ten embryos at each stage, for each treatment, and for each probe were collected and submitted to whole-mount *in situ* hybridization, totalling 2700 embryos, 45 probes, 3 stages per treatment, and 2 treatments. Despite the observation that transcripts were found to be misregulated in a range from 16-fold downregulated to 10-fold upregulated as assayed by microarray, none of the probes showed significant or obvious misregulation by whole-mount *in situ* hybridization (Table 4.1; data not shown). This may be due to the lack of sensitivity inherent in whole-mount *in situ* hybridization analysis. However, 27% of the transcripts were found to be specifically expressed in developing cardiac tissue, in corroboration with our findings that a defect in cardiogenesis is a primary phenotype of TBX20 depletion (Table 4.1; Chapter III). One of these ESTs, EST25, was found to be dramatically expressed throughout developing cardiac and skeletal muscle. This transcript was subsequently sequenced and characterized, resulting in the identification of the *X. laevis* orthologue of *titin novex 3* (*Xtn3*; see Chapter V).

In order to identify genes involved in cardiogenesis and putatively downstream of TBX20 function, we undertook a candidate-approach to identify the unknown ESTs that were both expressed in the developing heart and contained full-length sequences against which we could design antisense morpholino oligonucleotides. By this method we found that EST31 contains a full-length cDNA, including 5' UTR, 3' UTR, and polyA tail. The sequence, expression, and requirement for this transcript was subsequently characterized, resulting in the identification of *Hsp27* as a critical regulator of cardiac progenitor fusion and actin cytoskeletal dynamics (see Chapter VI).

Results from depletion of TBX5 yielded a list of 303 genes misregulated in response to loss of TBX5 protien. Forty nine of these transcripts appear to be involved with cell-cycle regulation (Table 4.2). These results have led to a subsequent study performed by Sarah Goetz in which she has demonstrated that a subset of cell cycle regulators expressed in S phase of the cell cycle are misregulated in response to loss of TBX5 (Goetz et al., 2006). We did not observe overlap between genes misregulated in response to loss of TBX20 or TBX5, suggesting that the loss of either TBX20 or TBX5 is insufficient to induce a 2-fold change of targets on which both factors act. Alternatively, it may be that perhaps only one gene or a few genes are targeted by both TBX20 and TBX5 and these genes were not present on the microarray. Further analysis of genes misregulated in response to loss of TBX5 is ongoing by F. Conlon and colleagues.

D. Discussion

In the present study I have identified a large number of genes putatively misregulated in response to loss of either TBX20 or TBX5 protein using microarray analysis. The majority

of transcripts misregulated at least 2-fold were found to consist of previously unknown ESTs. However, secondary screening by whole-mount *in situ* hybridization reveals that 27% of the transcripts misregulated by TBX20 depletion are expressed in the developing heart, suggesting that the misregulation is in fact due to loss of *Tbx20* or to indirect effects on cardiogenesis by TBX20 depletion. Unfortunately, significant misregulation of these ESTs could not be validated via whole-mount *in situ* hybridization, suggesting either that these targets are not bona fide downstream targets of TBX20 function, or that the screening method is not sensitive enough to detect the difference in expression. However, results from the concurrent screen for targets of TBX5 function identified a large number of genes involved in cell cycle regulation to be putatively downstream of TBX5. These results were followed up in a collaboration with Sarah Goetz, in which she demonstrated that a subset of genes involved in S-phase prgression are misregulated in TBX5-depleted embryos (Goetz et al., 2006). These findings suggest that at least a portion of targets identified by microarray analysis are downstream of TBX5 function. Considering that both the TBX20 and TBX5 experiments were performed at the same time, using the same batch of microarrays, and the same batch of embryos, the above results support the validity of the microarray data and suggest that the method of secondary screening used for TBX20 target validation is insufficent. An ideal secondary screen would involve performing chromatin immunoprecipitation and microarray analysis (ChIP-on-chip) by immunoprecipitating TBX20 and the genomic sequences bound by TBX20, followed by hybridization of the co-precipitated DNA to a genomic microarray. Unfortunately, highly-specific TBX20 antibodies are currently unavailable. Furthermore, only ~3500 genes are currently known in *X. laevis*,

and the *X. tropicalis* genome is only partially annotated, thus complicating this potential technique.

While *in situ* hybridization has not yielded insights into whether particular putative targets are directly downstream of TBX20 function, these data have resulted in the identification of several novel transcripts expressed in the developing heart, and thus potentially involved in cardiogenesis (Table 4.1). In collaboration with Anna Davis, I have sequenced one of these ESTs (EST25; Table 4.1) and characterized its expression within developing cardiac and skeletal muscle, thus identifying the *X. laevis* orthologue of *novex titin-3* (*XTn3*; Chapter V). In addition, we sought to identify putative targets that result in cardiac phenotypes when depleted by antisense morpholinos (Chapter IV). These results led to the identification of *X. laevis heat shock protein 27* (*XHsp27*) as being expressed n developing cardiac and skeletal muscle, and demonstrated a requirement for XHSP27 function in cardiac precursor fusion (Chapter VI). Thus, microarray analysis of TBX20 and TBX5 depletion has resulted in the demonstration of TBX5 function in cell cycle regulation, the identification of *XHsp27* as being critical for proper cardiogenesis, as well as the identification of a large number of genes expressed in the developing heart, including *XTn3*.

Table 4.1. List of Trascripts Misregulated by *Tbx20* Depletion as Assayed by Microarray

Fold change for each of two independent microarrays are shown in columns two and three. EST nomenclature refers to my own assigned nomenclature. GenBank accession numbers are shown in column four. All assigned gene names and degree of similarity with known homologues in column five are based on annotation by the Affymetrix GeneChip. Domains of expression in column six were based on secondary whole-mount *in situ* hybridization screens using embryos at stages 19, 26, and 36. Highlighted genes indicate detection of expression in the developing heart.

Table 4.1. List of Trascripts Misregulated by *Tbx20* Depletion as Assayed by Microarray

Gene/ EST	Fold Change Experiment 1	Fold Change Experiment 2	GenBank Accession	Name or Similarity	Expression by in situ hybridization
Ath5a	2.3	-1.2	U93170.1	Atonal Homologue 5a	
MMP9	1.3	-2.1	CB756686	matrix metalloproteinase 9	
TMB44	-3.5	-7.0	M87307.1	tropomyosin beta 44	
Vent2	3.8	1.4	U53529.1	vent 2	
EST02	-2.1	-2.4	BC041283.1	Sim. to calsequestrin 2	
EST05	1.7	-6.0	BG884821	myosin light chain 1 (mlc1v) - moderately similar	somites
EST06	-2.0	-3.6	BG884964	myosin light chain 1 (mlc1v') - moderatley similar	heart, somites, facial muscle
EST12	-5.7	-10.4	BC046678.1	Clusterin	eye,neural tube
EST13	-1.2	-16.3	BG555819	Beta Crystallin B1	eye
EST14	2.6	6.0	BC044283.1	hypothetical protein 4931421J16 - similar	eye,arch,hypaxial
EST18	-3.8	-5.4	BM192591	hyaluronan proteoglycan link protein 3 - similar	heart
EST20	-3.2	-3.0	BC041721.1	Ca calmodulin-dependent protein kinase I (CamKI) - similar	skin
EST22	-4.5	-3.1	CD328853	2211263A breast epithelial BA46 antigen - weakly similar	heart,head
EST23	-4.1	-3.9	BC045019.1	C1-tetrahydrofolate synthase - similar	heart?,arch,pronephros,kidney
EST24	-3.8	-4.2	BF428365	unknown	ubiquitous (arch,tailbud)
EST25	-3.9	-3.4	CB564652	titin novex 3 (Xtn3)	heart,somite,hypaxial
EST27	-2.6	-4.5	BM180904	unknown	ubiquitous (arch,eye,somite)
EST28	-2.4	-4.3	AW766698	metaxin - weakly similar	ubiquitous (arch,eye,somite)
EST29	-1.7	-4.0	BF048520	unknown	heart, pronephros
EST30	-1.3	-4.0	BM180258	unknown	ubiquitous (arch,eye,somite, pronephros)
EST31	-1.4	-4.4	AW766262	heat shock protein 27 (XHsp27)	heart
EST32	-1.4	-8.1	CD329675	unknown	heart
EST33	-1.4	-3.8	BC044084.1	nectin-lke 1 - similar	cranial nerves
EST34	4.5	1.0	BF232412	putative heme-binding protein - weakly similar	ubiquitous (arch,eye,somite)
EST35	6.1	5.9	BG513761	polyadenylate-binding protein 4 - weakly similar	ubiquitous (arch,eye,somite)
EST36	3.5	4.6	BC044085.1	splicing factor arginine serine-rich 5 - weakly similar	arch,eye,pronephros
EST38	-9.6	-6.9	BJ052119	unknown	ubiquitous (arch,eye,somite)
EST39	-6.8	-2.3	BJ075657	human reversion-induced LIM protein - weakly similar	ubiquitous (arch,eye,somite)
EST40	-4.2	-4.2	BJ045367	unknown	skin cells, pronephros
EST41	-3.8	-4.1	BJ075760	unknown	arch,eye,brain
EST42	-3.0	-4.4	BJ078949	unknown	gill,eye,brain,pronephros,tailbud
EST43	-2.8	-4.0	BJ053913	osteonidogen - moderately similar	heart,somite,hypaxial
EST44	-1.7	-4.4	BJ054774	unknown	heart,brain,head
EST45	3.9	1.4	BJ081438	EGLN3 (EGL nine homologue 3)	heart,brain,head, pronephros
EST46	3.7	-1.0	BJ092551	unknown	heart,brain,head
EST47	1.7	4.4	BJ047968	SL55 Sodium iodide cotransporter - weakly similar	liver,pronephros,tailbud
EST48	-4.1	-4.0	BJ088604	unknown	brain, eye, endoderm
EST49	-4.1	-3.2	BJ054524	chloride channel protein CLC-KA - weakly similar	head, cloaca
EST50	-4.0	-2.2	BJ081023	AP-3 complex beta3A chain	pronephros, cement gland, heart, mesoderm
EST51	-3.8	-5.9	BJ054660	adenylate kinase isoenzyme 2 - weakly similar	surface ectoderm, brain
EST52	-3.5	-3.4	BJ055892	Ewing sarcoma breakpoint region 1 - similar	pronephros, arch, tailbud
EST53	-3.4	-1.6	BJ091200	angiopoietin-related protein 2 precursor - weakly similar	diffuse
EST54	-3.3	-3.0	BJ088598	hatching enzyme	LPM, hatching gland, pronephros
EST55	-3.3	-2.5	BJ046996	kinesin central motor 1 (XKCM)	surface ectoderm, tail
EST56	-3.1	-2.0	BJ091176	UBHU5B tubulin beta chain - moderately similar	brain, eye, arch

Table 4.2. List of Transcripts Associated with Cell Cycle Regulation Misregulated by *Tbx5* Depletion as Assayed by Microarray

Column one shows fold change. Column two contains GenBank accession numbers. Column three shows gene names and similarity with known homologues as annotated by the Affymettrix GeneChip.

Table 4.2. List of Transcripts Associated with Cell Cycle Regulation Misregulated by *Tbx5* Depletion as Assayed by Microarray

Fold Change	GenBank Accession	Gene Description
-6.3	U51234.1	XMCM7
-4.8	BC043950.1	pescadillo - similar
-4.5	BG163172	14S cohesin SMC3 subunit
-4.3	AF200212.1	CPEB-associated factor Maskin
-3.7	BC049395.1	primase, polypeptide 1 - similar
-3.6	BC044094.1	N-acetyltransferase ARD1 homolog - similar
-3.6	BJ045437	14S cohesin SMC3 subunit
-3.6	U66558.1	cell division control protein 6 (cdc6)
-3.4	BG163172	14S cohesin SMC3 subunit
-3.4	CB564116	ubiquitin protein ligase E3 component n-recognin 1 - weakly similar
-3.3	U44049.1	cdc21
-3.2	U13674.1	XCAP-E
-3.0	AI031506	replication protein A
-3.0	AB003582.1	Dr1
-3.0	BJ086613	Talin - moderately similar
-2.9	BJ048846	bromodomain containing protein 3 - moderately similar
-2.6	U28931.1	membrane-associated tyrosinethreonine Cdc2-specific inhibitory kinase (MYT1)
-2.5	BJ051599	bromodomain containing protein 3 - moderately similar
-2.5	AY253231.1	PCNA-like DNA checkpoint protein Rad9 (Rad9)
-2.4	BJ055178	dynein intermediate chain 1 - moderately similar
-2.4	BC045030.1	cytoplasmic dynein light-intermediate chain - similar
-2.3	BQ385845	anaphase-promoting complex subunit 7 - moderately similar
-2.3	BC044291.1	dynamin 1-like - similar
-2.3	BJ044039	novel MCM235 family member - moderately similar
-2.3	BC043855.1	cyclin E2 - similar
-2.3	U75681.1	histone stem-loop binding protein (SLBP)
-2.2	BG161706	dynamin-1 - weakly similar
-2.2	BQ388347	chromosome segregation 1-like protein - moderately similar
-2.2	AF134570.1	exonuclease ExoI (EXOI)
-2.2	AF307841.1	Blooms syndrome-like protein
-2.2	X82012.1	kinesin like protein 1
-2.1	BG022153	early endoderm-specific nuclear factor (Xenf)
-2.1	BQ400620	alpha-centractin - highly similar
-2.1	BC044291.1	dynamin 1-like - similar
-2.1	BE505964	replication licensing factor MCM5 - moderately similar
-2.1	BF072231	DNA damage binding protein 1 - highly similar
-2.1	AB091779.1	Cut5-related protein
-2.1	AF134569.1	putative nuclease Mre11 (MRE11)
-2.0	AF393653.1	allurin
2.1	BC049393.1	cyclin G1 - similar
2.2	X53745.1	cyclin A1
2.3	BC044046.1	growth arrest and DNA-damage-inducible, alpha - similar
2.4	BG347352	Ubiquitin carboxyl-terminal hydrolase 2 - moderately similar
2.4	U44050.1	mis5
2.4	BI314319	bifunctional methylenetetrahydrofolate dehydrogenase - moderately similar
2.5	BG022307	microtubule-associated proteins 1A1B light chain 3 - highly similar
2.6	M36962.1	p53 homologue
3.0	AJ414384.1	xgadd45-gamma
3.8	BJ090673	sudD suppressor of bimD6 homolog - moderately similar

CHAPTER V

XTN3 IS A DEVELOPMENTALLY EXPRESSED CARDIAC AND SKELETAL MUSCLE-SPECIFIC *NOVEX-3 TITIN* ISOFORM[3]

A. Introduction

The process of myogenesis in *Xenopus laevis* appears to be unique compared to mammalian and avian systems in that it is characterized by two completely distinct types of myogenesis (reviewed in Chanoine and Hardy, 2003). Initially, primary myogenesis results in formation of uninucleate myofibers assembled during early neurula embryos that become functional following neurulation (stage 24). These primary muscles are initially composed entirely of one "fast" fiber type, but by late tailbud stage (stage 37), a second "slow" fiber type appears. During metamorphosis the primary myocytes begin a wave of autonomous programmed cell death resulting in a complete replacement of these primary muscles with "adult" multinucleate muscles produced by a process of secondary myogenesis. Furthermore, this process has been shown to involve switching from embryonic to adult muscle protein isoforms by differential mRNA splicing (Hardy et al., 1999; Radice and Malacinski, 1989).

The giant muscle protein titin is the largest known protein in the biological world and the single human titin gene contains 363 exons with a coding potential of 38,138 amino acids. Many splice-variants of titin have been described and full-length isoforms have been shown to span half the sarcomere length from the Z-line to the M-line, serving to link the two

[3] This work was originally published in Brown, D. D., Davis, A. C. and Conlon, F. L. (2006). Xtn3 is a developmentally expressed cardiac and skeletal muscle-specific novex-3 titin isoform. *Gene Expr Patterns* 6, 913-918.

regions and stabilize sarcomere length by acting as a molecular spring (reviewed in Granzier et al., 2002). To date, the cloning or expression of *Xenopus* titin orthologues has not been reported. Recently a novel human titin exon, termed novex-3, was identified within the human titin locus and shown to encode an alternative C-terminal exon resulting in a truncated titin isoform that is too short to reach the A-band (Bang et al., 2001). This isoform was shown to be expressed in human skeletal and cardiac muscle and the protein was shown to bind the signaling molecule, obscurin (Bang et al., 2001). The novex-3 titin/obscurin complex extends in a spring-like manner when sarcomeres are stretched and has been hypothesized to be involved in stretch-initiated sarcomeric restructuring during muscle adaptation and disease (Bang et al., 2001). This observation also lends to the possibility that the novex-3 titin/obscurin contributes to the development and remodeling of embryonic skeletal and cardiac muscles during embryonic myogenesis. Alternatively, this complex may be involved in the process of switching from the embryonic "fast" fiber type to the "slow" fiber type that occurs during late tailbud stage.

B. Materials and Methods

DNA Constructs

The *Xtn3* EST clone was obtained from OpenBiosystems (IMAGE ID: 5537366). The *Xtn3*-pCMV-SPORT6 plasmid was linearized using SalI and digoxigenin-conjugated *in situ* hybridization probes were synthesized using T7 polymerase.

Whole-mount RNA *in situ* Hybridization

Embryos were collected and fixed in MEMFA for 1.5 hours at room temperature. Whole-mount *in situ* hybridization was performed as previously described (Harland, 1991). Embryos were paraffin-embedded using a Tissue-Tek II Tissue Embedding Center and sectioned at a depth of 16 μm on a Microm HM 340 E microtome. Protein alignments were performed using the GeneDoc program.

Reverse Transcription Polymerase Chain Reaction

RNA for RT-PCR was extracted from 30 st.13 embryos, 30 st.38 embryos, 500 mg adult heart tissue, and 500 mg adult thigh muscle tissue using the RNeasy Kit (QIAgen). First-strand cDNA synthesis was performed using Superscript II Kit (Invitrogen) and random hexamers. PCR reactions with Taq polymerase (Promega) were performed according to established protocol using 2 μl of the resulting cDNA. *MHCα*, *m. actin*, and *EF1α* primers sequences were obtained from the website of Eddie DeRobertis. Primers: *Xtn3*: forward- AGT TGA TAA TAC CTT CAA TGC CAC, reverse- AGA TTA TTG CAT GAA ACC CTG C; *Tbx20*: forward- GAG AAT GTT TCC TAC AAT CCG, reverse- TTC CCT CTC AAT ATC AGT GAG; *m. actin*: forward-GCT GAC AGA ATG CAG AAG, reverse-TTG CTT GGA GGA GTG TGT; *MHCα*: forward-GCC AAC GCG AAC CTC TCC AAG TTC CG, reverse-GGT CAC ATT TTA TTT CAT GCT GGT TAA CAG G; *EF1α*: forward-CAG ATT GGT GCT GGA TAT GC, reverse-ACT GCC TTG ATG ACT CCT AG.

C. Results and Discussion

Sequence Comparisons Between Titin Novex-3 Homologues

Xtn3, the partial *Xenopus* novex-3 titin isoform (GenBank accession: DQ241814) was initially identified in a screen for differentially expressed cardiac genes as an expressed-sequence tag (EST; GenBank accession: CB564652) expressed in the developing heart. This EST was subsequently sequenced and a BLAST search revealed that the EST is highly similar to the human truncated titin isoform, novex-3 titin. The partial *Xenopus* novex-3 titin EST consists of 2771 nucleotides, encodes for 544 putative amino acids, and appears to lie completely within the putative novex-3 exon as identified by comparisons with human novex-3 titin (Fig. 5.1A). Furthermore, this EST appears to align with a single exon within the titin gene in the *Xenopus tropicalis* genome (JGI, ver. 4.1, scaffold 163). Protein alignments performed against a predicted chick titin (GenBank accession: XM_421979), predicted mouse novex-3 titin (GenBank accession: XM_619766), predicted cow novex-3 titin (GenBank accession: XM_617216), and human novex-3 titin (GenBank accession: NM_133379) reveal identities in the range of 39-48% (Fig. 5.1A,B). Furthermore, all three immunoglobulin cell adhesion molecule (IGcam) domains are conserved between human and frog, as identified by the NCBI conserved domain search (cd#: cd00931.2; Fig. 5.1A). Thus, the partial *Xenopus* titin clone is likely the *Xenopus* orthologue of human novex-3 titin and we refer to this transcript as *Xtn3* for *Xenopus titin novex 3*.

XTn3 Expression Pattern

Human novex-3 titin consists of 5604 amino acids and 16,812 nucleotides. Due to the large size of the titin gene and the many titin isoforms, it was not feasible to clone the full-

length version of *Xtn3*, thus the partial *Xtn3* EST was used for whole-mount *in situ* hybridization analyses. The novex-3 exon is contained only in the novex-3 titin isoform mRNA, thus the partial *Xtn3* probe is specific for this titin isoform. Expression analyses of *Xtn3* reveal that this transcript is initially detected during the onset of neurulation (stage 14/15) throughout the developing presomitic mesoderm. At this stage, *Xtn3* is expressed in a narrow anterior domain which flares laterally toward the posterior region of the presomitic mesoderm (Fig. 5.2A). This pattern mirrors that of the presomitic mesoderm as it constricts in a wave from anterior to posterior during somite formation. By mid-neurula stage (stage 19) *Xtn3* expression becomes more restricted as the forming somites develop into vertical stripes (Fig. 5.2B, C). In higher magnifications of tailbud stage embryos (stage 35) it is apparent that the somitic expression lies within a thin stripe down the center of the somite as well within a lower intensity stripe along the anterior and posterior borders of individual somites (inset, Fig. 5.2H). The somitic expression continues through development until tadpole stage at which point *Xtn3* expression is almost completely undetectable (Fig. 5.2N). By stage 37, *Xtn3* also becomes expressed in the migrating ventral myoblasts, which will eventually become the ventral abdominal muscles (Fig. 5.2J, L). Also at this stage *Xtn3* expression becomes apparent in the developing facial and jaw muscles (Fig. 5.2J, L). Expression in the migrating heart primordia was first detected prior to fusion of the primordia at the midline (stage 26; Fig. 5.2D, E). Cardiac expression persists throughout all stages of heart development until tadpole stages, at which point *Xtn3* expression is almost completely lost (Fig. 5.2N-P). By tadpole stage (stage 46), only weak expression is detected in the jaw muscles. Staining of the adult heart shows very little *Xtn3* expression globally. However, discrete groups of *Xtn3*-expressing cells can be detected near the surface of the myocardium

(Fig. 5.2O, P). Thus, it appears that a global downregulation of *Xtn3* corresponds with fully differentiated muscle and completion of heart development, although some expression remains in adult tissues.

Histological sectioning of embryos stained by whole-mount *in situ* hybridization revealed that *Xtn3* is initially expressed more highly in the dorsal medial lip and medial regions of the developing myotome during neurula stage (stage 19; Fig. 5.3A). *Xtn3* expression then becomes expanded throughout the entire dorsal/ventral axis of the somitic domain during later stages of myotome development (Fig. 5.3A, C, E, G). Cardiac expression is detected exclusively in the myocardium, consistent with the defined role of titin as a sarcomeric structural protein (Fig. 5.3D-H). *Xtn3* appears to be expressed in a gradient during looping stages of cardiogenesis, with higher levels in the ventral cardiac regions (Fig. 5.3F, H). Sectioning further demonstrates *Xtn3* expression throughout the developing jaw muscles in the head (Fig. 5.3I).

To test whether *Xtn3* transcripts are detectable in adult heart and muscle tissues, RT-PCR was performed on RNA isolated from st.13, st.38, adult heart and adult muscle tissues. *Xtn3* transcripts were present in st.38, adult heart and adult muscle tissues, as were transcripts for *myosin heavy chain* α (*MHC*α) and *muscle actin*. In contrast, the heart marker *Tbx20* was only detectable in st.38 embryos and in adult heart tissue. Thus, it appears that while *Xtn3* may be downregulated at tadpole stages as assayed by whole-mount *in situ* hybridization, *Xtn3* transcripts can be detected by sensitive methods in adult muscle tissues.

Figure 5.1. XTN3 is a conserved titin isoform.

(A) Schematic depicting human novex-3 titin and the partial XTN3 proteins, including positions of conserved Ig domains and amino acid lengths. (B) Protein alignment of *Xenopus laevis* XTN3, a predicted chick titin, a predicted mouse novex-3 titin, a predicted cow titin, and human novex-3 titin. Alignment was performed using the GeneDoc program. Red underlines indicate conserved Ig domains as identified by the NCBI conserved domain search. (C) Table showing degree of protein identity and similarity between the putative novex-3 titin orthologues.

Figure 5.1. XTN3 is a conserved titin isoform.

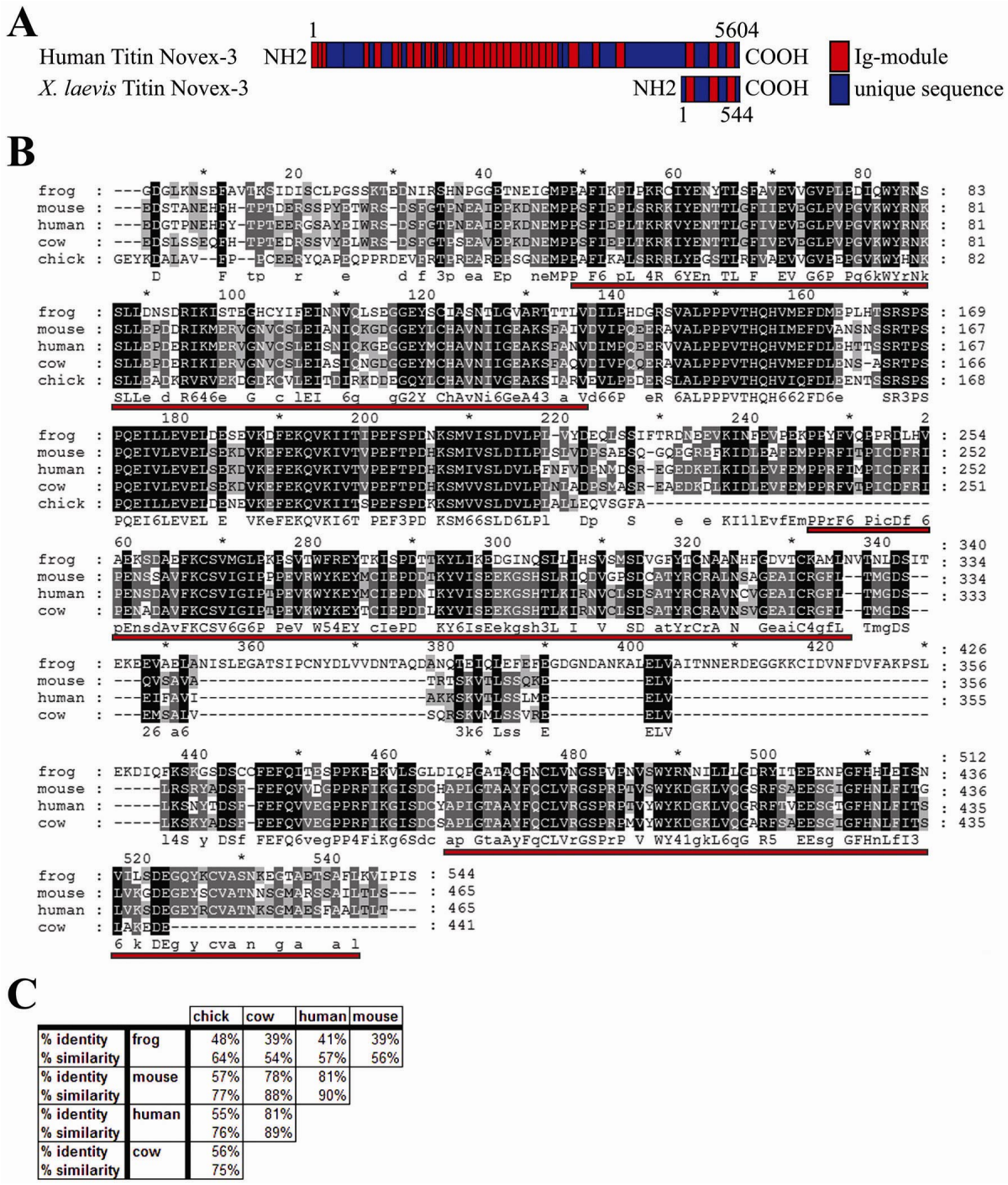

Figure 5.2. *Xtn3* is developmentally expressed throughout the somites, heart, and jaw myoblasts from early neurula to late tailbud stages.

(A-P) *In situ* hybridization showing expression of the *Xtn3* at the indicated stages. (A-C) Neurula stage embryos. Anterior is to the left. (A) and (C) are dorsal views. (B) is a lateral view. (D-M). Tailbud stage embryos. (E,G,I,K,M). Ventral anterior views. Anterior is up. (H). Inset shows higher magnification of somite region. Bracket indicates one individual somite. (N). Tadpole stage embryo. Note the lack of staining in trunk and heart. Some light staining remains in facial muscles. (O, P). Adult heart lacking global *Xtn3* expression. (P) is a magnification of (O). Black arrowhead indicates isolated group of *Xtn3*-expressing cells. *h*, heart; *hp*, heart primordia; *jm*, jaw myoblasts; *psm*, presomitic mesoderm; *pc*, pigment cells; *vm*, ventral myoblasts; *s*, somites; *t*, trunk.

Figure 5.2. *Xtn3* is developmentally expressed throughout the somites, heart, and jaw myoblasts from early neurula to late tailbud stages.

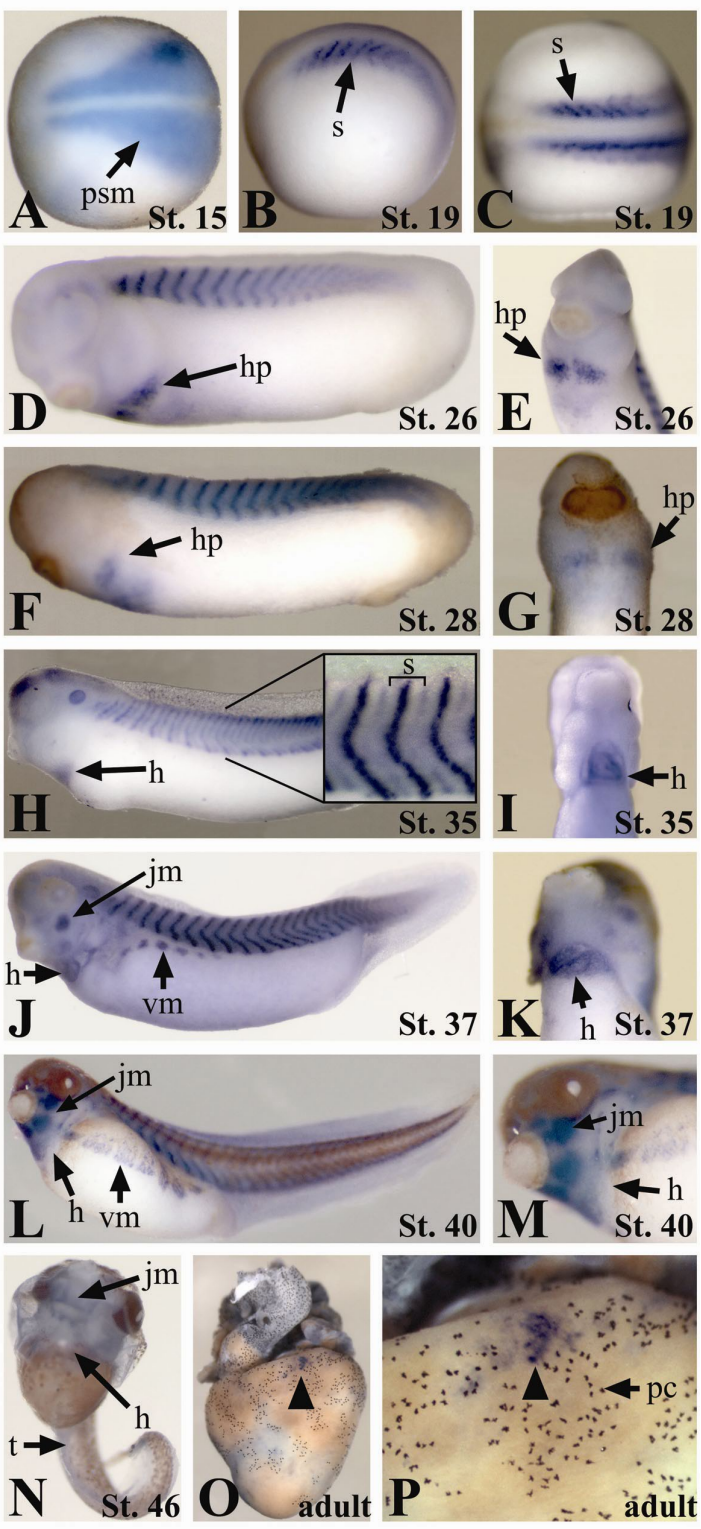

Figure 5.3. Histology of *Xtn3* expression.

Paraffin embedded embryos were sectioned at a depth of 16 μm after *in situ* hybridization. (A, C, E, G) Transverse sections through developing somites. (B, D, F, H) Transverse sections through developing cardiac region. (I) Transverse section showing jaw myoblasts in the head. *a*, atrium; *ec*, endocardium; *hp*, heart primordia; *jm*, jaw myoblasts; *mc*, myocardium; *nc*, notochord; *nt*, neural tube; *s*, somites; *v*, ventricle; *vm*, ventral myoblasts.

Figure 5.3. Histology of *Xtn3* expression.

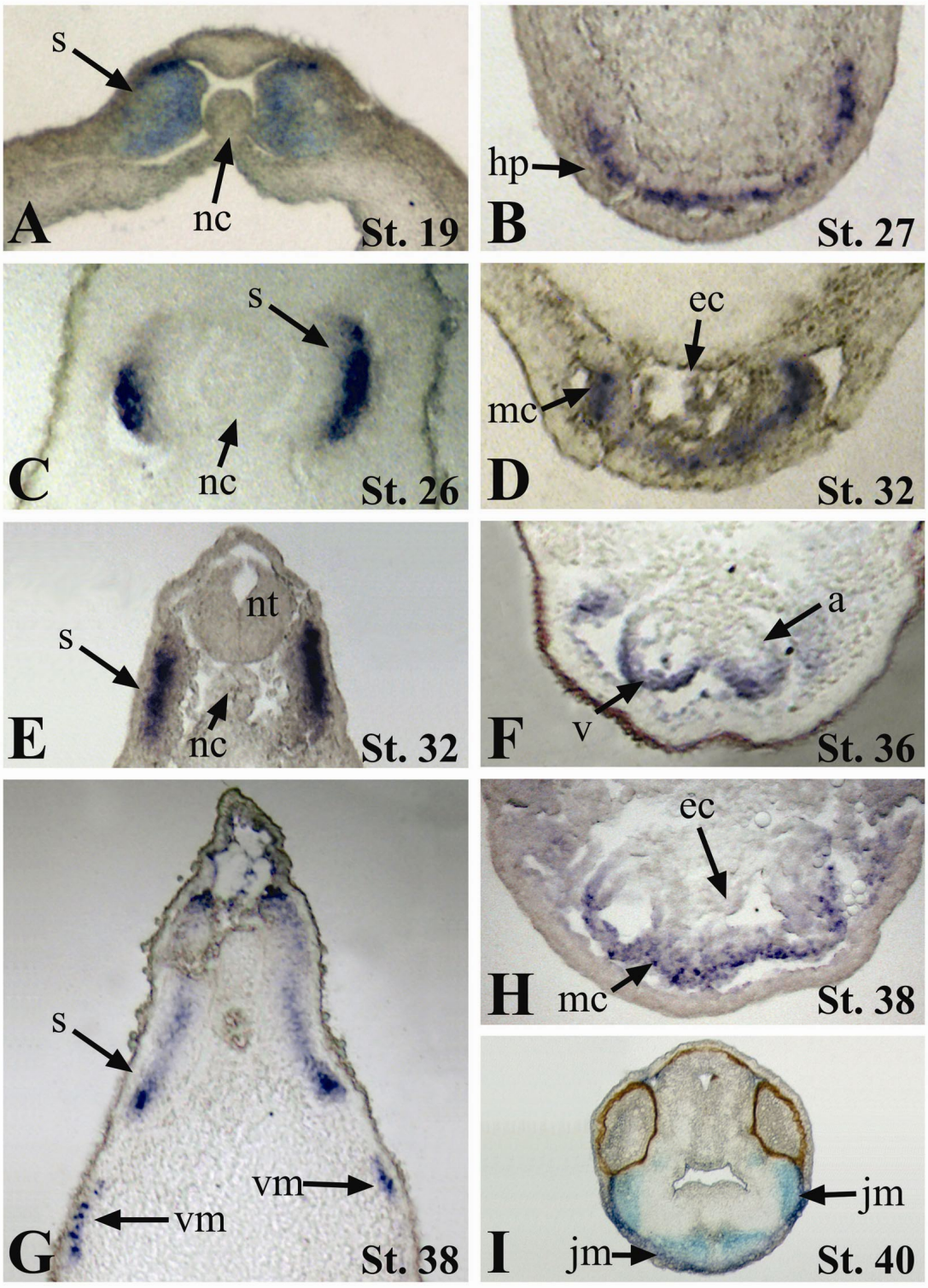

Figure 5.4. *Xtn3* is expressed in adult heart and skeletal muscle.

RNA from st.13 embryos, st.38 embryos, adult heart and adult muscle tissue was isolated and 100 ng of RNA subjected to RT-PCR. *Xtn3* RT-PCR shows expression in St. 38, adult heart and adult muscle tissues. "-RT" controls lack reverse transcriptase to show lack of genomic contamination. *Tbx20* primers serve as controls for heart tissue, *MHC*α and *muscle actin* serve as controls for muscle tissue, and *EF1*α serves as loading control.

Figure 5.4. *Xtn3* is expressed in adult heart and skeletal muscle.

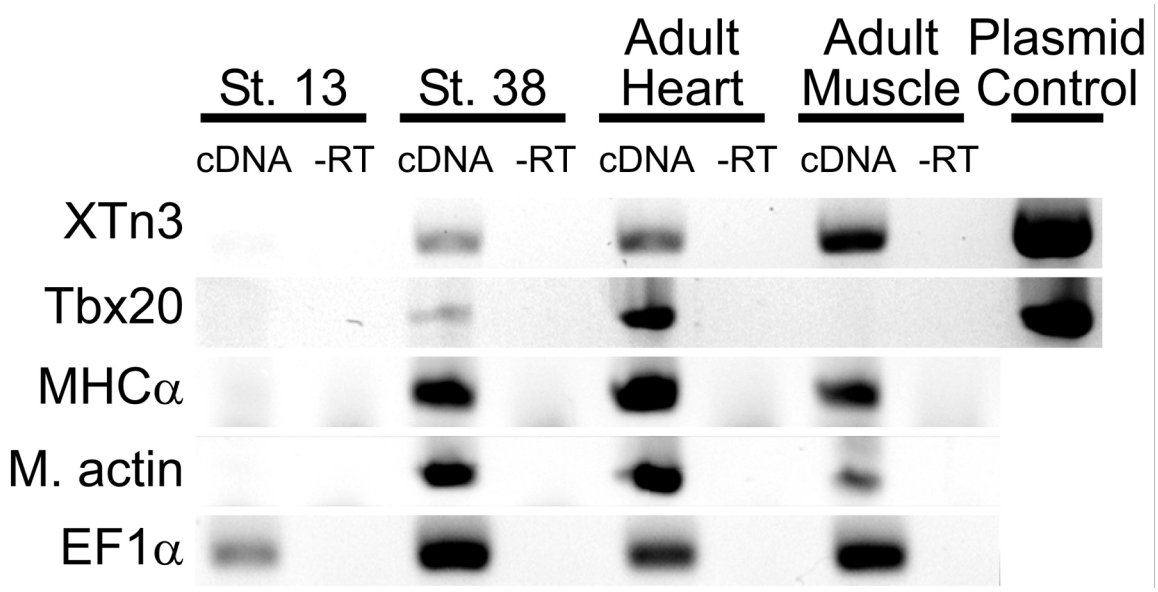

CHAPTER VI

HSP27 EXPRESSION IS DEVELOPMENTALLY REGULATED IN DIFFERENTIATING MUSCLE AND IS REQUIRED FOR PROPER CARDIAC PRECURSOR FUSION

A. Introduction

Of the many known congenital diseases that affect humans, those affecting development of the heart are among the most severe. Cardiogenesis is an incredibly complex process requiring the coordination of many events within well-defined spatial and temporal dimensions (reviewed in Harvey, 2002). The complex nature and multitude of coordinated steps within cardiogenesis makes this process inherently sensitive to genetic perturbation. As such, it is not surprising that congenital heart diseases are estimated to be present in about thirty percent of all infant deaths due to congenital disease (Thom et al., 2006). Furthermore, current data from the Centers for Disease Control estimates that one out of every one hundred and ten babies born in the United States is afflicted with a congenital heart disease (Botto et al., 2001).

Formation of a functioning heart requires the organization and synchronization of many cellular and tissue-level processes, including proper cell movements and polarity establishment, specification and differentiation of cardiac precursors, and morphogenesis of the heart. During gastrulation a bilaterally symmetric pair of fields within the anterior lateral

plate mesoderm (LPM) is initially specified as cardiac precursors. Once the cardiac precursor fields are specified, they undergo two separate migration events as neurulation proceeds. The large-scale tissue movements involved in neurulation result in the anterior migration of the cardiac progenitors toward more anterior regions. This process seems to be largely controlled by FGF factors such as FGF8 and FGF4 (Beiman et al., 1996; Ciruna and Rossant, 1999; Gisselbrecht et al., 1996; Sun et al., 1999). Soon after migration to more anterior positions in the embryo, the cardiac progenitors then migrate ventrally as an epithelial sheet towards the anterior ventral midline where they proceed to fuse and form a linear heart tube (DeHaan, 1963; Kolker et al., 2000; Mohun et al., 2003).

Several requirements for the ventral migration and fusion of the cardiac fields have thus far been identified, including proper cardiomyocyte differentiation (Reiter et al., 1999; Yelon et al., 2000), interaction or signaling from the endoderm (Alexander et al., 1999; Kikuchi et al., 2000; Reiter et al., 1999; Schier et al., 1997), epithelial organization of the cardiac fields, and migration cues from the midline (Trinh and Stainier, 2004). Recent work by Trihn and Stanier has demonstrated a requirement for *fibronectin* (*Fn*) in the migrating cardiac precursor fields in zebrafish; fish mutant for *Fn* exhibit cardia bifida, which is characterized by unfused cardiac progenitors that independently differentiate into cardiac tissue (Trinh and Stainier, 2004). Their results indicate that a gradient of *Fn* at the junction between the endoderm and mesoderm appears to be required for epithelial integrity within the cardiac fields. Furthermore, deposition of *Fn* at the ventral midline appears to regulate the timing of migration. Other studies have shown that mutant mice lacking *Fn* display defects in cardiogenesis, despite normal specification of the cardiac precursors (George et al., 1997; George et al., 1993). It is also well established that the anterior endoderm is required for

cardiac progenitor migration (reviewed in Lough and Sugi, 2000). For example, many genes involved in endoderm differentiation and maturation, including *Gata4*, *Gata5*, *one-eyed pinhead* (*oep*), *casanova*, and *miles apart* result in cardia bifida when mutated in mice or fish (Kuo et al., 1997; Kupperman et al., 2000; Reiter et al., 1999; Stainier, 2001). Furthermore, studies have shown that abrogation of proper myocardial differentiation can also result in cardia bifida (Reiter et al., 1999; Yelon et al., 2000). In the present study we report an additional requirement for proper cardiac fusion: expression and function of the small heat shock protein, *Hsp27*.

Hsp27, also called *Hsp25* in mice and *HspB1* in humans, is one of the most widely distributed and most studied of the small heat shock proteins (reviewed in Ferns et al., 2006). Changes in *Hsp27* expression have been observed in cells and tissues exposed to many stress conditions, including oxidative damage (Arrigo, 2001; Baek et al., 2000; Dalle-Donne et al., 2001; Escobedo et al., 2004; Huot et al., 1996; Komatsuda et al., 1999; Mehlen et al., 1995), metal toxicity (Bonham et al., 2003; Leal et al., 2002; Somji et al., 1999), and ischemia (Hollander et al., 2004; Reynolds and Allen, 2003; Shelden et al., 2002; Vander Heide, 2002), as well as in disease states such as cardiac hypertrophy (Knowlton et al., 1998; Scheler et al., 1999), and muscle myopathies (Benndorf and Welsh, 2004). In addition, a role for HSP27 function has been implicated in many cellular processes, including protein chaperone activity (Jakob et al., 1993), regulation of cellular glutathione levels (Arrigo, 2001; Baek et al., 2000), apoptotic signaling (Bruey et al., 2000; Paul et al., 2002), inhibition of actin polymerization (Benndorf et al., 1994; Miron et al., 1991; Rahman et al., 1995), and stabilization of actin filament arrays (Huot et al., 1996; Lavoie et al., 1993a; Lavoie et al., 1993b; Lavoie et al., 1995).

Hsp27 is known to be expressed during both skeletal and cardiac muscle development in several organisms, including human (Shama et al., 1999), mouse (Gernold et al., 1993), pig (David et al., 2000) and zebrafish (Mao et al., 2005; Mao and Shelden, 2006). However, to date the biological significance of this developmentally regulated expression has not been analyzed in developing embryos. Furthermore, previous attempts to identify *Xenopus laevis* (*X. laevis*) orthologues of the *Hsp27* family have reportedly failed (Norris et al., 1997). Here we report the sequence and expression of the *X. laevis* orthologue of *heat shock protein 27* (*XHsp27*). We demonstrate using anti-sense morpholinos that XHSP27 is required for proper fusion of cardiac precursors and for actin organization in developing cardiac and skeletal muscle. We further demonstrate that cardiac specification and differentiation appear unaltered as assayed by several markers of cardiac precursor and differentiated cardiomyocyte populations.

B. Materials and Methods

Embryo Culture and Injections

Preparation and injection of *X. laevis* embryos was carried out as previously described (Wilson and Hemmati-Brivanlou, 1995). Embryos were staged according to Nieuwkoop and Faber (Nieuwkoop and Faber, 1967). An antisense morpholino oligonucleotide was designed against the translation start site of *XHsp27*. XHSP27 morpholinos were obtained from Gene Tools, LLC. with the following sequence: 5' AAT TCT GCG TTC TGA CAT TTT CTC T 3'. The human β-globin splice-mutant standard control morpholino from Gene Tools was used as control. For the *in vitro* translation studies,

TBX20MO was used to show specificity of the HSP27MO (Brown et al., 2005). HSP27MO was injected at 60 ng/embryo.

Translation Inhibition by Morpholinos

In vitro translations were performed using TNT Coupled Reticulocyte Lysate System (Promega) following the manufacturer's protocol. Reactions were carried out in the presence or absence of HSP27MO or TBX20MO. A carboxy-terminal hemagluttin tagged version of HSP27 was generated using the pSP64T-HA vector (generous gift of Masazuma Tada). An HA-tagged TBX20 was also used in the *in vitro* translation study (Brown et al., 2005). We have recently demonstrated that *X. laevis* SHP2 is uniformly expressed throughout early development (Brown et al., 2005) and anti-PTP1D/SHP2 primary antibody was used at 1:2500 (Transduction Laboratories) as a loading control with peroxidase-conjugated AffiniPure donkey anti-mouse (H+L) 2° antibody (1:10,000). HA-tagged proteins were probed with anti-HA primary antibody (Covance) at 1:1000 dilution, and peroxidase-conjugated AffiniPure Donkey anti-mouse (H+L) secondary antibody (Jackson ImmunoResearch Laboratories) at 1:10,000 dilution. For *in vivo* translation analyses, embryos were injected with MOs and mRNA at the one-cell stage. At stage 19, 40 embryos per treatment were collected and lysed in 300 μl of lysis buffer: 140 mM NaCl, 50 mM Tris (pH 7.6), 10 mM EDTA, 1% Surfact-Amps Triton-100 (Pierce), Complete EDTA-free Protease Inhibitor (Roche), and 25mM PMSF (Roche). Lysates were resolved on 12% SDS-PAGE gels, and visualization was carried out using luminol-based chemi-luminescence solutions at 1:1 ratio: solution A: 100 mM Tris pH8.5, 2.5 mM Luminol (Sigma), 0.4 mM p-Coumaric acid (Sigma); solution B: 100 mM Tris pH 8.5, 0.02% H_2O_2 (Sigma).

Whole-mount RNA *in situ* Hybridization

Whole-mount *in situ* hybridization was performed as previously described (Harland, 1991). Probes used include *Tbx20* (Brown et al., 2003), *Nkx2.5* (Brown et al., 2005), *Gata4* and *Gata6* (generous gifts of Roger Patient; (Jiang and Evans, 1996), *Mlc1v'* (IMAGE clone 4408657, GenBank Accession No.: BG884964), and *Titin Novex 3* (Brown et al., 2006).

Immunohistochemistry

Embryos were prepared for whole-mount immunohistochemistry as previously described (Kolker et al., 2000). Briefly, fixed embryos were incubated overnight at 4°C with an antibody against *myosin heavy chain* α (Abcam), at a dilution of 1:500. Following washes, the embryos were incubated overnight at 4°C with a Cy3-conjugated anti-mouse secondary antibody (Sigma) at a dilution of 1:100. For imaging, embryos were cleared with 2:1 benzyl benzoate: benzyl alcohol and viewed on a Leica MZFLIII fluorescence dissecting microscope. For immunostaining of histological sections, embryos were collected at the indicated stages, fixed for 2 hours in 4% paraformaldehyde, and embedded in OCT cryosectioning medium (Tissue Tek). Cryostat sections (14 μm) were rinsed with wash buffer (PBS with 1% Triton and 1% heat inactivated calf serum), and incubated at 4°C overnight, as indicated, with mouse anti-*myosin heavy chain* α (Abcam), at a dilution of 1:500 or anti-tropomyosin 1:50 (Developmental Studies Hybridoma Bank), and phalloidin conjugated to Alexa 488 flourophore (Molecular Probes). Sections were then rinsed with wash buffer and incubated with anti-mouse Cy3-conjugated secondary antibody (1:200; Sigma). Sections were rinsed and incubated for 20 minutes at room temperature with DAPI, cover slipped and visualized on a Zeiss LSM410 confocal microscope.

Transmission Electron Microscopy

Briefly, stage 37 embryos were fixed in 2% paraformaldehyde/2.5% gluteraldehyde overnight (Goetz et al., 2006). Embryos were post-fixed in ferrocyanide-reduced osmium and embedded in Spurr's epoxy resin. Transverse ultra-thin (70 nm) sections were mounted on copper grids, and post-stained with 4% aqueous uranyl acetate followed by Reynolds' lead citrate. Sections were imaged with a LEO EM-910 transmission electron microscope.

C. Results

XHsp27 Expression is Developmentally Regulated in Differentiating Cardiac and Skeletal Muscle.

XHsp27, the *X. laevis* orthologue of *Hsp27* (HSP25, HspB1; GenBank Accession No.: EF066483) was initially identified in a screen for differentially expressed cardiac genes as an expressed sequence tag (GenBank Accession No.: AW766262) expressed in the developing heart (D. Brown and F.L.C., unpublished data). This EST was subsequently sequenced and a BLASTn search revealed that the EST is highly similar to several members of the small heat shock protein 27 subfamily. The *X. laevis Hsp27* transcript consists of at least 1123 nucleotides and encodes for 213 putative amino acids (Fig. 6.1A). The *XHsp27* transcript appears to align with a single locus within the *Xenopus tropicalis* (*X. tropicalis*) genome (JGI, ver. 4.1, scaffold 72), consisting of 3 exons separated by two introns. This organization appears to mirror that of mouse *Hsp27* (Ferns et al., 2006), which also consists of three exons. In addition, a synteny search using Metazome (**www.metazome.net**) reveals that the genomic locus within *X. tropicalis* is highly syntenic with the *Hsp27* orthologue locus on human chromosome 7, mouse chromosome 5, rat chromosome 12, and chick

chromosome 19. (Fig. 6.1C). Protein alignments performed against *Hsp27* orthologues in human (GenBank Accession No.: BC073768), rat (GenBank Accession No.: NM_031970), mouse (GenBank Accession No.: AK003119), pig (GenBank Accession No.: NM_001007518), dog (GenBank Accession No.: NM_001003295), chick (GenBank Accession No.: NM_205290), and zebrafish (GenBank Accession No.: NM_001008615) reveal conservation of identities in the range of 64-70% (Fig. 6.1A-B). An "alpha-crystallin-hsps" domain within the transcript is conserved between the *Hsp27* orthologues, as identified by the NCBI conserved domain search (cd#: cd00298; Fig. 6.1A). The crystallin domain is known to be important in homo- and heterodimerization between various sHSPs (Feil et al., 2001). Furthermore, one of two putative actin interacting domains appears to be highly conserved between *XHsp27* and the various orthologues, with a second domain showing a smaller degree of conservation (Fig 6.1A; Mao et al., 2005). Thus, this transcript is likely the *X. laevis* orthologue of *Hsp27* and we refer to this transcript as *XHsp27*.

By whole-mount *in situ* hybridization, *XHsp27* appears to be expressed diffusely throughout the developing embryo during gastrulation, consistent with recent findings in zebrafish (Fig. 6.2; Mao and Shelden, 2006). Shortly after gastrulation *XHsp27* becomes restricted to thin dorsal-ventral stripes within a subdomain of each developing myotome within the somitic mesoderm (Fig. 6.2A). This expression initially begins in the anterior most somites and proceeds in a wave towards the posterior end, mirroring the wave of somitic formation and development (Fig 6.2B-L). As myogenesis progresses, the thickness of each vertical stripe expands to encompass the entire myotome and this expression remains in the developing muscle until at least stage 40 (Fig 6.2B-I). During cardiac precursor fusion and linear heart tube formation, *XHsp27* expression commences throughout the developing

myocardium and remains expressed throughout the developing heart at all stages examined (Fig 6.2G-I, L, M). Furthermore, as muscle development continues during early tadpole stages, *XHsp27* expression becomes evident in other muscle domains such as those in the developing jaw and the body wall (Fig 6.2I). Expression is also detected in the brain of tadpole stage embryos (Fig 6.2I). These results indicate that *XHsp27* is a developmentally regulated gene and may be involved in gastrulation, cardiac and skeletal myogenesis, and neural development.

XHSP27 Morpholinos Specifically Inhibit XHSP27 Translation

In order to test whether *XHsp27* protein is required during embryogenesis, we sought to knock down endogenous XHSP27 protein levels using antisense morpholino oligonucleotides. To this end we designed morpholinos targeted against the start site of *XHsp27*, which we refer to as HSP27MO (Fig. 6.3A). Unfortunately, attempts to detect endogenous or *in vitro* translated *X. laevis* HSP27 were unsuccessful using several of the available commercial HSP27 antibodies. Thus we sought to test the efficiency and specificity of morpholino translation inhibition using a hemagglutinin (HA) epitope-tagged version of XHSP27 both *in vitro* and *in vivo*. For the *in vitro* inhibition study, transcription/translation reactions were incubated with HA-HSP27 construct alone and together with increasing concentrations of HSP27MO (Fig. 6.3B). TBX20MO was included as a negative control (Brown et al., 2005). Furthermore, HSP27MO was incubated with HA-*Tbx20* to show specificity of the HSP27MO. Results from these assays show that HSP27MO efficiently blocks translation of HA-*XHsp27 in vitro* while TBX20MO and ControlMO do not. In contrast, HSP27MO does not block translation of HA-TBX20 (Fig. 6.3B).

In order to test whether HSP27MO can knock down XHSP27 translation *in vivo*, HA-Hsp27 capped mRNA was injected into one-cell stage embryos along with HSP27MO. To insure that the MOs did not bind the mRNA prior to injection, embryos were first injected with 30 ng or 60 ng HSP27MO or 60 ng ControlMO. Embryos were then re-injected with 100pg HA-HSP27 capped mRNA prior to first cleavage. Embryos were then collected at stage 20, lysed, submitted to Western blotting with an anti-HA antibody. An antibody against the protein phosphatases, SHP2, was used as loading control (Brown et al., 2005). As shown in Figure 6.3C, embryos injected with HSP27MO completely lack HA-HSP27 protein, in contrast to ControlMO injected embryos, which display no inhibition of HA-HSP27 translation.

XHSP27 misexpression results in gastrulation defects and can be partially rescued by XHSP27 morpholinos

As described above, we sought to test morpholino efficiency by coinjecting morpholinos and capped HA-XHsp27 capped mRNA into one-cell stage embryos. Surprisingly, injection of 1ng HA-*XHsp27* resulted in dramatic gastrulation defects characteristic of exogastrulation, which is a failure of blastopore closure (Fig. 6.4A). *Hsp27* is known to regulate actin filament polymerization and stability, suggesting that the failure of blastopore closure may be due to defects in actin dynamics (reviewed in Mounier and Arrigo, 2002). The fact that *XHsp27* is normally expressed diffusely in gastrulating embryos, combined with the observation that misexpression of *XHsp27* results in gastrulation defects, suggest that regulation of *XHsp27* expression or activity is necessary for proper gastrulation. Furthermore, embryos co-injected with HA-*XHsp27* mRNA and HSP27MO displayed a

partial rescue of the gastrulation phenotype (Fig. 6.4B, C). Injection of HA-XHsp27 alone results in 99.5% exogastrulation. However, embryos co-injected with 60 ng HSP27MO display exogastrulation 66% of the time, and the gastrulation defects appear less severe (Fig. 6.4). These results suggest that the gastrulation defects are a specific effect of HA-*XHsp27* misexpression and that HSP27MO can inhibit translation of the injected HA-*XHsp27* mRNA.

The Cardiac Transcriptional Program Appears to be Unaltered in XHSP27 Morphants.

To assess whether the cardiac and skeletal muscle precursors are properly specified and differentiate, embryos were injected with HSP27MO or ControlMO at the one-cell stage. Whole-mount *in situ* hybridizations were then performed using a panel of cardiac and skeletal muscle markers. *Tbx20*, *Nkx2.5*, *Gata4*, and *Gata6* probes were used to mark both early cardiac precursors and terminally differentiated cardiomyocytes, while *titin novex-3* (*XTn3*) and myosin light chain 1v' (*Mlc1v'*) were used to mark differentiated skeletal and cardiac muscle. As shown in Figure 6.5, the cardiac and skeletal muscle domains appeared normal in all cases. This data, combined with the observation that the hearts are contractile, suggests that the cardiac and skeletal muscle precursors are properly specified, migrate to the correct location within the embryo and can initiate terminal differentiation.

Knockdown of XHSP27 Protein Translation Results in Cardia Bifida.

To determine the requirement for XHSP27 during development, we again injected HSP27MO into one-cell stage embryos. Despite *XHsp27* expression in gastrula embryos, no defects in gastrulation were observed, suggesting that XHSP27 is not required for this process. However, by linear heart tube formation stage (stage 33), defects in heart tube fusion

became apparent as assayed by myosin heavy chain (MHC) whole-mount antibody staining (Fig. 6.6J-L). As shown in Figure 6.4, XHSP27 morphants display a bifurcation in the posterior inflow region of the linear heart tube. The degree of bifurcation varies between embryos, and in the most severe cases the hearts appear to be almost entirely divided, resulting in complete cardia bifida (Fig. 6.6P-R). Despite aberrant morphogenesis of the heart, the extant cardiac tissue becomes rhythmically contractile, although blood flow is not evident in these embryos (data not shown). This data suggests that the cardiomyocytes differentiate, but the cardiovascular system is not functional. Furthermore, XHSP27 morphant embryos arrest development by early tadpole stages (stage 40) and die shortly thereafter, presumably due to the lack of a functioning cardiovascular system. These results suggest that XHSP27 is critical for proper cardiac morphogenesis.

XHSP27 Morphants Display Actin Filament Disorganization in the Developing Heart and Somites.

Recent studies have shown that in addition to a requirement for cardiac differentiation and endoderm maturation in heart tube formation, proper epithelial organization, adhesion and migration are absolutely critical for heart tube formation. Furthermore, HSP27 has been shown to stabilize the actin cytoskeleton in response to stress (Huot et al., 1996; Lavoie et al., 1993a; Lavoie et al., 1993b; Lavoie et al., 1995). Thus considering that the cardiomyocytes are apparently specified and differentiate properly, *XHsp27* is not detected in endoderm tissue, and *XHsp27* is known to be involved in cytoskeletal dynamics, we hypothesized that actin organization may be disrupted in the developing myotomes and heart of XHSP27 morphants. To address this possibility we injected HSP27MO into one-cell stage embryos

and collected the embryos at stages during cardiac fusion (stage 28), linear heart tube formation (stage 33), and cardiac looping (stage 37). Embryos were then transversely cryosectioned and cardiac sections were immunostained for *myosin heavy chain α* (*MHC*) using a *MHC*-specific antibody and F-actin using phalloidin. Somitic sections were stained for F-actin and with DAPI to mark nuclei in somitic sections. In control hearts, actin staining is most apparent at the basal and apical surfaces of the cells in the forming heart tube, which consists of a single layer of cardiac cells, as well as in fibers perpendicular to the lumen, which appear to correspond with the lateral membranes of cardiac cells (Fig. 6.7A-C, G-I). However, in XHSP27 morphant hearts, actin staining appears diffuse and disorganized (Fig. 6.7D-F, J-L). Few distinct fibers are apparent within the morphant hearts, except where lumen formation occurs (Fig. 6.7L). A similar and more dramatic defect in actin organization is evident within the developing somites. In control morpholino-injected embryos, the somites display thick, highly organized actin bundles oriented along the anterior-posterior axis (Fig. 6.7M-O, S-U). However, in XHSP27 morphants, the actin appears disorganized and scattered throughout the somites (Fig. 6.7P-R, V-X). Furthermore, the somitic domain itself appears to be larger and less well-defined (Fig. 6.7P-R, V-X). This appearance is similar to the appearance of the somites at earlier stages, after which the somites normally become smaller and more compact, possibly due to the formation of the thick actin bundles. These results suggest that *XHsp27* is required for proper regulation of cytoskeletal dynamics during myogenesis.

In order to gain further insight into the nature of microfilament disorganization in XHSP27 morphants, embryos were injected with control or XHSP27 morpholinos, collected at stage 38 and visualized using transmission electron microscopy (TEM). As shown in

Figure 6.8, ControlMO hearts display many myofibril bundles, the majority of which were found to be oriented along the anterior-posterior axis, as demonstrated by transversely sectioned myofibers (Fig. 6.8-C). In regions where longitudinal sections of myofibers are present, clear z-lines are evident showing the fusion between individual sarcomeres (Fig. 6.8A, B). Furthermore, in transverse myofiber sections, the highly organized myosin structure can be seen (Fig. 6.8C inset). In contrast, XHSP27 morphant hearts show very few myofiber structures (Fig. 6.8D-E). In addition, the occasional myofibers are very short and no z-lines or connections between multiple fibers were apparent, indicating a lack of sarcomeric assembly (Fig. 6.8D-E). In some sections, large aggregates of bodies are apparent that appear very similar to cross-sectional views of myosin in control myofibrils (Fig. 6.8F inset). However, these aggregates lack any of the obvious structure in spacing or organization characteristic of myofibrils (Fig. 6.8F inset). Similar results are observed within the developing myotomes in the somitic region of XHSP27 morphants. In the forming skeletal muscle, all myofibers analyzed appeared to be sectioned transversely, indicating that these fibers are arranged along the anterior-posterior axis. ControlMO-injected myotomes display thick myofiber structures that generally extend throughout the entire cell (Fig. 7G, H). In higher magnifications, the myofibril structure is visible as highly ordered arrays of microfilaments (Fig. 7H). In contrast, XHSP27 morphants display much fewer apparent myofibers and most of these appear abnormal in morphology (Fig. 7I, J). Magnification of these myofibers reveal a less-ordered structure and an apparent lack of thick myosin filaments in these structures (Fig. 7J). These observations suggest that the lack in actin organization is accompanied by a failure of myofibril assembly and sarcomere formation.

D. Discussion

Developmental Regulation of Hsp27 Expression

Hsp27 has been shown to be involved in a diverse array of cellular processes. In general, the majority of functional data on *Hsp27* comes from experiments performed both *in vitro* and in cell culture, and much of this research has focused on the function of *Hsp27* in response to various cellular stressors. However, surprisingly little has been done to address the potential role of *Hsp27* in developing embryos. In this study, we report the identification of *X. laevis Hsp27* and demonstrate that this orthologue is expressed in a developmentally regulated manner throughout developing gastrula, skeletal muscle and cardiac tissues. The temporal and spatial expression appears to be highly conserved between *X. laevis* and zebrafish (Mao and Shelden, 2006). As in the fish, *XHsp27* is initially detected diffusely throughout the gastrulating embryo, suggesting that *Hsp27* may be involved in gastrulation. However, embryos depleted of *XHsp27* protein by antisense morpholinos did not display any defects in gastrulation, suggesting either that XHSP27 is not required for gastrulation or that a functionally redundant sHSP is present in *X. laevis*. During neurulation, *XHsp27* expression commences in the anterior most developing somites, followed by a posterior wave of expression in newly forming somites. As development proceeds, expression within the somitic myotomes expands to encompass the entire myotome, suggesting that XHSP27 may be involved in morphogenesis or differentiation of muscle tissue. However, our data from XHSP27-depleted embryos suggest that XHSP27 functions in cytoskeletal dynamics but is not involved in differentiation. In addition to its role in skeletal muscle, *XHsp27* is expressed in developing cardiac tissue, beginning at heart tube formation, with this expression continuing through stage 40. During tadpole stages, additional domains of expression within

developing jaw and body wall muscles also become evident, suggesting that XHSP27 may be involved in general mechanisms of muscle formation and development.

Hsp27 in gastrulation

As in the fish, *Hsp27* is initially detected diffusely throughout the gastrulating embryo, suggesting that *Hsp27* may be involved in gastrulation. Surprisingly, embryos depleted of *Hsp27* protein by antisense morpholinos did not display any defects in gastrulation. There are several reasons as to why this might be the case. It may be that *Hsp27* is simply not required for gastrulation per se. However, *Hsp27* is known to be a primary protective agent in response to stress, thus expression during gastrulation may serve as insurance against stressors during this brief but critical moment in development. It is also possible that functional redundancy between other sHSPs in the gastrulating embryo might compensate for the loss of *Hsp27*. In support of this hypothesis, bovine *Hsp20*, a related sHSP member, has been shown to bind actin, similar to turkey *Hsp27*, suggesting a possible similarity in function (Brophy et al., 1999; Miron et al., 1988). Furthermore, *Hsp27* has been found by yeast 2-hybrid studies to bind several sHSPs, including *Hsp20*, *Hsp22* and *αB-crystallin* (Benndorf et al., 2001; Liu and Welsh, 1999). However, *Hsp20* and *Hsp22* have yet to be described in *Xenopus*, and *αB-crystallin* is not known to be expressed in muscle tissues. It will be interesting to learn whether other sHSP members are also involved in embryogenesis. It is also formally possible that our *Hsp27* morpholino does not eliminate all HSP27 protein, allowing enough to be translated to perform its function during gastrulation. This seems unlikely considering the fact that the morpholinos efficiently induce muscular

and cardiac phenotypes at much later stages after the morpholino is significantly diluted in the embryo.

Even more interesting is the finding that misexpression of an epitope-tagged *Hsp27* results in severe defects in blastopore closure. *Hsp27* has been shown to be an effective inhibitor of actin polymerization *in vitro*, and many studies have implicated *Hsp27* in actin cytoskeletal dynamics (reviewed in (Mounier and Arrigo, 2002). In addition, studies have shown that a dominant-negative form of *Xenopus Ral*, a downstream effector of the *Ras* pathway, results in actin disorganization leading to failure of blastopore closure (Lebreton et al., 2003). Thus, it is possible that an alteration of actin organization due to overexpression of *Hsp27* is the primary cause of the failure of blastopore closure. In support of this hypothesis are the findings that dominant-negative *Hsp27* results in aberrant microfilament morphology and defects in endothelial cell motility and that *Hsp27* regulates fibroblast adhesion, migration, and matrix contraction during wound healing (Hirano et al., 2004; Piotrowicz et al., 1998).

Hsp27 in Cardiogenesis and Myogenesis

Formation of a linear heart tube requires the coordination of cardiac specification, differentiation, and cell behavior within defined spatial and temporal domains. In the present study, we identify the small heat shock protein, *Hsp27*, as being integral to this process. Several studies have shown that *Hsp27* is expressed in developing muscle tissues. While it is clear that *Hsp27* is critical in mediating the cellular response to a wide variety of stressors, it is unclear what role *Hsp27* may be playing during cardiogenesis and myogenesis under un-stressed physiological conditions. Evidence from studies of embryonic stem cell

differentiation has suggested that *Hsp27* can function as a molecular switch between differentiation and apoptosis (Mehlen et al., 1997). Furthermore, it is known that proper cardiomyocyte differentiation is necessary for cardiac fusion and heart tube formation (Reiter et al., 1999; Yelon et al., 2000). However, while our data does not rule this out as a possible function for *XHsp27*, it at least suggests that a primary function of *Hsp27* may be to regulate actin dynamics in the context of myogenesis. Our results show that the cardiac and skeletal muscle appears to be specified and to differentiate normally, at least as assayed by several markers of specification and terminal myocyte differentiation. Furthermore, the total amount of cardiac and skeletal tissue appears grossly normal in *XHsp27*-depleted embryos. With the exception of actin, all markers examined appear to be normally expressed and the defects in heart development appear to be primarily morphogenetic in nature. These data suggest that the cause of the cardiac defect is not a failure of cardiomyocyte differentiation. It remains formally possible that the cardiac fusion defects may result from a loss of differentiation or an increase in apoptosis in a subset of cardiac precursors at the midline, essentially creating a barrier between the two cardiac fields. However, further studies must be conducted to precisely define whether *Hsp27* can influence differentiation or apoptosis in the developing embryo.

Abrogation of *XHsp27* function in *X. laevis* embryos results in improper fusion of the cardiac progenitors, resulting in two unfused or partially fused contractile hearts. Our data suggest that the primary role of *Hsp27* in cardiogenesis is to regulate actin dynamics, and thus cell motility or adhesion. In support of this hypothesis, previous research has shown that cardiac epithelial integrity and cell motility and adhesion are critical for proper fusion of the cardiac primordia (Trinh and Stainier, 2004). In addition, the precardiac field was shown to

consist of a single polarized epithelial layer. Our results demonstrate that actin fibers are visible primarily at the cell membrane in the single-cell layered cardiac precursors. However, in XHSP27-depleted embryos, few discreet fibers are visible. These results suggest that epithelial organization or polarization is defective in the cardiac fields and that XHSP27 is required for this organization. Actin fiber organization appears to be morphologically different in developing skeletal muscle. Within the developing myotomes, thick actin fibers are arranged in an anterior-posterior orientation and do not appear to delineate the membranes in an epithelial manner. However, similar to what is seen in cardiac primordia, actin protein appears to be completely disorganized in XHSP27 morphant embryos, again suggesting that cell polarity or tissue integrity is affected by HSP27 loss.

Figure 6.1. *XHsp27* is a conserved member of the *Hsp27* subfamily of proteins.

(A) Protein sequence alignments of *X. laevis Hsp27* with various *Hsp27* orthologues. Alignment was performed using the GeneDoc program. Blue underline indicates conserved crystallin domain. Red underline indicates putative actin interacting domains. (B) Percent identity and similarity between *Hsp27* orthologues. (C) Synteny between *X. tropicalis*, human, mouse, rat, and chick *Hsp27* loci as revealed by Metazome. *Hsp27* is indicated in black. Upstream and downstream genes are colored as indicated.

Figure 6.1. *XHsp27* is a conserved member of the *Hsp27* subfamily of proteins.

A

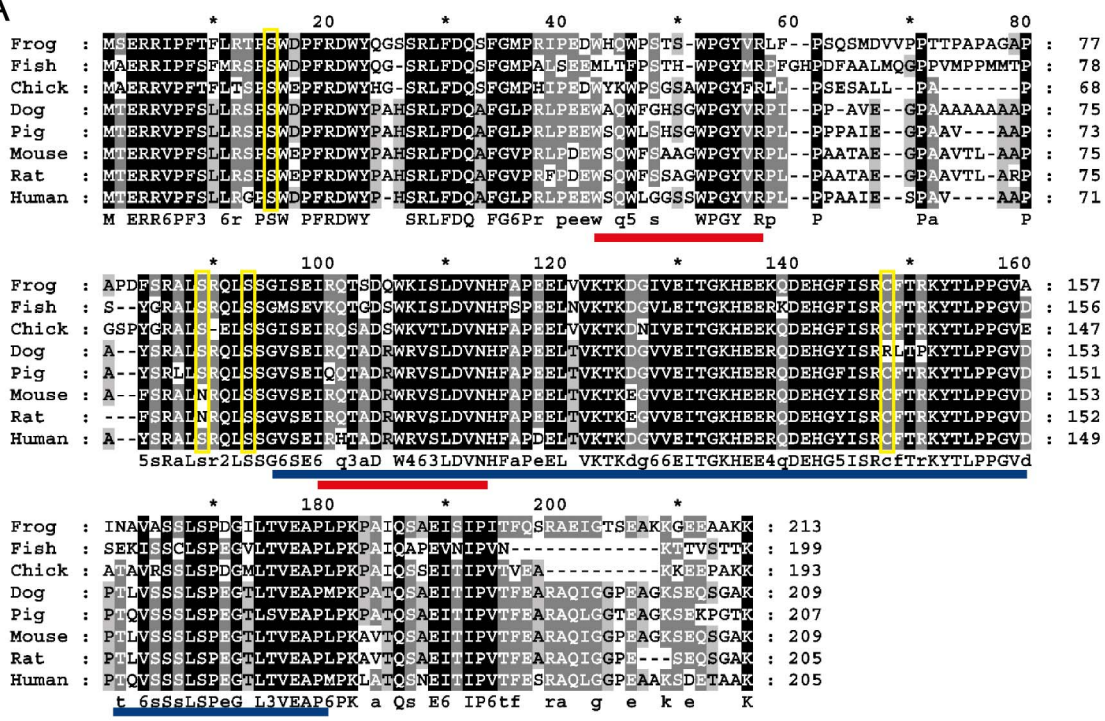

B

		Human	Rat	Mouse	Pig	Dog	Chick	Fish
Frog	% Identity	66	64	66	67	67	70	61
	% Similarity	81	80	82	83	82	80	74
Fish	% Identity	58	58	58	61	59	61	
	% Similarity	71	72	71	72	70	76	
Chick	% Identity	64	63	63	65	62		
	% Similarity	76	75	75	76	73		
Dog	% Identity	85	85	88	88			
	% Similarity	91	90	93	93			
Pig	% Identity	87	84	87				
	% Similarity	91	90	93				
Mouse	% Identity	83	96					
	% Similarity	90	97					
Rat	% Identity	80						
	% Similarity	88						

C

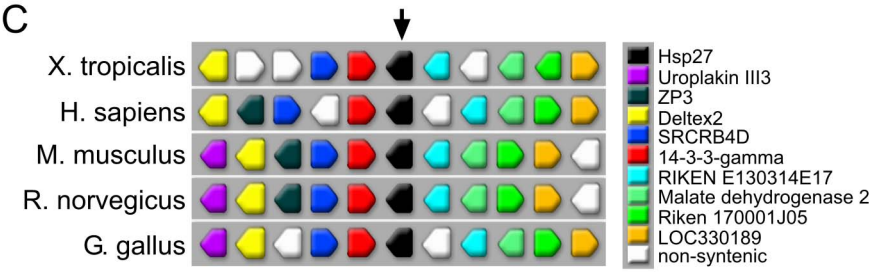

Figure 6.2. *XHsp27* is expressed in the gastrula, and developing skeletal and cardiac muscle

Whole mount *in situ* hybridization of *X. laevis* embryos using an antisense probe specific for *XHsp27* at the indicated stages. (A) Dorsal is to the top. (B-I) Anterior is to the left. b, body muscle; br, brain; h, heart; j, jaw muscle, m, myotome.

Figure 6.2. *XHsp27* is expressed in the gastrula, and developing skeletal and cardiac muscle

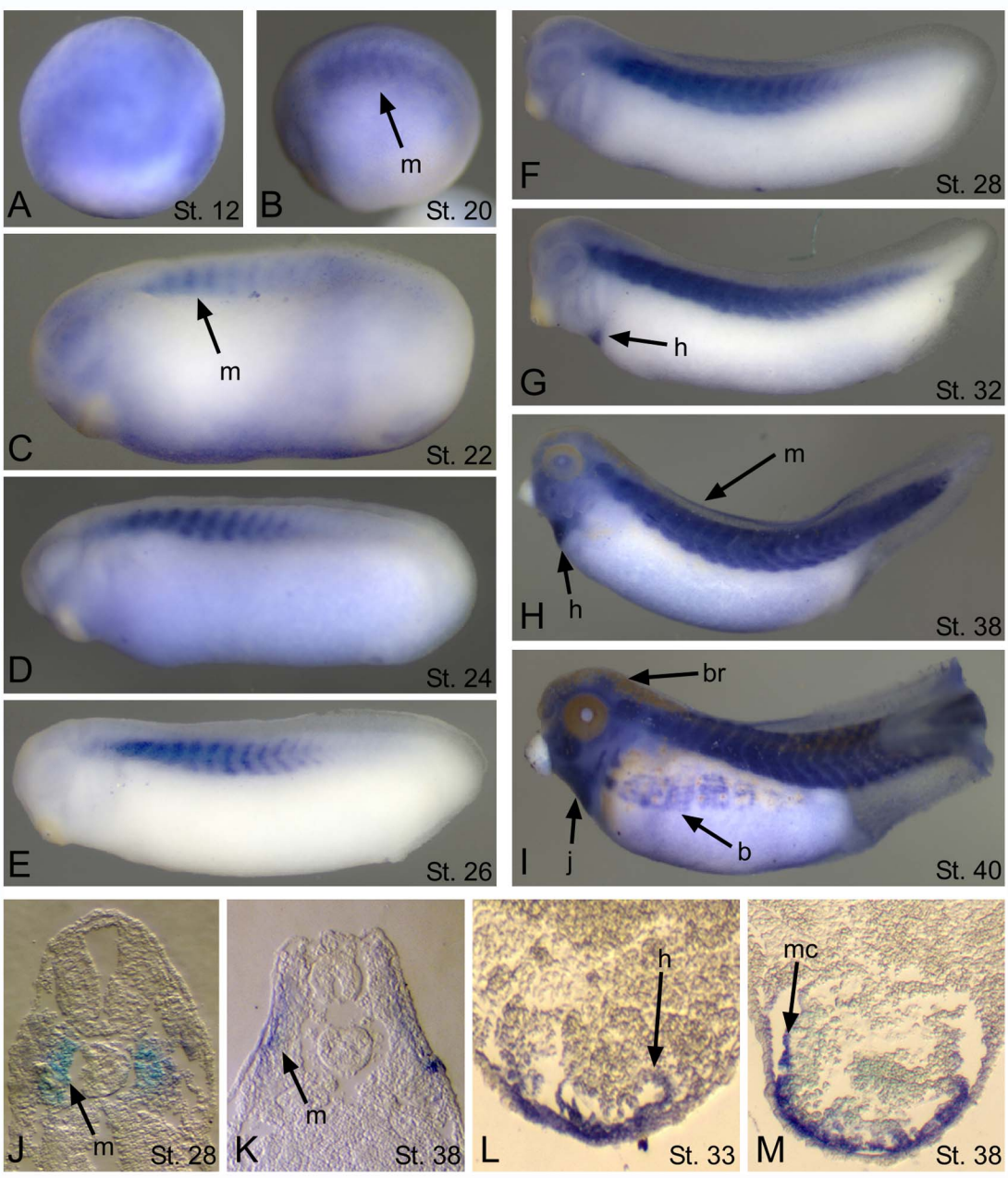

Figure 6.3. HSP27 morpholinos specifically block translation *in vitro*.

(A) Diagram depicting *XHsp27* mRNA structure and morpholino-targeted region. (B) Western blot demonstrating translation inhibition *in vitro* using rabbit reticulocyte lysate. Reactions were incubated with the indicated amounts of HA-*Hsp27* mRNA and/or HSP27MO. TBX20MO was included as a negative control. HSP27MO was incubated with HA-*Tbx20* mRNA to show specificity of the HSP27MO. HA-HSP27 and HA-TBX20 was visualized using anti-HA antibody, and SHP2 antibody was used as loading control. (C) Western blot demonstrating translation inhibition *in vivo* by coinjection of HA-*Hsp27* mRNA with HSP27MO. Embryos were injected with the indicated amount of HSP27MO, ControlMO, and/or HA-*Hsp27* mRNA. Embryos were collected at stage 20. Western blotting was performed on lysate using anti-HA antibody. SHP2 antibody was used as loading control.

Figure 6.3. HSP27 morpholinos specifically block translation *in vitro*.

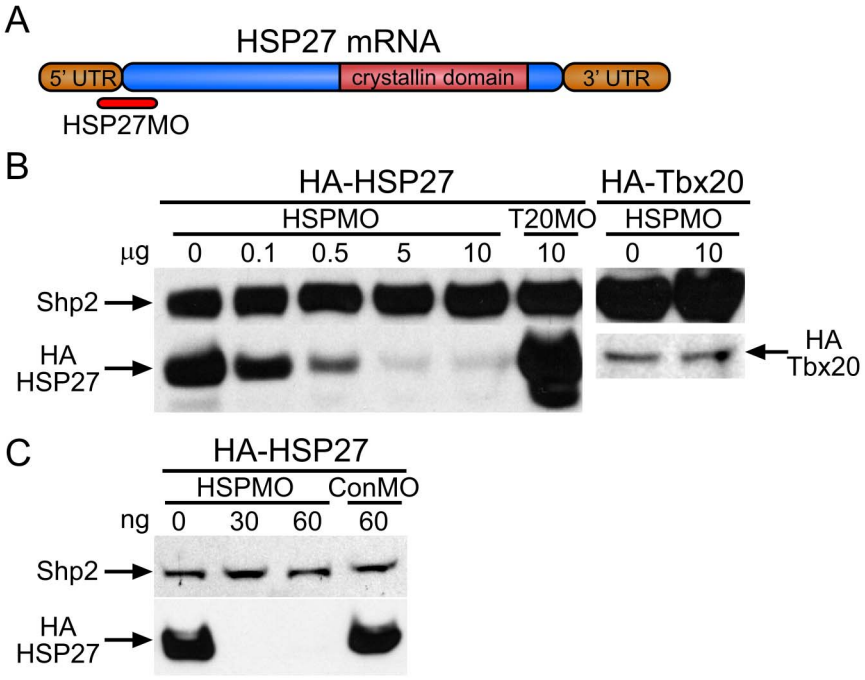

Figure 6.4. XHSP27 misexpression results in gastrulation defects and can be partially rescued by XHSP27 morpholinos.

Embryos were injected with 1 ng HA-XHsp27 mRNA (A-C) and co-injected with either 30 ng HSP27MO (B) or 60 ng HSP27MO (C). Wild-type embryos are shown as a control (D). Numbers at the bottom show the percent of embryos displaying exogastrulation and the total number of embryos assayed per treatment. All embryos shown are displayed with anterior to the left and posterior to the right.

Figure 6.4. XHSP27 misexpression results in gastrulation defects and can be partially rescued by XHSP27 morpholinos.

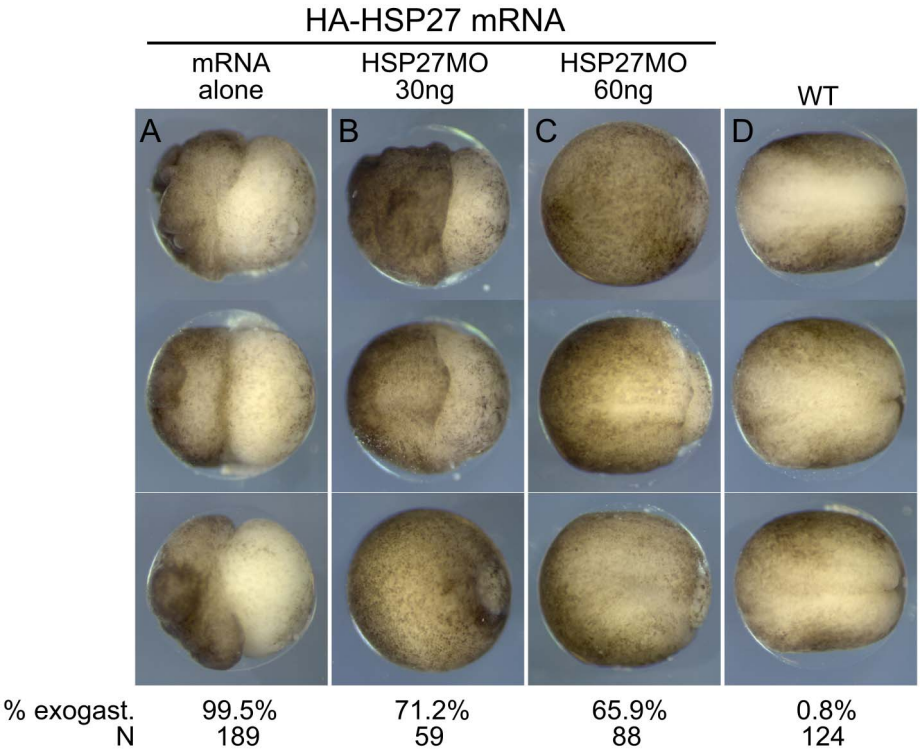

Figure 6.5. Specification and differentiation of cardiac and skeletal muscle appear unaltered in HSP27 morphants.

Whole-mount *in situ* hybridizations using antisense probes against (A) *Nkx2.5*, (B) *Tbx20*, (C) *Gata4*, (D) *Gata6*, (E) *Mlc1v'*, and (F) *Titin novex 3* (*Tn3*). Embryos were injected with either HSP27MO or ControlMO and fixed at the indicated stages. (A-F) Ventral views with anterior upward. (E, F) Stage 37 embryos shown laterally with anterior to the left. All markers analyzed appear normal between control and HSP27 morphant embryos.

Figure 6.5. Specification and differentiation of cardiac and skeletal muscle appear unaltered in HSP27 morphants.

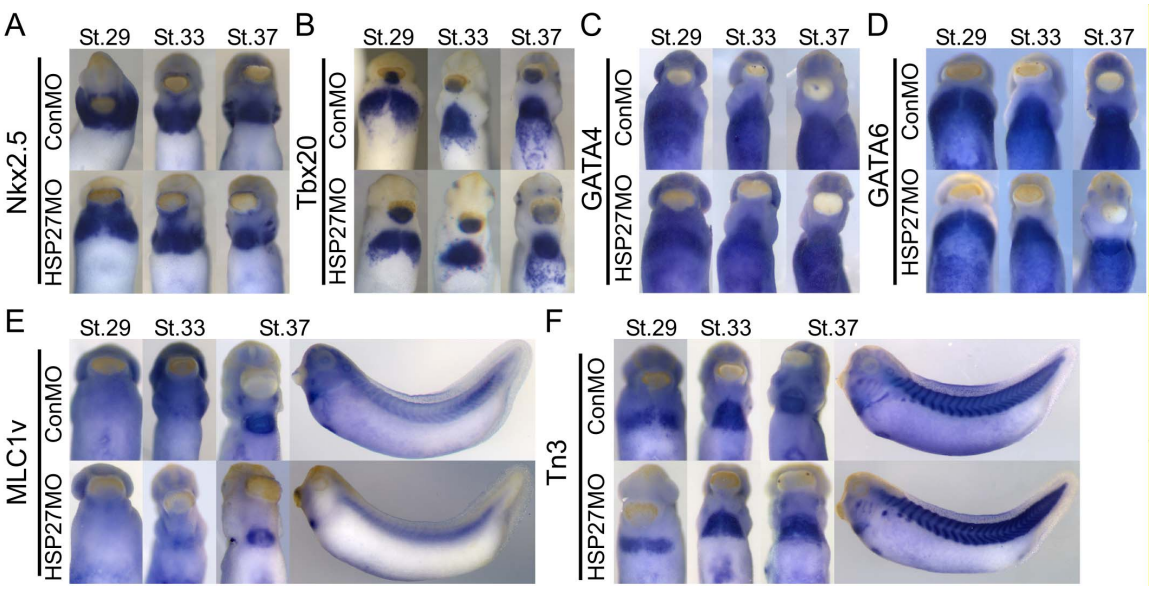

Figure 6.6. Depletion of XHSP27 results in unfused or partially fused hearts.

Whole-mount antibody staining using anti-myosin heavy chain α (MHC). Embryos were injected at the one-cell stage with either HSP27MO or ControlMO, fixed, and stained for MHC at the indicated stages. All views are ventral with anterior upwards. Arrows indicate separation between the two cardiac fields or developing hearts. a, atrium; i, inflow tract; o, outflow tract; v, ventricle.

Figure 6.6. Depletion of XHSP27 results in unfused or partially fused hearts.

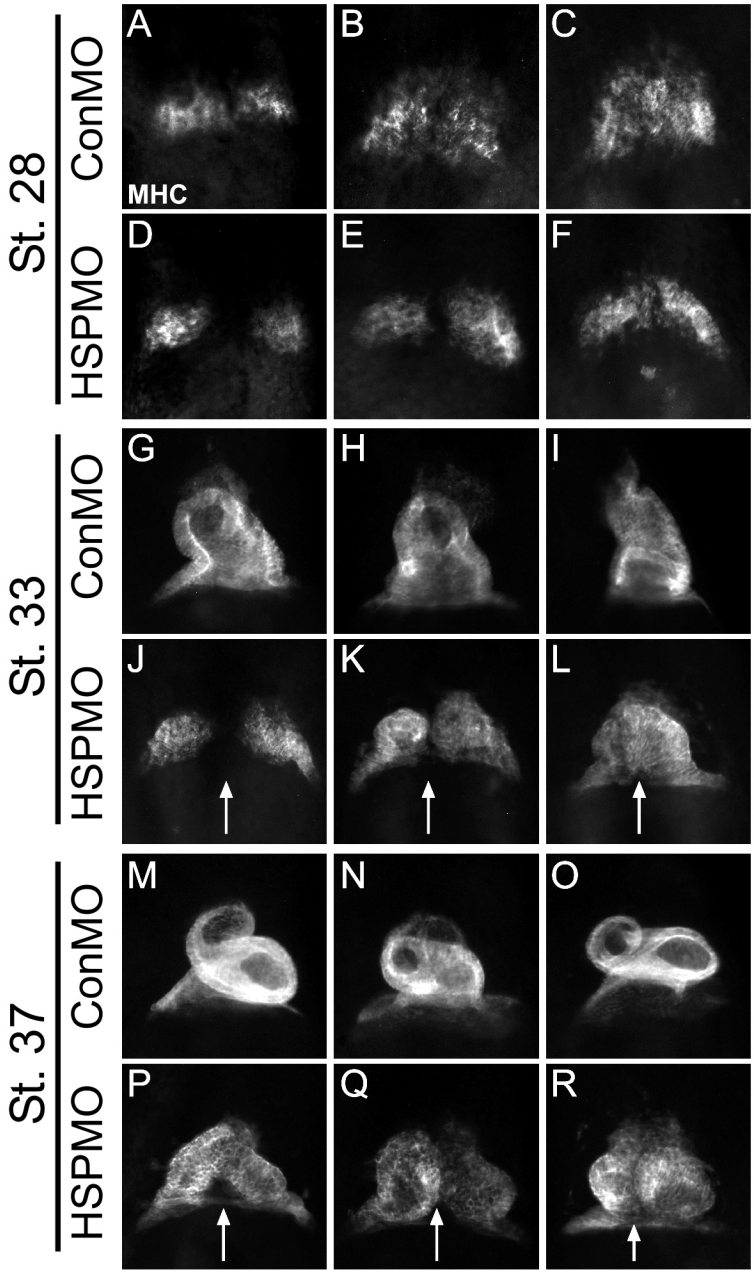

Figure 6.7. Depletion of XHSP27 results in actin disorganization in developing skeletal and cardiac muscle.

Transverse 12 μm sections through the heart (A-L) and somite (M-X). All sections are shown with dorsal upward. Heart sections were immunostained for F-actin using phalloidin (A, D, G, J) and MHC using anti-MHC antibody (B, E, H, K). Overlays are shown in (C, F, I, L). Somite sections were immunostained for F-actin using phalloidin (M, P, S, V) and stained with DAPI to visualize the nuclei (N, Q, T, W). Overlays are shown in (O, R, U, X).

Figure 6.7. Depletion of XHSP27 results in actin disorganization in developing skeletal and cardiac muscle.

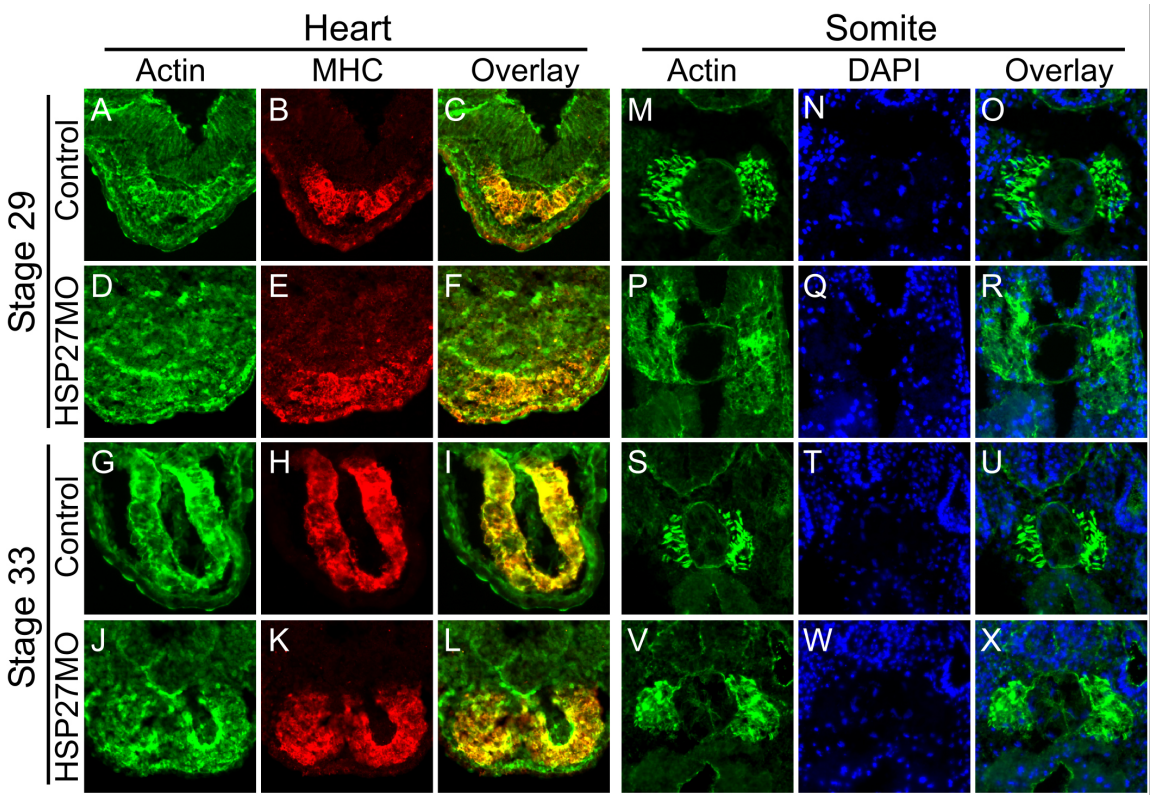

Figure 6.8. XHSP27 morphant ultrastructure analysis reveals a lack in myofibril assembly.

Transmission electron microscopy of ventral myocardium in stage 38 control and XHSP27 morphant hearts. (A-C) Ventral myocardium of ControlMO injected embryo. (D-F) Ventral myocardium of XHSP27MO injected embryo. Inset in (C) shows magnification of myofibril structure and inset in (F) shows magnification of apparent myosin aggregates. Scale bars depicts 2µm distance. *l*, longitudinal myofibers section; *t*, transverse myofibers section; *z*, z-line. (G, H) Muscle fibers within the myotome in stage 38 control morpholino injected embryos. (I, J) Muscle fibers within the myotome in stage 38 *XHsp27* morpholino injected embryos. *l*, longitudinal myofibers section; *t*, transverse myofibers section; *z*, z-line.

Figure 6.8. XHSP27 morphant ultrastructure analysis reveals a lack in myofibril assembly.

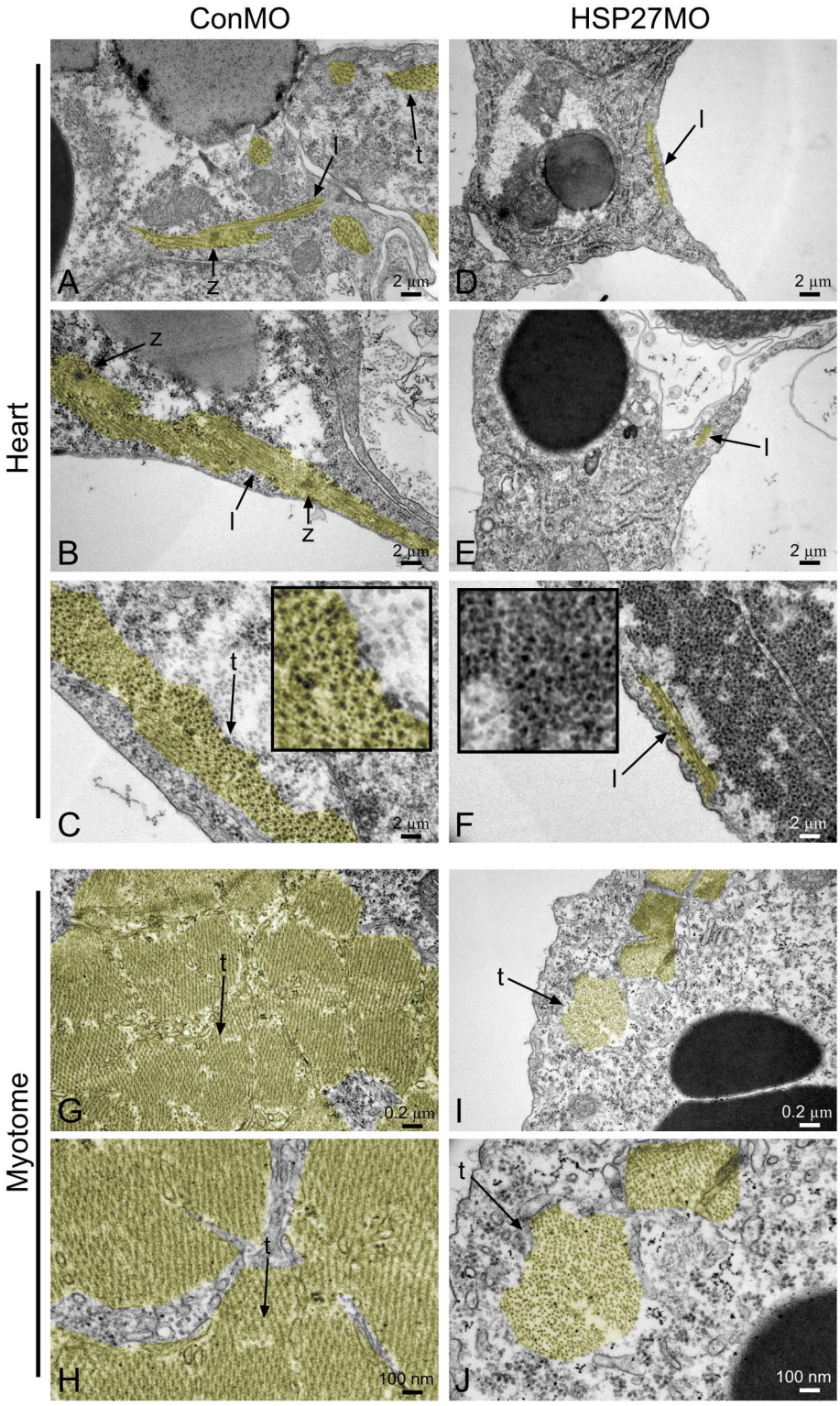

CHAPTER VII

GENERAL DISCUSSION

The development of a functional multi-chambered contractile heart from a simple patterned tube involves a number of interacting transcriptional networks acting within well-defined temporal and spatial parameters. While many of the regulatory transcription factors have been identified and shown to be required for proper cardiogenesis, much remains to be deciphered regarding how these pathways interact at different times and within different cell populations during cardiogenesis. In addition, very little is currently known as to the specific downstream pathways affected by the various transcriptional regulators known to be involved in cardiac morphogenesis. Thus, one of the main challenges within the field of heart development is to not only identify the transcriptional regulators involved in cardiogenesis, but to also place these factors within specific pathways and cellular contexts and to understand how these pathways interconnect to direct the precise morphogenetic changes required for heart formation.

A. The Role of *Tbx20* in Cardiogenesis

Many studies on various T-box genes have shown this family of transcription factors to be integral to numerous developmental processes during embryogenesis (reviewed in Naiche et al., 2005; Showell et al., 2004). Prior to the work included herein, previous studies had indicated that several vertebrate homologues of *Tbx20* are expressed at the proper time

and place to potentially regulate cardiogenesis (Ahn et al., 2000; Griffin et al., 2000; Iio et al., 2001; Kraus et al., 2001; Meins et al., 2000). These data, combined with the observation that *Tbx20* is likely ancient in evolutionary origin, existing as far back as invertebrates (Brook and Cohen, 1996b), suggest that *Tbx20* likely plays a critical role in embryogenesis, particularly within heart development. In this work I demonstrate the identification of the *X. laevis* orthologue of *Tbx20* and demonstrate high homology to other vertebrate orthologues of *Tbx20* in both sequence and expression (Chapter II; Brown et al., 2003). I further demonstrate that removal of *Tbx20* from the amphibian heart results in a dramatic decrease in cardiac cell numbers and a complete lack of looping morphogenesis (Chapter III; Brown et al., 2005). These findings are corroborated by findings in both mouse and zebrafish which display nearly identical phenotypes upon removal of functional *Tbx20* (Cai et al., 2005; Singh et al., 2005; Stennard et al., 2005; Szeto et al., 2002; Takeuchi et al., 2005). A somewhat surprising finding among all of these studies is the observation that cardiac specification and development in *Tbx20*-depleted embryos appears to be completely normal until formation of a linear heart tube. Experiments from my work and others have shown that *Tbx20* is expressed in the cardiac precursor fields within the lateral plate mesoderm at very early stages prior to ventral migration of the precursors (Chapter II, Ahn et al., 2000; Brown et al., 2003; Carson et al., 2000; Griffin et al., 2000; Iio et al., 2001; Kraus et al., 2001; Meins et al., 2000). Despite this early expression, the specification, migration, and differentiation of the cardiac progenitors appears to be normal in *Tbx20*-depleted embryos as assayed by several cardiac markers, including *Nkx2.5*, *ANF*, and *TnIc* (Chapter III; Brown et al., 2005). Thus, it remains to be determined whether *Tbx20* plays a role within the cardiac progenitors during these early time periods. One possible explanation for this finding is the possibility

that removal of *Tbx20* results in subtle changes within the cell that only become apparent during heart tube formation and morphogenesis. These changes may be in the proliferative capacity of the cardiac progenitors, such that early *Tbx20* expression is required to initiate events that eventually lead to proliferation during cardiac morphogenesis. Alternatively, it may be that other transcription factors can function in place of TBX20 upon its removal. Evidence from mice indicates that removal of TBX20 results in misexpression of a related T-box gene, *Tbx2*, throughout the *Tbx20* expression domain in both early cardiac progenitors and the later heart tube (Cai et al., 2005; Singh et al., 2005; Stennard et al., 2005). Both of these transcription factors have been show to be repressive in activity (Cai et al., 2005; Carreira et al., 1998; Plageman and Yutzey, 2004). It is thus possible that TBX2 may be able to bind targets of TBX20, thus taking over the repressive role of TBX20 on these targets. However, if this is indeed the case, it appears that TBX2 expression cannot compensate for the loss of TBX20 during later cardiac morphogenesis, as the heart is severely abnormal in the absence of TBX20. One way to test this hypothesis involves the co-injection of morpholinos against *Tbx20* and *Tbx2* to determine if removal of both proteins can result in earlier cardiac phenotypes. It is also formally possible that TBX5 may be functionally redundant with TBX20 during early cardiac progenitor development; however two lines of evidence suggest that this is not likely. Studies have indicated that TBX20 primarily acts as a transcriptional repressor, in contrast to TBX5 which is known to activate target genes (Cai et al., 2005; Ghosh et al., 2001; Plageman and Yutzey, 2004). Furthermore, *Tbx5* and *Tbx20* do not share fully overlapping domains of expression; for example, *Tbx5* is not expressed in the future outflow region, which is a domain of very high *Tbx20* expression (Ahn et al., 2000;

Brown et al., 2003; Chapman et al., 1996b; Iio et al., 2001; Kraus et al., 2001; Meins et al., 2000). Thus, it seems unlikely that TBX5 can function in place of TBX20.

My own studies on embryos lacking TBX20 or TBX5 indicate that morphant hearts show significant decreases in numbers of cells within the heart (Chapter III; Brown et al., 2005). Furthermore, work in collaboration with Sarah Goetz has indicated that in the case of *Tbx5*, it appears that a primary defect of TBX5 depletion is a delay or halt in cell cycle progression (Goetz et al., 2006). In addition, studies of *Tbx20*-null mice indicate that TBX20 depletion leads to repression of *Nmyc1*, a cell cycle regulator, via deregulation of *Tbx2* expression (Cai et al., 2005). Taken together these results suggest that a primary role of TBX20 during cardiac morphogenesis is to regulate cardiomyocyte proliferation which leads to the patterned growth required for proper looping and morphogenesis. However, there is one inconsistency in the results showing *Tbx2* de-repression in mice (Cai et al., 2005). In this study, the authors propose a model whereby TBX2 normally represses *Nmyc1* and thus proliferation in the developing outflow tract, while TBX20 represses *Tbx2* in chamber myocardium resulting in higher proliferation rates. However, they fail to note that the outflow tract is one of the regions in which *Tbx20* is very highly expressed. Thus, by this model TBX20 should repress *Tbx2* expression in the outflow region. To the contrary, both factors are found to be highly expressed within this region (Ahn et al., 2000; Brown et al., 2003; Carreira et al., 1998; Iio et al., 2001; Kraus et al., 2001; Meins et al., 2000). Thus it appears that the relative functions of these factors in cardiogenesis are more complex and will be likely found to be highly context dependent, being affected by the presence of numerous other transcription factors and perhaps post-translational modifications depending on the specific cell type. This is evidenced by findings from my work and others

demonstrating that TBX20 can physically and functionally interact with several other factors, including TBX5, NKX2.5, GATA4, and GATA5, which can in turn interact with each other (Brown et al., 2005; Stennard et al., 2003). These studies have shown that the specific interactions between various transcription factors can lead to either synergistic activation or repression of target promoters, depending on which factors are present and which promoter is being assayed. The above findings highlight the apparent complexity of interconnectedness between the various transcriptional networks within developing cardiac tissue and pose significant challenges for future studies on cardiogenesis.

The major findings that will likely help in elucidating this incredibly complex network of pathways, will be the identification of targets of these factors' transcriptional activity. While studies have succeeded in identifying targets for individual transcription factors, such as *connexin40* and *atrial natriuretic factor* (*ANF*) for TBX5, very little is known as to the biological significance of binding to these targets (Bruneau et al., 2001; Hiroi et al., 2001). More importantly, even less is known about the effects of the various putative complexes containing multiple cardiac transcription factors on target regulation. However, a leap forward in this understanding will likely come with the advent of the bourgeoning techniques of performing large scale chromatin immunoprecipitation (ChIP) and microarray-based chromatin immunoprecipitation (ChIP-on-chip) screens (reviewed in Buck and Lieb, 2004; Hanlon and Lieb, 2004). Using ChIP-on-chip, researchers can immunoprecipitate a transcription factor, pulling along any genomic fragments to which the factor is bound, and hybridize the genomic fragments to a microarray, thus learning which sequences within the genome are being regulated by the particular transcription factor. However, this technique relies heavily on two major requirements: a highly-specific antibody

and a well annotated complete genome sequence. With the completion of the *Xenopus tropicalis* genome, this technique may well provide many new insights into cardiogenesis and biology in general. However, in the case of T-box genes, very few antibodies have been found that will bind the T-box proteins efficiently and specifically. Thus, antibody development will remain a large challenge for T-box research and cardiogenesis research in the future.

B. Transcriptional Activity of *Tbx20*

One of the main challenges for understanding the role of *Tbx20* during cardiogenesis remains the elucidation of the specific transcriptional activity of *Tbx20* on endogenous promoters. Current evidence from our work and others indicates that the precise transcriptional activity appears to be highly context dependent, with *Tbx20* activating transcription in some cases while repressing it in others. Much of the work analyzing *Tbx20* transcriptional activity has relied on use of the *ANF* promoter. In the present study, we have shown that TBX20 can activate transcription of the *ANF* promoter to an even greater degree than TBX5, although total activation is low for both factors (Chapter III; Brown et al., 2005). Similar results were obtained by two other reports in which the authors reported low activation by TBX20 of either the *ANF* or *connexin 40* promoters or a minimal promoter containing multiple tandem NKX2.5 binding elements (Plageman and Yutzey, 2004; Stennard et al., 2003). We have further demonstrated that at low doses, TBX20 can synergistically activate transcription with TBX5 on the *ANF* promoter, while at higher doses it can repress activation by TBX5 (Chapter III; Brown et al., 2005). In contrast, Takeuchi and colleagues (2003) have demonstrated that TBX20 has no effect on transcription by TBX5 on

the *ANF* promoter, while inhibiting synergistic activation by TBX5 and GATA4 together or TBX5 and NKX2.5 together (Takeuchi et al., 2003). Similarly, Plageman and Yutzey (2004) have demonstrated that co-expression of *Tbx20* with *Tbx5* can result in repression of activation on the *ANF* promoter by TBX5. However, in this study the presence of TBX20 had no effect on activation by NKX2.5 or GATA4 (Plageman and Yutzey, 2004).

The specific activity of TBX20 has become further complicated by the identification of additional *Tbx20* isoforms that lack the carboxy-terminal domains, which are presumably the domains necessary for transcriptional activity (Stennard et al., 2003). In this study, the long form of *Tbx20*, *Tbx20a*, which contains the entire carboxy terminus, was shown to elicit low levels of transcriptional activity on the *ANF* promoter (Stennard et al., 2003). This same isoform was shown to synergistically activate transcription by NKX2.5 and GATA4 on the *ANF* and *connexin40* promoters, while the isoform of *Tbx20* lacking the carboxy terminus, *Tbx20c*, was shown to increase transcription by NXK2.5 and GATA4 to an even greater extent (Stennard et al., 2003). Their study thus suggests that TBX20 can synergistically activate transcription with NKX2.5 and GATA4, in contrast to the study by Plageman and Yutzey, demonstrating no synergistic activity (Plageman and Yutzey, 2004; Stennard et al., 2003). The above experiments were all performed using reporter constructs driven by promoters not known to be direct targets of TBX20 transcriptional activity, such as the *ANF* and *connexin40* promoters. Furthermore, DNA binding assays have shown that TBX20 can only weakly bind a modified consensus T-box binding element within the *ANF* promoter (Stennard et al., 2003). Thus, a major determinant in our understanding of the *in vivo* activity and binding potential of TBX20 must come with the identification of direct targets of TBX20 function.

Recent evidence from mice lacking *Tbx20* has demonstrated that a primary defect of TBX20 depletion is a direct loss of repression of *Tbx2* within the heart (Cai et al., 2005; Singh et al., 2005; Stennard et al., 2005). Furthermore, TBX20 has been show to directly bind to and repress transcription of the *Tbx2* promoter (Cai et al., 2005). Thus, it appears that in some contexts TBX20 can activate transcription by itself, repress transcription by TBX5, synergistically activate transcription by NKX2.5 and GATA4, or repress transcription of *Tbx2*. It remains to be determined which, if any, of these activities occur within the embryonic heart and on which targets this activity occurs, with the exception of *Tbx2* repression, which appears to be a bona fide function of TBX20.

C. *Tbx20* and Human Disease

As described in Chapter I, two members of the T-box gene family have been implicated in human congenital heart disease, with *Tbx5* mutations being associated with the autosomal dominant Holt-Oram Syndrome (Basson et al., 1997; Li et al., 1997) and *Tbx1* deletion frequently associated with DiGeorge Syndrome (Merscher et al., 2001; Yagi et al., 2003). Mutation of another T-box family member, *Tbx3* has been shown to cause human autosomal dominant Ulnar-Mammary Syndrome, a disease characterized by upper limb defects, mammary hypoplasia and genital abnormalities (Bamshad et al., 1997). The defects associated with all three disorders appear to arise due to haploinsufficiency of the respective T-box genes. Consistent with this hypothesis, patients with Holt-Oram Syndrome or Ulnar-Mammary Syndrome are typically heterozygous for *Tbx5* and *Tbx3*, respectively, and *Tbx1* heterozygous mice phenotypically recapitulate DiGeorge Syndrome (Bamshad et al., 1997;

Basson et al., 1997; Li et al., 1997; Lindsey et al., 2001). These observations suggest that cardiac morphogenesis and embryogenesis are sensitive to T-box gene dosage.

Mice heterozygous for *Tbx5* recapitulate the Holt-Oram Syndrome abnormalities, displaying atrial and septal defects as well as upper limb abnormalities (Bruneau et al., 2001). Furthermore, mice completely lacking *Tbx5* show more severe phenotypes characterized by hypoplastic, unlooped, and non-functional hearts (Bruneau et al., 2001). This finding is further supported by my own work which demonstrates a nearly identical cardiac phenotype in *X. laevis* embryos depleted of TBX5 protein using antisense morpholinos (Chapter III; Brown et al., 2005). These results suggest that in addition to mutations in *Tbx5* that can cause a survivable cardiac abnormality, mutation of both *Tbx5* alleles may be responsible for some pregnancies that fail to come to term.

At the present time, no inheritable cardiac disorders have been mapped to the locus of *Tbx20*, chromosome 7p14. However, given that studies have shown that precise *Tbx5* gene dosage is critical in proper cardiac and limb development, combined with work by myself and others demonstrating a requirement for *Tbx20* in cardiogenesis, it remains possible that human congenital heart defects may arise from mutation of *Tbx20*. It is further possible that mutation of only one allele of *Tbx20* may be sufficient to prevent proper cardiogenesis and thus preclude a pregnancy from coming to term. One possible outcome of *Tbx20* mutation may lie in the development of neurological disorders. As described in Chapter II, *Tbx20* is expressed within rhombomeres in the hindbrain that contribute to motor development and function (Brown et al., 2003). Furthermore, as mentioned in Chapter III, depletion of TBX20 using antisense morpholinos results in a complete lack of motor function in *X. laevis* embryos. These results suggest that *Tbx20* may play a role in neuronal development.

Recently, studies have mapped a subset of human congenital neuropathies to the locus of *Tbx20* in humans, namely chromosome 7p14 (Ellsworth et al., 1999). Charcot-Marie-Tooth (CMT) disease is a progressive neuropathy of the peripheral nervous system, and is the single most-common inherited neuropathy at an estimated prevalence of 1 in 2,500 (Skre, 1974). The non-demyelinated forms of CMT are denoted "CMT2" and four subclasses of this disease have been found mapping to four distinct loci. One such subclass, CMT2D, has been demonstrated to map to a region of chromosome 7p14, the same region containing *Tbx20* (Ellsworth et al., 1999). It is thus tempting to hypothesize that mutation of *Tbx20* may be involved in the development of CMT2D. Of further interest is the fact that, as mentioned in Chapter VI, a separate subclass of CMT2 has been demonstrated to arise from mutations within the *Hsp27* gene in a separate locus on chromosome 7 (Evgrafov et al., 2004). I initially identified *Hsp27* in *X. laevis* due to its' apparent misregulation in response to loss of TBX20 as assayed by microarray analysis. Although it remains to be determined whether *Hsp27* is truly downstream of TBX20 function and whether CMT2D can result from *Tbx20* mutation, these apparent connections suggest that this is indeed a possibility.

TBX20 may also be a candidate for contributing to retinal diseases. Work by myself and others have demonstrated that *Tbx20* is expressed in the developing eye (Chapter II; Brown et al., 2003; Carson et al., 2000; Kraus et al., 2001; Meins et al., 2000). Furthermore, misexpression of *Tbx20* in *X. laevis* results in defects in eye development (Carson et al., 2004). Consistent with these observations, two inherited eye disorders have been found to map to loci on chromosome 7 in regions encompassing the *Tbx20* locus, with retinitis pigmentosa (RP9) having been mapped to chromosome 7p13-15 (Inglehearn et al., 1994) and blepharophlemosis syndrome (BPES) having been mapped to chromosome 7p13-21 (Maw et

al., 1996). However, the potential role of *Tbx20* in BPES has been brought into question by a recent study by Meins and colleagues (2000) demonstrating that BPES may map to a locus 16 cM distal to *Tbx20* (Meins et al., 2000). In addition, the study failed to detect mutations within *Tbx20* exons 3, 4, or 5 in a patient with RP9 (Meins et al., 2000). Despite these findings, it remains formally possible that mutation in other regions of *Tbx20* or in regulatory elements of *Tbx20* may be causative in RP9.

D. HSP27, Cardiogenesis, and Myogenesis

In Chapter VI, I describe the identification of the *X. laevis* orthologue of the small heat shock protein *Hsp27* and demonstrate that this orthologue is expressed in a developmentally regulated manner throughout developing skeletal and cardiac muscle tissues. I further demonstrate that *Hsp27* function is essential for cardiac precursor fusion and actin organization. As described in Chapter I, formation of a linear heart tube requires the coordination of cardiac specification, differentiation, and cell behavior within defined spatial and temporal domains. Furthermore, fusion of the cardiac progenitors to create a single heart tube requires the coordination of many processes, including proper cardiomyocyte differentiation (Reiter et al., 1999; Yelon et al., 2000), signaling from the endoderm (Alexander et al., 1999; Kikuchi et al., 2000; Reiter et al., 1999; Schier et al., 1997), epithelial organization of the cardiac fields, and migration cues from the midline (Trinh and Stainier, 2004). In the present study, I identify the small heat shock protein, *Hsp27*, as being integral to this process. While it is clear that *Hsp27* is critical in mediating the cellular response to a wide variety of stressors, it is unclear what role *Hsp27* may be playing during cardiogenesis and myogenesis under unstressed physiological conditions. While

cardiomyocyte differentiation is known to be required for proper cardiac fusion (Reiter et al., 1999; Yelon et al., 2000), and *Hsp27* is known to affect differentiation in some contexts (Mehlen et al., 1997), my data suggest that *Hsp27* is dispensable for differentiation within developing cardiac and skeletal muscle precursors. It appears instead that HSP27 is necessary for initiating or maintaining actin cytoskeleton organization, as loss of HSP27 results in dramatically disorganized actin networks. In support of these findings, previous research has shown that cardiac epithelial integrity and cell motility and adhesion are critical for proper fusion of the cardiac primordia (Trinh and Stainier, 2004). Our results demonstrate that actin fibers are visible primarily at the cell membrane in the single-cell layered cardiac precursors. However, few discreet fibers are visible in HSP27-depleted embryos. These findings suggest that epithelial organization or polarization is defective in the cardiac fields. An even more dramatic actin network disorganization is apparent in the developing myotomes of HSP27 morphant embryos. Within the developing myotomes, thick actin fibers are arranged in an anterior-posterior orientation. However, similar to what is seen in cardiac primordia, actin protein appears to be completely disorganized in HSP27 morphant embryos. Thus I have demonstrated that HSP27 is critical in regulating actin networks in developing muscle tissue and that proper actin organization is required for cardiac fusion.

E. Conclusions

The work included herein represents a contribution to our understanding of the factors and mechanisms involved in the formation of the vertebrate heart. Prior to my studies, the function and requirement of the T-box gene, *Tbx20*, in cardiogenesis was completely unknown, and the *X. laevis* orthologue of *Tbx20* had not been previously identified. By

isolating and characterizing the sequence and expression of *X. laevis Tbx20*, I have shown this gene to be very highly conserved throughout evolution, indicating a likely critical function of this gene in heart development (Chapter II; Brown et al., 2003). Through a series of experiments, primarily utilizing protein depletion approaches, I have demonstrated that *Tbx20* function is critical in the developing organism for controlling morphogenetic processes that result in proper cardiac formation (Chapter III; Brown et al., 2005). I have further shown that at least one role of *Tbx20* is to coordinately regulate cardiogenesis along with *Tbx5* (Chapter III; Brown et al., 2005). As mentioned in Chapter I, a main challenge within the field of cardiogenesis is to decipher not only what factors are involved in cardiogenesis, but how these different factors within different molecular pathways coalesce in different cell types and contexts to regulate the complex changes involved in heart formation. By demonstrating a physical and functional interaction between TBX20 and TBX5 I have identified one step at which multiple pathways may converge to modulate transcription of genes involved in cardiogenesis (Chapter III; Brown et al., 2005). Findings from a microarray-based screen I conducted to identify genes downstream of TBX5 function resulted in the identification of several cell cycle genes putatively misregulated in response to loss of *Tbx5* (Chapter IV). This observation has directly led to a study conducted by Sarah Goetz in which she demonstrated a requirement for *Tbx5* for proper cell cycle progression, thus further elucidating downstream pathways in heart development (Goetz et al., 2006). A similar screen I performed to identify genes misregulated in response to loss of TBX20 has yielded the identification of many previously uncharacterized genes expressed within the developing heart, indicating a potential role for these genes in controlling cardiogenesis and setting up the basis for many future studies to come (Chapter IV). Furthermore, I have

characterized the expression of two of these genes during cardiac and skeletal muscle development, *titin novex 3* (*XTn3*; Chapter V), and *heat shock protein 27 (XHsp27*; Chapter VI*)*. By eliminating XHSP27 protein in the embryo I have further shown that this gene is critical for fusion of cardiac precursors and proper organization of actin filament networks, thus furthering our understanding of small heat shock proteins in embryonic development (Chapter VI). Thus, this dissertation work represents a significant advance in our understanding of cardiogenesis at multiple levels, including the identification of factors involved in cardiogenesis, interactions between these factors, and downstream cellular behaviors affected by these factors.

REFERENCES

Agulnik, S. I., Ruvinsky, I. and Silver, L. M. (1997). Three novel T-box genes in Caenorhabditis elegans. *Genome* **40**, 458-64.

Ahn, D. G., Ruvinsky, I., Oates, A. C., Silver, L. M. and Ho, R. K. (2000). tbx20, a new vertebrate T-box gene expressed in the cranial motor neurons and developing cardiovascular structures in zebrafish. *Mech Dev* **95**, 253-8.

Alexander, J., Rothenberg, M., Henry, G. L. and Stainier, D. Y. (1999). casanova plays an early and essential role in endoderm formation in zebrafish. *Dev Biol* **215**, 343-57.

Alsan, B. H. and Schultheiss, T. M. (2002). Regulation of avian cardiogenesis by Fgf8 signaling. *Development* **129**, 1935-43.

Andree, B., Duprez, D., Vorbusch, B., Arnold, H. H. and Brand, T. (1998). BMP-2 induces ectopic expression of cardiac lineage markers and interferes with somite formation in chicken embryos. *Mech Dev* **70**, 119-31.

Araki, I. and Brand, M. (2001). Morpholino-induced knockdown of fgf8 efficiently phenocopies the acerebellar (ace) phenotype. *Genesis* **30**, 157-9.

Arrigo, A. P. (2001). Hsp27: novel regulator of intracellular redox state. *IUBMB Life* **52**, 303-7.

Baek, S. H., Min, J. N., Park, E. M., Han, M. Y., Lee, Y. S., Lee, Y. J. and Park, Y. M. (2000). Role of small heat shock protein HSP25 in radioresistance and glutathione-redox cycle. *J Cell Physiol* **183**, 100-7.

Baldini, A. (2004). DiGeorge syndrome: an update. *Curr Opin Cardiol* **19**, 201-4.

Bamshad, M., Lin, R. C., Law, D. J. and al., e. (1997). Mutations in human TBX3 alter limb, apocrine and genital development in ulnar-mammary syndrome. *Nat Genet.* **16**, 311-315.

Bang, M. L., Centner, T., Fornoff, F., Geach, A. J., Gotthardt, M., McNabb, M., Witt, C. C., Labeit, D., Gregorio, C. C., Granzier, H. et al. (2001). The complete gene sequence

of titin, expression of an unusual approximately 700-kDa titin isoform, and its interaction with obscurin identify a novel Z-line to I-band linking system. *Circ Res* **89**, 1065-72.

Bar, H., Kreuzer, J., Cojoc, A. and Jahn, L. (2003). Upregulation of embryonic transcription factors in right ventricular hypertrophy. *Basic Res Cardiol* **98**, 285-94.

Basson, C. T., Bachinsky, D. R., Lin, R. C., Levi, T., Elkins, J. A., Soults, J., Grayzel, D., Kroumpouzou, E., Traill, T. A., Leblanc Straceski, J. et al. (1997). Mutations in human cause limb and cardiac malformation in Holt-Oram syndrome. *Nat. Genet.* **15**, 30-35.

Basson, C. T., Huang, T., Lin, R. C., Bachinsky, D. R., Weremowicz, S., Vaglio, A., Bruzzone, R., Quadrelli, R., Lerone, M., Romeo, G. et al. (1999). Different TBX5 interactions in heart and limb defined by Holt-Oram syndrome mutations. *Proc Natl Acad Sci U S A* **96**, 2919-2924.

Beddington, R. S. P., Rashbass, P. and Wilson, V. (1992). *Brachyury* - a gene affecting mouse gastrulation and early organogenesis. *Development (suppl.)*, 157-165.

Beiman, M., Shilo, B. and T., V. (1996). Heartless, a Drosophila FGF receptor homolog, is essential for cell migration and establishment of several mesodermal lineages. *Genes Dev.* **10**, 2993-3002.

Benndorf, R., Hayess, K., Ryazantsev, S., Wieske, M., Behlke, J. and Lutsch, G. (1994). Phosphorylation and supramolecular organization of murine small heat shock protein HSP25 abolish its actin polymerization-inhibiting activity. *J Biol Chem* **269**, 20780-4.

Benndorf, R., Sun, X., Gilmont, R. R., Biederman, K. J., Molloy, M. P., Goodmurphy, C. W., Cheng, H., Andrews, P. C. and Welsh, M. J. (2001). HSP22, a new member of the small heat shock protein superfamily, interacts with mimic of phosphorylated HSP27 ((3D)HSP27). *J Biol Chem* **276**, 26753-61.

Benndorf, R. and Welsh, M. J. (2004). Shocking degeneration. *Nat Genet* **36**, 547-8.

Benson, D. W., Basson, C. T. and MacRae, C. A. (1996). New understandings in the genetics of congenital heart disease. *Curr. Opin. Pediatr.* **8**, 505-511.

Bisaha, J. G. and Bader, D. (1991). Identification and characterization of a ventricular-specific avian myosin heavy chain, VMHC1: expression in differentiating cardiac and skeletal muscle. *Dev Biol* **148**, 355-64.

Bodmer, R. (1993). The gene *tinman* is required for the specification of theheart and visceral muscles in Drosphila. *Development* **118**, 719-729.

Bonham, R. T., Fine, M. R., Pollock, F. M. and Shelden, E. A. (2003). Hsp27, Hsp70, and metallothionein in MDCK and LLC-PK1 renal epithelial cells: effects of prolonged exposure to cadmium. *Toxicol Appl Pharmacol* **191**, 63-73.

Botto, L. D., Correa, A. and Erickson, J. D. (2001). Racial and temporal variations in the prevalence of heart defects. *Pediatrics* **107**, E32.

Brook, W. J. and Cohen, S. M. (1996a). Antagonistic interactions between wingless and decapentaplegic responsible for dorsal-ventral pattern in the Drosophila Leg. *Science* **273**, 1373-7.

Brook, W. J. and Cohen, S. M. (1996b). Antagonistic interactions between wingless and decapentaplegic responsible for dorsal-ventral pattern in the Drosophila Leg. *Science* **273**, 1373-7.

Brophy, C. M., Lamb, S. and Graham, A. (1999). The small heat shock-related protein-20 is an actin-associated protein. *J Vasc Surg* **29**, 326-33.

Brown, D. D., Binder, O., Pagratis, M., Parr, B. A. and Conlon, F. L. (2003). Developmental expression of the Xenopus laevis Tbx20 orthologue. *Dev Genes Evol* **212**, 604-7.

Brown, D. D., Davis, A. C. and Conlon, F. L. (2006). Xtn3 is a developmentally expressed cardiac and skeletal muscle-specific novex-3 titin isoform. *Gene Expr Patterns* **6**, 913-918.

Brown, D. D., Martz, S. N., Binder, O., Goetz, S. C., Price, B. M. J., Smith, J. C. and Conlon, F. L. (2005). Tbx5 and Tbx20 act synergistically to control vertebrate heart morphogenesis. *Development* **132**, 553-563.

Bruey, J. M., Ducasse, C., Bonniaud, P., Ravagnan, L., Susin, S. A., Diaz-Latoud, C., Gurbuxani, S., Arrigo, A. P., Kroemer, G., Solary, E. et al. (2000). Hsp27 negatively regulates cell death by interacting with cytochrome c. *Nat Cell Biol* **2**, 645-52.

Bruneau, B. G. (2002). Transcriptional regulation of vertebrate cardiac morphogenesis. *Circ Res* **90**, 509-19.

Bruneau, B. G., Bao, Z. Z., Tanaka, M., Schott, J. J., Izumo, S., Cepko, C. L., Seidman, J. G. and Seidman, C. E. (2000). Cardiac expression of the ventricle-specific homeobox gene Irx4 is modulated by Nkx2-5 and dHand. *Dev Biol* **217**, 266-77.

Bruneau, B. G., Logan, M., Davis, N., Levi, T., Tabin, C. J., Seidman, J. G. and Seidman, C. E. (1999). Chamber-specific cardiac expression of Tbx5 and heart defects in Holt-Oram syndrome. *Dev Biol* **211**, 100-8.

Bruneau, B. G., Nemer, G., Schmitt, J. P., Charron, F., Robitaille, L., Caron, S., Conner, D. A., Gessler, M., Nemer, M., Seidman, C. E. et al. (2001). A Murine Model of Holt-Oram Syndrome Defines Roles of the T-Box Transcription Factor Tbx5 in Cardiogenesis and Disease. *Cell* **106**, 709-721.

Buck, M. J. and Lieb, J. D. (2004). ChIP-chip: considerations for the design, analysis, and application of genome-wide chromatin immunoprecipitation experiments. *Genomics* **83**, 349-60.

Cai, C. L., Zhou, W., Yang, L., Bu, L., Qyang, Y., Zhang, X., Li, X., Rosenfeld, M. G., Chen, J. and Evans, S. (2005). T-box genes coordinate regional rates of proliferation and regional specification during cardiogenesis. *Development* **132**, 2475-87.

Carinato, M. E., Walter, B. E. and Henry, J. J. (2000). Xenopus laevis gelatinase B (Xmmp-9): development, regeneration, and wound healing. *Dev Dyn* **217**, 377-87.

Carreira, S., Dexter, T. J., Yavuzer, U., Easty, D. J. and Goding, C. R. (1998). Brachyury-related transcription factor Tbx2 and repression of the melanocyte-specific TRP-1 promoter. *Mol Cell Biol* **18**, 5099-108.

Carson, C. T., Kinzler, E. R. and Parr, B. A. (2000). Tbx12, a novel T-box gene, is expressed during early stages of heart and retinal development. *Mech Dev* **96**, 137-40.

Carson, C. T., Pagratis, M. and Parr, B. A. (2004). Tbx12 regulates eye development in Xenopus embryos. *Biochem Biophys Res Commun* **318**, 485-9.

Chanoine, C. and Hardy, S. (2003). Xenopus muscle development: from primary to secondary myogenesis. *Dev Dyn* **226**, 12-23.

Chapman, D. L., Agulnik, I., Hancock, S., Silver, L. M. and Papaioannou, V. E. (1996a). Tbx6, a mouse T-Box gene implicated in paraxial mesoderm formation at gastrulation. *Dev Biol* **180**, 534-42.

Chapman, D. L., Garvey, N., Hancock, S., Alexiou, M., Agulnik, S. I., Gibson-Brown, J., Cebra-Thomas, J., Bollag, R., Silver, L. M. and Papaionnou, V. E. (1996b). Expression of the T-box family genes, *Tbx1-Tbx5*, during early mouse development. *Dev. Dynam.* **206**, 379-390.

Chen, J. N. and Fishman, M. C. (2000). Genetics of heart development. *Trends Genet.* **16**, 383-388.

Chieffo, C., Garvey, N., Gong, W., Roe, B., Zhang, G., Silver, L., Emanuel, B. S. and Budarf, M. L. (1997). Isolation and characterization of a gene from the DiGeorge chromosomal region homologous to the mouse Tbx1 gene. *Genomics* **43**, 267-77.

Christoffels, V. M., Habets, P. E., Franco, D., Campione, M., de Jong, F., Lamers, W. H., Bao, Z. Z., Palmer, S., Biben, C., Harvey, R. P. et al. (2000). Chamber formation and morphogenesis in the developing mammalian heart. *Dev Biol* **223**, 266-78.

Ciruna, B. G. and Rossant, J. (1999). Expression of the T-box gene Eomesodermin during early mouse development. *Mech Dev* **81**, 199-203.

Collavoli, A., Hatcher, C. J., He, J., Okin, D., Deo, R. and Basson, C. T. (2003). TBX5 nuclear localization is mediated by dual cooperative intramolecular signals. *J Mol Cell Cardiol* **35**, 1191-5.

Cripps, R. M. and Olson, E. N. (2002). Control of cardiac development by an evolutionarily conserved transcriptional network. *Dev Biol* **246**, 14-28.

Crispino, J. D., Lodish, M. B., Thurberg, B. L., Litovsky, S. H., Collins, T., Molkentin, J. D. and Orkin, S. H. (2001). Proper coronary vascular development and heart morphogenesis depend on interaction of GATA-4 with FOG cofactors. *Genes Dev* **15**, 839-44.

Dalle-Donne, I., Rossi, R., Milzani, A., Di Simplicio, P. and Colombo, R. (2001). The actin cytoskeleton response to oxidants: from small heat shock protein phosphorylation to changes in the redox state of actin itself. *Free Radic Biol Med* **31**, 1624-32.

David, J. C., Landry, J. and Grongnet, J. F. (2000). Perinatal expression of heat-shock protein 27 in brain regions and nonneural tissues of the piglet. *J Mol Neurosci* **15**, 109-20.

DeHaan, R. L. (1963). Migrating patterns of precardiac mesoderm in the early chick embryo. *Exp. Cell Res.* **29**, 544-560.

DeHaan, R. L. and Ursprung, H. (1965). Organogenesis. New York: Holt, Rinehart Winston.

DeRuiter, M. C., Poelmann, R. E., VanderPlas-de Vries, I., Mentink, M. M. and Gittenberger-de Groot, A. C. (1992). The development of the myocardium and endocardium in mouse embryos. Fusion of two heart tubes? *Anat Embryol (Berl)* **185**, 461-73.

Drysdale, T. A., Tonissen, K. F., Patterson, K. D., Crawford, M. J. and Kreig, P. A. (1994). Cardiac troponin I is a heart specific marker in the Xenopus embryo: Expression during abnormal heart heart morphogenesis. *Dev. Biol.* **154**, 432-441.

Edmondson, D. G., Lyons, G. E., Martin, J. F. and Olson, E. N. (1994). Mef2 gene expression marks the cardiac and skeletal muscle lineages during mouse embryogenesis. *Development* **120**, 1251-63.

Eisenberg, L. M. and Markwald, R. R. (2004). Cellular recruitment and the development of the myocardium. *Dev Biol* **274**, 225-32.

Elliott, D. A., Kirk, E. P., Yeoh, T., Chandar, S., McKenzie, F., Taylor, P., Grossfeld, P., Fatkin, D., Jones, O., Hayes, P. et al. (2003). Cardiac homeobox gene NKX2-5 mutations and congenital heart disease: associations with atrial septal defect and hypoplastic left heart syndrome. *J Am Coll Cardiol* **41**, 2072-6.

Ellsworth, R. E., Ionasescu, V., Searby, C., Sheffield, V. C., Braden, V. V., Kucaba, T. A., McPherson, J. D., Marra, M. A. and Green, E. D. (1999). The CMT2D locus: refined genetic position and construction of a bacterial clone-based physical map. *Genome Res* **9**, 568-74.

Escobedo, J., Pucci, A. M. and Koh, T. J. (2004). HSP25 protects skeletal muscle cells against oxidative stress. *Free Radic Biol Med* **37**, 1455-62.

Evgrafov, O. V., Mersiyanova, I., Irobi, J., Van Den Bosch, L., Dierick, I., Leung, C. L., Schagina, O., Verpoorten, N., Van Impe, K., Fedotov, V. et al. (2004). Mutant small heat-shock protein 27 causes axonal Charcot-Marie-Tooth disease and distal hereditary motor neuropathy. *Nat Genet* **36**, 602-6.

Fan, C., Liu, M. and Wang, Q. (2003). Functional analysis of TBX5 missense mutations associated with Holt-Oram syndrome. *J Biol Chem* **278**, 8780-5.

Feil, I. K., Malfois, M., Hendle, J., van Der Zandt, H. and Svergun, D. I. (2001). A novel quaternary structure of the dimeric alpha-crystallin domain with chaperone-like activity. *J Biol Chem* **276**, 12024-9.

Ferns, G., Shams, S. and Shafi, S. (2006). Heat shock protein 27: its potential role in vascular disease. *Int J Exp Pathol* **87**, 253-74.

Fishman, M. C. and Chien, K. R. (1997). Fashioning the vertebrate heart: earliest embryonic decisions. *Development* **124**, 2099-2117.

Foley, A. C. and Mercola, M. (2005). Heart induction by Wnt antagonists depends on the homeodomain transcription factor Hex. *Genes Dev* **19**, 387-96.

Fujimoto, A., Baba, N. and Wakasugi, N. (1991). A tail length modifier gene discovered in the Japanese wild mice (Mus musculus molossinus). *Jpn J Genet* **66**, 141-54.

Gajewski, K., Fossett, N., Molkentin, J. D. and Schulz, R. A. (1999). The zinc finger proteins Pannier and GATA4 function as cardiogenic factors in Drosophila. *Development* **126**, 5679-88.

Garg, V., Kathiriya, I. S., Barnes, R., Schluterman, M. K., King, I. N., Butler, C. A., Rothrock, C. R., Eapen, R. S., Hirayama-Yamada, K., Joo, K. et al. (2003). GATA4 mutations cause human congenital heart defects and reveal an interaction with TBX5. *Nature* **424**, 443-7.

Garrity, D. M., Childs, S. and Fishman, M. C. (2002). The heartstrings mutation in zebrafish causes heart/fin Tbx5 deficiency syndrome. *Development* **129**, 4635-45.

Gei, A. F. and Hankins, G. D. (2001). Cardiac disease and pregnancy. *Obstet Gynecol Clin North Am* **28**, 465-512.

George, E. L., Baldwin, H. S. and Hynes, R. O. (1997). Fibronectins are essential for heart and blood vessel morphogenesis but are dispensable for initial specification of precursor cells. *Blood* **90**, 3073-81.

George, E. L., Georges-Labouesse, E. N., Patel-King, R. S., Rayburn, H. and Hynes, R. O. (1993). Defects in mesoderm, neural tube and vascular development in mouse embryos lacking fibronectin. *Development* **119**, 1079-91.

Gernold, M., Knauf, U., Gaestel, M., Stahl, J. and Kloetzel, P. M. (1993). Development and tissue-specific distribution of mouse small heat shock protein hsp25. *Dev Genet* **14**, 103-11.

Ghosh, T. K., Packham, E. A., Bonser, A. J., Robinson, T. E., Cross, S. J. and Brook, J. D. (2001). Characterization of the TBX5 binding site and analysis of mutations that cause Holt-Oram syndrome. *Hum Mol Genet* **10**, 1983-1994.

Gisselbrecht, S., Skeath, J., Doe, C. and Michelson, A. (1996). heartless encodes a fibroblast growth factor receptor (DFR1/DFGF-R2) involved in the directional migration of early mesodermal cells in the Drosophila embryo. *Genes Dev.*. **1**, 3003-3017.

Goetz, S. C., Brown, D. D. and Conlon, F. L. (2006). TBX5 is required for embryonic cardiac cell cycle progression. *Development* **133**, 2575-84.

Goldmuntz, E., Geiger, E. and Benson, D. W. (2001). NKX2.5 mutations in patients with tetralogy of fallot. *Circulation* **104**, 2565-8.

Gordon, M. D. and Nusse, R. (2006). Wnt signaling: multiple pathways, multiple receptors, and multiple transcription factors. *J Biol Chem* **281**, 22429-33.

Granzier, H., Labeit, D., Wu, Y. and Labeit, S. (2002). Titin as a modular spring: emerging mechanisms for elasticity control by titin in cardiac physiology and pathophysiology. *J Muscle Res Cell Motil* **23**, 457-71.

Grepin, C., Robitaille, L., Antakly, T. and Nemer, M. (1995). Inhibition of transcription factor GATA-4 expression blocks in vitro cardiac muscle differentiation. *Mol Cell Biol* **15**, 4095-102.

Griffin, K. J. and Kimelman, D. (2002). One-Eyed Pinhead and Spadetail are essential for heart and somite formation. *Nat Cell Biol* **4**, 821-5.

Griffin, K. J., Stoller, J., Gibson, M., Chen, S., Yelon, D., Stainier, D. Y. and Kimelman, D. (2000). A conserved role for H15-related T-box transcription factors in zebrafish and Drosophila heart formation. *Dev Biol* **218**, 235-47.

Hanlon, S. E. and Lieb, J. D. (2004). Progress and challenges in profiling the dynamics of chromatin and transcription factor binding with DNA microarrays. *Curr Opin Genet Dev* **14**, 697-705.

Hardy, S., Hamon, S., Cooper, B., Mohun, T. and Thiebaud, P. (1999). Two skeletal alpha-tropomyosin transcripts with distinct 3'UTR have different temporal and spatial patterns of expression in the striated muscle lineages of Xenopus laevis. *Mech Dev* **87**, 199-202.

Hardy, S. and Thiebaud, P. (1992). Isolation and characterization of cDNA clones encoding the skeletal and smooth muscle Xenopus laevis beta tropomyosin isoforms. *Biochim Biophys Acta* **1131**, 239-42.

Harland, R. and Gerhart, J. (1997). Formation and function of Spemann's organizer. *Ann. Rev. Cell Dev. Biol.* **13**, 611-667.

Harland, R. M. (1991). In situ hybridization: an improved whole mount method for Xenopus embryos. *Meth. Cell Biol.* **36**, 675-685.

Harvey, R. P. (2002). Patterning the vertebrate heart. *Nat Rev Genet* **3**, 544-56.

Haworth, K., Putt, W., Cattanach, B., Breen, M., Binns, M., Lingaas, F. and Edwards, Y. H. (2001). Canine homolog of the T-box transcription factor T; failure of the protein to bind to its DNA target leads to a short-tail phenotype. *Mamm Genome* **12**, 212-8.

Heasman, J., Kofron, M. and Wylie, C. (2000). Beta-catenin signaling activity dissected in the early Xenopus embryo: a novel antisense approach. *Dev Biol* **222**, 124-34.

Hemmati Brivanlou, A. and Thomsen, G. H. (1995). Ventral mesodermal patterning in Xenopus embryos: expression patterns and activities of BMP-2 and BMP-4. *Dev. Genet.* **17**, 78-89.

Herrmann, B. G. and Lehrach, H. (1988). From phenotype to gene: molecular cloning in the Brachyury (T) locus region. *Curr Top Microbiol Immunol* **137**, 77-81.

Hirano, S., Shelden, E. A. and Gilmont, R. R. (2004). HSP27 regulates fibroblast adhesion, motility, and matrix contraction. *Cell Stress Chaperones* **9**, 29-37.

Hiroi, Y., Kudoh, S., Monzen, K., Ikeda, Y., Yazaki, Y., Nagai, R. and Komuro, I. (2001). Tbx5 associates with Nkx2-5 and synergisticallly promotes cardiomyocyte differentiation. *Nature Genetics* **28**, 276-280.

Hoffman, J. I. (1995a). Incidence of Congenital Heart Disease: I. Postnantal Incidence. **16**, 103-113.

Hoffman, J. I. (1995b). Incidence of Congenital Heart Disease: II Prenatal Incidence. *Pediatr. Cardiol* **16**, 155-165.

Hollander, J. M., Martin, J. L., Belke, D. D., Scott, B. T., Swanson, E., Krishnamoorthy, V. and Dillmann, W. H. (2004). Overexpression of wild-type heat shock protein 27 and a nonphosphorylatable heat shock protein 27 mutant protects against ischemia/reperfusion injury in a transgenic mouse model. *Circulation* **110**, 3544-52.

Horb, M. E. and Thomsen, G. H. (1997). A vegetally localized T-box transcription factor in Xenopus eggs specifies mesoderm and endoderm and is essential for embryonic mesoderm formation. *Development* **124**, 1689-1698.

Horb, M. E. and Thomsen, G. H. (1999). Tbx5 is essential for heart development. *Development* **126**, 1739-1751.

Huot, J., Houle, F., Spitz, D. R. and Landry, J. (1996). HSP27 phosphorylation-mediated resistance against actin fragmentation and cell death induced by oxidative stress. *Cancer Res* **56**, 273-9.

Iio, A., Koide, M., Hidaka, K. and Morisaki, T. (2001). Expression pattern of novel chick T-box gene, Tbx20. *Dev Genes Evol* **211**, 559-62.

Inglehearn, C., Keen, T. J., al-Maghtheh, M. and Bhattacharya, S. (1994). Loci for autosomal dominant retinitis pigmentosa and dominant cystoid macular dystrophy on chromosome 7p are not allelic. *Am J Hum Genet* **55**, 581-2.

Isaacs, H. V., Tannahill, D. and Slack, J. M. W. (1992). Expression of a novel FGF in the Xenopus embryo. A new candidate inducing factor for mesoderm formation and anteroposterior specification. *Development* **114**, 711-720.

Jakob, U., Gaestel, M., Engel, K. and Buchner, J. (1993). Small heat shock proteins are molecular chaperones. *J Biol Chem* **268**, 1517-20.

Jerome, L. A. and Papaioannou, V. E. (2001). DiGeorge syndrome phenotype in mice mutant for the T-box gene, Tbx1. *Nat. Genet.* **27**, 286-291.

Jiang, Y. and Evans, T. (1996). The Xenopus GATA-4/5/6 genes are associated with cardiac specification and can regulate cardiac-specific transcription during embryogenesis. *Dev Biol* **174**, 258-70.

Kanekar, S., Perron, M., Dorsky, R., Harris, W. A., Jan, L. Y., Jan, Y. N. and Vetter, M. L. (1997). Xath5 participates in a network of bHLH genes in the developing Xenopus retina. *Neuron* **19**, 981-94.

Kappe, G., Franck, E., Verschuure, P., Boelens, W. C., Leunissen, J. A. and de Jong, W. W. (2003). The human genome encodes 10 alpha-crystallin-related small heat shock proteins: HspB1-10. *Cell Stress Chaperones* **8**, 53-61.

Keller, R. E. (1976). Vital dye mapping of the gastrula and neurula of Xenopus laevis. II. Prospective areas and morphogenetic movements of the deep layer. *Dev Biol* **51**, 118-37.

Kikuchi, Y., Trinh, L. A., Reiter, J. F., Alexander, J., Yelon, D. and Stainier, D. Y. (2000). The zebrafish bonnie and clyde gene encodes a Mix family homeodomain protein that regulates the generation of endodermal precursors. *Genes Dev* **14**, 1279-89.

Klein, L. L. and Galan, H. L. (2004). Cardiac disease in pregnancy. *Obstet Gynecol Clin North Am* **31**, 429-59, viii.

Knowlton, A. A., Kapadia, S., Torre-Amione, G., Durand, J. B., Bies, R., Young, J. and Mann, D. L. (1998). Differential expression of heat shock proteins in normal and failing human hearts. *J Mol Cell Cardiol* **30**, 811-8.

Kochanek, K. D., Murphy, S. L., Anderson, R. N. and Scott, C. (2004). Deaths: final data for 2002. *Natl Vital Stat Rep* **53**, 1-115.

Kolker, S., Tajchman, U. and Weeks, D. L. (2000). Confocal Imaging of early heat development in Xenopus laevis. *Dev. Biol.* **218**, 64-73.

Komatsuda, A., Wakui, H., Oyama, Y., Imai, H., Miura, A. B., Itoh, H. and Tashima, Y. (1999). Overexpression of the human 72 kDa heat shock protein in renal tubular cells confers resistance against oxidative injury and cisplatin toxicity. *Nephrol Dial Transplant* **14**, 1385-90.

Koshiba-Takeuchi, K., Takeuchi, J. K., Matsumoto, K., Momose, T., Uno, K., Hoepker, V., Ogura, K., Takahashi, N., Nakamura, H., Yasuda, K. et al. (2000). Tbx5 and the retinotectum projection. *Science* **287**, 134-7.

Kraus, F., Haenig, B. and Kispert, A. (2001). Cloning and expression analysis of the mouse T-box gene tbx20. *Mech Dev* **100**, 87-91.

Kuo, C. T., Morrisey, E. E., Anandappa, R., Sigrist, K., Lu, M. M., Parmacek, M. S., Soudais, C. and Leiden, J. M. (1997). GATA4 transcription factor is required for ventral morphogenesis and heart tube formation. *Genes Dev* **11**, 1048-60.

Kupperman, E., An, S., Osborne, N., Waldron, S. and Stainier, D. Y. (2000). A sphingosine-1-phosphate receptor regulates cell migration during vertebrate heart development. *Nature* **406**, 192-5.

Ladd, A. N., Yatskievych, T. A. and Antin, P. B. (1998). Regulation of avian cardiac myogenesis by activin/TGFbeta and bone morphogenetic proteins. *Dev Biol* **204**, 407-19.

Ladher, R., Mohun, T. J., Smith, J. C. and Snape, A. M. (1996). Xom: a Xenopus homeobox gene that mediates the early effects of BMP-4. *Development* **122**, 2385-94.

Laverriere, A. C., MacNeill, C., Mueller, C., Poelmann, R. E., Burch, J. B. and Evans, T. (1994). GATA-4/5/6, a subfamily of three transcription factors transcribed in developing heart and gut. *J Biol Chem* **269**, 23177-84.

Lavoie, J. N., Gingras-Breton, G., Tanguay, R. M. and Landry, J. (1993a). Induction of Chinese hamster HSP27 gene expression in mouse cells confers resistance to heat shock. HSP27 stabilization of the microfilament organization. *J Biol Chem* **268**, 3420-9.

Lavoie, J. N., Hickey, E., Weber, L. A. and Landry, J. (1993b). Modulation of actin microfilament dynamics and fluid phase pinocytosis by phosphorylation of heat shock protein 27. *J Biol Chem* **268**, 24210-4.

Lavoie, J. N., Lambert, H., Hickey, E., Weber, L. A. and Landry, J. (1995). Modulation of cellular thermoresistance and actin filament stability accompanies phosphorylation-induced changes in the oligomeric structure of heat shock protein 27. *Mol Cell Biol* **15**, 505-16.

Leal, R. B., Cordova, F. M., Herd, L., Bobrovskaya, L. and Dunkley, P. R. (2002). Lead-stimulated p38MAPK-dependent Hsp27 phosphorylation. *Toxicol Appl Pharmacol* **178**, 44-51.

Lebreton, S., Boissel, L. and Moreau, J. (2003). Control of embryonic Xenopus morphogenesis by a Ral-GDS/Xral branch of the Ras signalling pathway. *J Cell Sci* **116**, 4651-62.

Leconte, L., Lecoin, L., Martin, P. and Saule, S. (2004). Pax6 Interacts with cVax and Tbx5 to Establish the Dorsoventral Boundary of the Developing Eye. *J Biol Chem* **279**, 47272-47277.

Lee, K. H., Evans, S., Ruan, T. Y. and Lassar, A. B. (2004). SMAD-mediated modulation of YY1 activity regulates the BMP response and cardiac-specific expression of a GATA4/5/6-dependent chick Nkx2.5 enhancer. *Development* **131**, 4709-23.

Li, Q. Y., Newbury Ecob, R. A., Terrett, J. A., Wilson, D. I., Curtis, A. R., Yi, C. H., Gebuhr, T., Bullen, P. J., Robson, S. C., Strachan, T. et al. (1997). Holt-Oram syndrome is caused by mutations in TBX5, a member of the Brachyury (T) gene family. *Nat. Genet.* **15**, 21-29.

Liberatore, C. M., Searcy-Schrick, R. D., Vincent, E. B. and Yutzey, K. E. (2002). Nkx-2.5 gene induction in mice is mediated by a Smad consensus regulatory region. *Dev Biol* **244**, 243-56.

Lien, C. L., McAnally, J., Richardson, J. A. and Olson, E. N. (2002). Cardiac-specific activity of an Nkx2-5 enhancer requires an evolutionarily conserved Smad binding site. *Dev Biol* **244**, 257-66.

Lien, C. L., Wu, C., Mercer, B., Webb, R., Richardson, J. A. and Olson, E. N. (1999). Control of early cardiac-specific transcription of Nkx2-5 by a GATA-dependent enhancer. *Development* **126**, 75-84.

Lindsey, E. A., Vitelli, F., Su, H., Morishima, M., Huynh, T., Pramparo, T., Jurecic, V., Ogunrinu, G., Sutherland, H. F., Scrambler, P. J. et al. (2001). Tbx1 haploinsufficiency in the DiGeorge syndrome region causes aortic arch defects in mice. *Nature* **410**, 97-101.

Liu, C. and Welsh, M. J. (1999). Identification of a site of Hsp27 binding with Hsp27 and alpha B-crystallin as indicated by the yeast two-hybrid system. *Biochem Biophys Res Commun* **255**, 256-61.

Logan, M. and Mohun, T. (1993). Induction of cardiac muscle differentiation in isolated animal pole explants of Xenopus laevis embryos. *Development* **118**, 865-875.

Lohr, J. L. and Yost, H. J. (2000). Vertebrate Model Systems in the Study of Early Heart Development: Xenopus and Zebrafish. *American Journal of Medical Genetics (Semin. Med. Genet).* **97**, 248-257.

Lough, J. and Sugi, Y. (2000). Endoderm and heart development. *Dev Dyn* **217**, 327-42.

Lyons, I., et al. (1995). Myogenic and morphogenic defects in the heart tubes of murine embrryos lacking thehomeobox gene Nkx-2.5. *Genes Dev.* **9**, 1654-1666.

Mao, L., Bryantsev, A. L., Chechenova, M. B. and Shelden, E. A. (2005). Cloning, characterization, and heat stress-induced redistribution of a protein homologous to human hsp27 in the zebrafish Danio rerio. *Exp Cell Res* **306**, 230-41.

Mao, L. and Shelden, E. A. (2006). Developmentally regulated gene expression of the small heat shock protein Hsp27 in zebrafish embryos. *Gene Expr Patterns* **6**, 127-33.

Marcellini, S., Technau, U., Smith, J. C. and Lemaire, P. (2003). Evolution of Brachyury proteins: identification of a novel regulatory domain conserved within Bilateria. *Dev Biol* **260**, 352-61.

Marvin, M. J., Di Rocco, G., Gardiner, A., Bush, S. M. and Lassar, A. B. (2001). Inhibition of Wnt activity induces heart formation from posterior mesoderm. *Genes Dev* **15**, 316-27.

Maw, M., Kar, B., Biswas, J., Biswas, P., Nancarrow, D., Bridges, R., Kumaramanickavel, G., Denton, M. and Badrinath, S. S. (1996). Linkage of blepharophimosis syndrome in a large Indian pedigree to chromosome 7p. *Hum Mol Genet* **5**, 2049-54.

Mehlen, P., Kretz-Remy, C., Briolay, J., Fostan, P., Mirault, M. E. and Arrigo, A. P. (1995). Intracellular reactive oxygen species as apparent modulators of heat-shock protein 27 (hsp27) structural organization and phosphorylation in basal and tumour necrosis factor alpha-treated T47D human carcinoma cells. *Biochem J* **312 (Pt 2)**, 367-75.

Mehlen, P., Mehlen, A., Godet, J. and Arrigo, A. P. (1997). hsp27 as a switch between differentiation and apoptosis in murine embryonic stem cells. *J Biol Chem* **272**, 31657-65.

Meins, M., Henderson, D. J., Bhattacharya, S. S. and Sowden, J. C. (2000). Characterization of the human TBX20 gene, a new member of the T-Box gene family closely related to the Drosophila H15 gene. *Genomics* **67**, 317-32.

Merscher, S., Funke, B., Epstein, J. A., Heyer, J., Puech, A., Lu, M. M., Xavier, R. J., Demay, M. B., Russell, R. G., Factor, S. et al. (2001). TBX1 is responsible for cardiovascular defects in velo-cardio- facial/DiGeorge syndrome. *Cell* **104**, 619-29.

Miron, T., Vancompernolle, K., Vandekerckhove, J., Wilchek, M. and Geiger, B. (1991). A 25-kD inhibitor of actin polymerization is a low molecular mass heat shock protein. *J Cell Biol* **114**, 255-61.

Miron, T., Wilchek, M. and Geiger, B. (1988). Characterization of an inhibitor of actin polymerization in vinculin-rich fraction of turkey gizzard smooth muscle. *Eur J Biochem* **178**, 543-53.

Miskolczi-McCallum, C. M., Scavetta, R. J., Svendsen, P. C., Soanes, K. H. and Brook, W. J. (2005). The Drosophila melanogaster T-box genes midline and H15 are conserved regulators of heart development. *Devlopmental Biology* **in press**.

Mohun, T., Orford, R. and Shang, C. (2003). The origins of cardiac tissue in the amphibian, Xenopus laevis. *Trends Cardiovasc Med* **13**, 244-8.

Mohun, T. J. and Leong, L. M. (1999). Heart Formation and the Heart Field in Amphibian Embryos.: Academic Press.

Mohun, T. J., Leong, L.M., Weninger, W. J., and Sparrow, D. B. (2000). The Morphology of Heart Development in Xenopus laevis. *Developmental Biology* **218**, 74-88.

Moskowitz, I. P., Pizard, A., Patel, V. V., Bruneau, B. G., Kim, J. B., Kupershmidt, S., Roden, D., Berul, C. I., Seidman, C. E. and Seidman, J. G. (2004). The T-Box

transcription factor Tbx5 is required for the patterning and maturation of the murine cardiac conduction system. *Development* **131**, 4107-16.

Mounier, N. and Arrigo, A. P. (2002). Actin cytoskeleton and small heat shock proteins: how do they interact? *Cell Stress Chaperones* **7**, 167-76.

Muller, C. W. and Herrmann, B. G. (1997). Crystallographic structure of the T domain-DNA complex of the Brachyury transcription factor. *Nature* **389**, 884-888.

Naiche, L. A., Harrelson, Z., Kelly, R. G. and Papaioannou, V. E. (2005). T-box genes in vertebrate development. *Annu Rev Genet* **39**, 219-39.

Narita, N., Bielinska, M. and Wilson, D. B. (1997). Cardiomyocyte differentiation by GATA-4-deficient embryonic stem cells. *Development* **124**, 3755-64.

Nascone, N. and Mercola, M. (1996). Endoderm and Cardiogenesis: New Insights. *Trends in Cardiovascular Medicine* **6**, 211-216.

Newbury-Ecob, R., Leanage, R., Raeburn, J. A. and Young, I. D. (1996). The Holt-Oram Syndrome: a clinical genetic study. *J. Med. Genet.* **33**, 300-307.

Newman, C. S. and Krieg, P. A. (1999). Specification and Differntiation of the Heart in Amphibia: Academic Press.

Newman, C. S., Krieg, P.A. (1998). tinman-related genes expressed during heart development in Xenopus. *Genet.* **22**, 230-238.

Niehrs, C., Kazanskaya, O., Wu, W. and Glinka, A. (2001). Dickkopf1 and the Spemann-Mangold head organizer. *Int J Dev Biol* **45**, 237-40.

Nieuwkoop, P. D. and Faber, J. (1967). Normal Table of *Xenopus laevis* (Daudin). Amsterdam: North Holland.

Nohe, A., Keating, E., Knaus, P. and Petersen, N. O. (2004). Signal transduction of bone morphogenetic protein receptors. *Cell Signal* **16**, 291-9.

Norris, C. E., Brown, M. A., Hickey, E., Weber, L. A. and Hightower, L. E. (1997). Low-molecular-weight heat shock proteins in a desert fish (Poeciliopsis lucida): homologs of human Hsp27 and Xenopus Hsp30. *Mol Biol Evol* **14**, 1050-61.

Olson, E. N. (2006). Gene regulatory networks in the evolution and development of the heart. *Science* **313**, 1922-7.

Orkin, S. H., Harosi, F. I. and Leder, P. (1975). Differentiation in erythroleukemic cells and their somatic hybrids. *Proc Natl Acad Sci U S A* **72**, 98-102.

Packham, E. A. and Brook, J. D. (2003). T-box genes in human disorders. *Hum Mol Genet* **12 Spec No 1**, R37-44.

Papaioannou, V. E. (2001). T-box genes in development: from hydra to humans. *Int Rev Cytol* **207**, 1-70.

Paul, C., Manero, F., Gonin, S., Kretz-Remy, C., Virot, S. and Arrigo, A. P. (2002). Hsp27 as a negative regulator of cytochrome C release. *Mol Cell Biol* **22**, 816-34.

Payne, R. M., Johnson, M. C., Grant, J. W. and Strauss, J. E. (1995). Toward a molecular understanding of congenital heart disease. *Circulation* **91**, 494-504.

Perea-Gomez, A., Rhinn, M. and Ang, S. L. (2001). Role of the anterior visceral endoderm in restricting posterior signals in the mouse embryo. *Int J Dev Biol* **45**, 311-20.

Piotrowicz, R. S., Hickey, E. and Levin, E. G. (1998). Heat shock protein 27 kDa expression and phosphorylation regulates endothelial cell migration. *Faseb J* **12**, 1481-90.

Plageman, T. F., Jr. and Yutzey, K. E. (2004). Differential expression and function of tbx5 and tbx20 in cardiac development. *J Biol Chem* **279**, 19026-34.

Prall, O. W., Elliott, D. A. and Harvey, R. P. (2002). Developmental paradigms in heart disease: insights from tinman. *Ann Med* **34**, 148-56.

Radice, G. P. and Malacinski, G. M. (1989). Expression of myosin heavy chain transcripts during Xenopus laevis development. *Dev Biol* **133**, 562-8.

Raffin, M., Leong, L. M., Rones, M. S., Sparrow, D., Mohun, T. and Mercola, M. (2000). Subdivision of the cardiac Nkx2.5 expression domain into myogenic and nonmyogenic compartments. *Dev Biol* **218**, 326-40.

Rahman, D. R., Bentley, N. J. and Tuite, M. F. (1995). The Saccharomyces cerevisiae small heat shock protein Hsp26 inhibits actin polymerisation. *Biochem Soc Trans* **23**, 77S.

Reim, I., Mohler, J. P. and Frasch, M. (2005). Tbx20-related genes, mid and H15, are required for tinman expression, proper patterning, and normal differentiation of cardioblasts in Drosophila. *Mech Dev* **122**, 1056-69.

Reiter, J. F., Alexander, J., Rodaway, A., Yelon, D., Patient, R., Holder, N. and Stainier, D. Y. (1999). Gata5 is required for the development of the heart and endoderm in zebrafish. *Genes Dev* **13**, 2983-95.

Reynolds, L. P. and Allen, G. V. (2003). A review of heat shock protein induction following cerebellar injury. *Cerebellum* **2**, 171-7.

Ryan, K. and Chin, A. J. (2003). T-box genes and cardiac development. *Birth Defects Res Part C Embryo Today* **69**, 25-37.

Sater, A. K. and Jacobson, A. G. (1989). The specification of heart mesoderm occurs during gastrulation in Xenopus laevis. *Development* **106**, 519-529.

Scheler, C., Li, X. P., Salnikow, J., Dunn, M. J. and Jungblut, P. R. (1999). Comparison of two-dimensional electrophoresis patterns of heat shock protein Hsp27 species in normal and cardiomyopathic hearts. *Electrophoresis* **20**, 3623-8.

Schier, A. F., Neuhauss, S. C., Helde, K. A., Talbot, W. S. and Driever, W. (1997). The one-eyed pinhead gene functions in mesoderm and endoderm formation in zebrafish and interacts with no tail. *Development* **124**, 327-42.

Schlange, T., Andree, B., Arnold, H. H. and Brand, T. (2000). BMP2 is required for early heart development during a distinct time period. *Mech Dev* **91**, 259-70.

Schneider, V. A. and Mercola, M. (2001). Wnt antagonism initiates cardiogenesis in Xenopus laevis. *Genes Dev* **15**, 304-15.

Schulte-Merker, S., van Eeden, F. J., Halpern, M. E., Kimmel, C. B. and Nusslein-Volhard, C. (1994). no tail (ntl) is the zebrafish homologue of the mouse T (Brachyury) gene. *Development* **120**, 1009-1015.

Schultheiss, T. M., Burch, J. B. and Lassar, A. B. (1997). A role for bone morphogenetic proteins in the induction of cardiac myogenesis. *Genes Dev* **11**, 451-462.

Schwartz, R. J. and Olson, E. N. (1999). Building the heart piece by piece: modularity of cis-elements regulating Nkx2-5 transcription. *Development* **126**, 4187-92.

Searcy, R. D., Vincent, E. B., Liberatore, C. M. and Yutzey, K. E. (1998). A GATA-dependent nkx-2.5 regulatory element activates early cardiac gene expression in transgenic mice. *Development* **125**, 4461-70.

Serbedzija, G. N., Chen, J. N. and Fishman, M. C. (1998). Regulation in the heart field of zebrafish. *Development* **125**, 1095-101.

Shama, K. M., Suzuki, A., Harada, K., Fujitani, N., Kimura, H., Ohno, S. and Yoshida, K. (1999). Transient up-regulation of myotonic dystrophy protein kinase-binding protein, MKBP, and HSP27 in the neonatal myocardium. *Cell Struct Funct* **24**, 1-4.

Shelden, E. A., Borrelli, M. J., Pollock, F. M. and Bonham, R. (2002). Heat shock protein 27 associates with basolateral cell boundaries in heat-shocked and ATP-depleted epithelial cells. *J Am Soc Nephrol* **13**, 332-41.

Shi, Y., Katsev, S., Cai, C. and Evans, S. (2000). BMP signaling is required for heart formation in vertebrates. *Dev Biol* **224**, 226-37.

Showell, C., Binder, O. and Conlon, F. L. (2004). T-box genes in early embryogenesis. *Dev Dyn* **229**, 201-18.

Singh, M. K., Christoffels, V. M., Dias, J. M., Trowe, M. O., Petry, M., Schuster-Gossler, K., Burger, A., Ericson, J. and Kispert, A. (2005). Tbx20 is essential for cardiac chamber differentiation and repression of Tbx2. *Development* **132**, 2697-707.

Sinha, S., Abraham, S., Gronostajski, R. M. and Campbell, C. E. (2000). Differential DNA binding and transcription modulation by three T-box proteins, T, TBX1 and TBX2. *Gene* **258**, 15-29.

Skre, H. (1974). Genetic and clinical aspects of Charcot-Marie-Tooth's disease. *Clin Genet* **6**, 98-118.

Small, E. M. and Krieg, P. A. (2000). Expression of atrial natriuretic factor (ANF) during Xenopus cardiac development. *Dev Genes Evol* **210**, 638-640.

Smith, J. (1999). T-box genes: what they do and how they do it. *Trends Genet.* **15**, 154-158.

Smith, J. C., Price, B. M., Green, J. B. A., Weigel, D. and Herrmann, B. G. (1991). Expression of a Xenopus homolog of *Brachyury* (T) is an immediate-early response to mesoderm induction. *Cell* **67**, 79-87.

Somji, S., Sens, D. A., Garrett, S. H., Sens, M. A. and Todd, J. H. (1999). Heat shock protein 27 expression in human proximal tubule cells exposed to lethal and sublethal concentrations of CdCl2. *Environ Health Perspect* **107**, 545-52.

Sparrow, D. B., Cai, C., Kotecha, S., Latinkic, B., Cooper, B., Towers, N., Evans, S. M. and Mohun, T. J. (2000). Regulation of the tinman homologues in Xenopus embryos. *Dev Biol* **227**, 65-79.

Stainier, D. Y. (2001). Zebrafish genetics and vertebrate heart formation. *Nat Rev Genet.* **2**, 39-48.

Stainier, D. Y., Lee, R. K. and Fishman, M. C. (1993). Cardiovascular development in the zebrafish. I. Myocardial fate map and heart tube formation. *Development* **119**, 31-40.

Stennard, F. A., Costa, M. W., Elliott, D. A., Rankin, S., Haast, S. J., Lai, D., McDonald, L. P., Niederreither, K., Dolle, P., Bruneau, B. G. et al. (2003). Cardiac T-box factor Tbx20 directly interacts with Nkx2-5, GATA4, and GATA5 in regulation of gene expression in the developing heart. *Dev Biol* **262**, 206-24.

Stennard, F. A., Costa, M. W., Lai, D., Biben, C., Furtado, M. B., Solloway, M. J., McCulley, D. J., Leimena, C., Preis, J. I., Dunwoodie, S. L. et al. (2005). Murine T-box transcription factor Tbx20 acts as a repressor during heart development, and is essential for adult heart integrity, function and adaptation. *Development* **132**, 2451-62.

Sugi, Y. and Lough, J. (1994). Anterior endoderm is a specific effector of terminal cardiac myocyte differentiation of cells from the embryonic heart forming region. *Dev Dyn* **200**, 155-62.

Sun, X., Meyers, E. N., Lewandoski, M. and Martin, G. R. (1999). Targeted disruption of Fgf8 causes failure of cell migration in the gastrulating mouse embryo. *Genes Dev* **13**, 1834-46.

Sun, Y. and MacRae, T. H. (2005). The small heat shock proteins and their role in human disease. *Febs J* **272**, 2613-27.

Szeto, D. P., Griffin, K. J. and Kimelman, D. (2002). HrT is required for cardiovascular development in zebrafish. *Development* **129**, 5093-101.

Takeuchi, J. K., Mileikovskaia, M., Koshiba-Takeuchi, K., Heidt, A. B., Mori, A. D., Arruda, E. P., Gertsenstein, M., Georges, R., Davidson, L., Mo, R. et al. (2005). Tbx20 dose-dependently regulates transcription factor networks required for mouse heart and motoneuron development. *Development* **132**, 2463-74.

Takeuchi, J. K., Ohgi, M., Koshiba-Takeuchi, K., Shiratori, H., Sakaki, I., Ogura, K., Saijoh, Y. and Ogura, T. (2003). Tbx5 specifies the left/right ventricles and ventricular septum position during cardiogenesis. *Development* **130**, 5953-64.

Tanaka, M., Chen, Z., Bartunkova, S., Yamasaki, N. and Izumo, S. (1999). The cardiac homeobox gene Csx/Nkx2.5 lies genetically upstream of multiple genes essential for heart development. *Development* **126**, 1269-80.

Thom, T., Haase, N., Rosamond, W., Howard, V. J., Rumsfeld, J., Manolio, T., Zheng, Z.-J., Flegal, K., O'Donnell, C., Kittner, S. et al. (2006). Heart Disease and Stroke Statistics--2006 Update: A Report From the American Heart Association Statistics Committee and Stroke Statistics Subcommittee. *Circulation* **113**, e85-151.

Tonissen, K. F., Drysdale, T. A., Lints, T. J., Harvey, R. P. and Krieg, P. A. (1994). XNkx-2.5, a Xenopus gene related to Nkx-2.5 and tinman: evidence for a conserved role in cardiac development. *Dev. Biol.* **162**, 325-328.

Trinh, L. A. and Stainier, D. Y. (2004). Fibronectin regulates epithelial organization during myocardial migration in zebrafish. *Dev Cell* **6**, 371-82.

Tzahor, E. and Lassar, A. B. (2001). Wnt signals from the neural tube block ectopic cardiogenesis. *Genes Dev* **15**, 255-60.

Vander Heide, R. S. (2002). Increased expression of HSP27 protects canine myocytes from simulated ischemia-reperfusion injury. *Am J Physiol Heart Circ Physiol* **282**, H935-41.

Wang, D., Chang, P. S., Wang, Z., Sutherland, L., Richardson, J. A., Small, E., Krieg, P. A. and Olson, E. N. (2001). Activation of cardiac gene expression by myocardin, a transcriptional cofactor for serum response factor. *Cell* **105**, 851-62.

Wilson, P. A. and Hemmati-Brivanlou, A. (1995). Induction of epidermis and inhibition of neural fate by Bmp-4. *Nature* **376**, 331-333.

Wilson, V. and Conlon, F. L. (2002). The T-box family. *Genome Biol* **3**, Reviews 3008.1-3008.7.

Yagi, H., Furutani, Y., Hamada, H., Sasaki, T., Asakawa, S., Minoshima, S., Ichida, F., Joo, K., Kimura, M., Imamura, S. et al. (2003). Role of TBX1 in human del22q11.2 syndrome. *Lancet* **362**, 1366-73.

Yatskievych, T. A., Ladd, A. N. and Antin, P. B. (1997). Induction of cardiac myogenesis in avian pregastrula epiblast: the role of the hypoblast and activin. *Development* **124**, 2561-70.

Yatskievych, T. A., Pascoe, S. and Antin, P. B. (1999). Expression of the homebox gene Hex during early stages of chick embryo development. *Mech Dev* **80**, 107-9.

Yelon, D., Ticho, B., Halpern, M. E., Ruvinsky, I., Ho, R. K., Silver, L. M. and Stainier, D. Y. (2000). The bHLH transcription factor hand2 plays parallel roles in zebrafish heart and pectoral fin development. *Development* **127**, 2573-82.

Zaffran, S. and Frasch, M. (2002). Early signals in cardiac development. *Circ Res* **91**, 457-69.

Zaragoza, M. V., Lewis, L. E., Sun, G., Wang, E., Li, L., Said-Salman, I., Feucht, L. and Huang, T. (2004). Identification of the TBX5 transactivating domain and the nuclear localization signal. *Gene* **330**, 9-18.

Zhang, H. and Bradley, A. (1996). Mice deficient for BMP2 are nonviable and have defects in amnion/chorion and cardiac development. *Development* **122**, 2977-86.

Zhang, X. M., Ramalho-Santos, M. and McMahon, A. P. (2001). Smoothened mutants reveal redundant roles for Shh and Ihh signaling including regulation of L/R asymmetry by the mouse node. *Cell* **105**, 781-92.